THE QUARTERLY JOURNAL OF MECHANICS AND APPLIED MATHEMATICS

VOLUME X
1957

OXFORD
AT THE CLARENDON PRESS

Oxford University Press, Amen House, London E.C.4

GLASGOW NEW YORK TORONTO MELBOURNE WELLINGTON
BOMBAY CALCUTTA MADRAS KARACHI KUALA LUMPUR
CAPE TOWN IBADAN NAIROBI ACCRA

PRINTED IN GREAT BRITAIN
AT THE UNIVERSITY PRESS, OXFORD
BY CHARLES BATEY, PRINTER TO THE UNIVERSITY

THE QUARTERLY JOURNAL OF

MECHANICS AND APPLIED MATHEMATICS

VOLUME X PART 1

FEBRUARY 1957

OXFORD

AT THE CLARENDON PRESS

1957

Price 18*s. net*

PRINTED IN GREAT BRITAIN BY CHARLES BATEY AT THE UNIVERSITY PRESS, OXFORD

THE QUARTERLY JOURNAL OF MECHANICS AND APPLIED MATHEMATICS

THE QUARTERLY JOURNAL OF MECHANICS AND APPLIED MATHEMATICS is published at 18*s.* net for a single number with an annual subscription (for four numbers) of 60*s.* post free.

NOTICE TO CONTRIBUTORS

1. *Communication.* Papers should be communicated to one or other of the Executive Editors, by name, at King's College, Strand, London, W.C. 2.

2. *Presentation.* Manuscripts should preferably be typewritten, and each paper should be preceded by a summary not exceeding 300 words in length. References to literature should be given in standard order, *author, title of journal, volume number, date, page.* These should be placed at the end of the paper and arranged according to the order of reference in the paper.

3. *Diagrams.* The number of diagrams should be kept to the minimum consistent with clarity. The lines of the figures should be drawn in ink either on draughtsman's paper or on good quality white paper. Each individual line in the figure should bear reducing to one-half of the size of the original, and great care should be exercised to see that the lines are regular in thickness, especially where they meet. Lettering of the figure should be in pencil and should be sufficient to define clearly the lines and curves in it. The writing of formulae or of explanations on the diagram itself should be avoided. All explanations of symbols, etc., should be given in underline. Contributors should indicate on their manuscripts where figures should be inserted.

4. *Tables.* Tables should preferably be arranged so that they can be printed with the columns parallel to the longer edge of the page.

5. *Notation.* All single letters used to denote vectors in the manuscript should be marked by underlining with a wavy line. Scalar and vector products should be denoted by $\underset{\sim}{a} . \underset{\sim}{b}$ and $\underset{\sim}{a} \wedge \underset{\sim}{b}$ respectively. Real and imaginary parts of complex quantities should be denoted by re and im respectively.

6. *Offprints.* Authors of papers will be entitled to 25 free offprints. This number is available for sharing between authors of joint papers.

7. All correspondence other than that dealing with contributions should be addressed to the publishers:

OXFORD UNIVERSITY PRESS
AMEN HOUSE, LONDON, E.C. 4

THE THEORY OF SYMMETRICAL GRAVITY WAVES OF FINITE AMPLITUDE

IV.† STEADY, SYMMETRICAL, PERIODIC WAVES IN A CHANNEL OF FINITE DEPTH

By A. J. GOODY *and* T. V. DAVIES

(*King's College, London*)

[Received 30 June 1955.—Revise received 12 April 1956]

SUMMARY

The perfect fluid problem of two-dimensional finite amplitude gravity waves in a channel of finite depth has been investigated and the four quantities, wave velocity (c), wave amplitude (a), wavelength (λ), and depth of the liquid (h), are shown to depend upon two parameters u and k, where $0 \leqslant u \leqslant u_{\max}$ and $0 \leqslant k \leqslant 1$. When $u = u_{\max}$ the wave is on the point of breaking. Tables have been prepared of four combinations of c, a, λ, and h against u and k from which it is possible to determine (say) the wave velocity when the three quantities a, h, and λ are given. An analytical formula is also derived for the relation between a, h, and λ when the wave is on the point of breaking.

1. Introduction

PART III (**1**) of this series of papers on symmetrical periodic gravity waves of finite amplitude establishes an *approximate* solution of the problem for a channel of finite depth, but no attempt was made in that paper to examine the results numerically. It is proposed in this paper to give tables and diagrams from which the wave velocity can be derived when the height and the length of the wave are known together with the depth of the channel and the liquid speed at one point.

The theoretical problem has received attention in the past from Korteweg and De Vries (**2**) and from Lamb (**3**), who uses the Rayleigh–Boussinesq method, and has developed what has been called the cnoidal wave (since it involves the Jacobi elliptic function cn); the solution of Part III is also expressed in terms of Jacobian elliptic functions, but not only is the nature of the approximation clearer in this investigation but it provides additional information, in that it is possible to discuss with relative simplicity the limiting or breaking wave. As far as the authors are aware no numerical results have been given for the cnoidal waves and no detailed comparison is therefore possible. It is clear, however, that the present solution bears

† Parts I, II, and III have been published elsewhere.

the same relation to the cnoidal solution as Packham's solution (**4**) of the solitary wave problem bears to the Rayleigh solution (cf. **3**). Comparison with earlier work is possible in the two special cases when the channel is infinite in depth and the wave is infinite in length. Parts I and II have

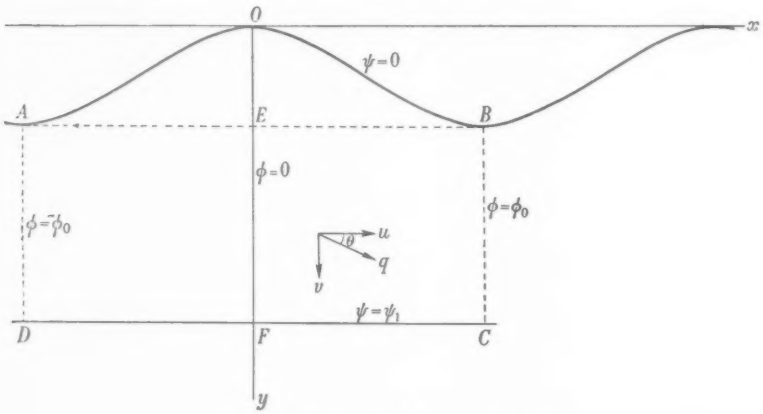

FIG. 1. $AB = \lambda$; $BC = h$; $OE = a$.

dealt adequately with these comparisons; the only results which need be mentioned are that the first approximate solution obtained by the present technique over-estimates the wave velocity and gives also an over-estimate of the critical ratio a/λ for the infinite depth problem and of the critical ratio a/h for the breaking solitary wave (see Fig. 1).

The axis Ox is horizontal, Oy is vertically downwards, and the origin O is always at a crest moving with a velocity c from right to left (see Fig. 1). With respect to these axes the motion is steady.

A velocity potential ϕ and stream function ψ exist, and are defined by

$$d\phi = u^* dx + v^* dy,$$

$$d\psi = -v^* dx + u^* dy, \tag{1.1}$$

where (u^*, v^*) are the velocity components relative to $O(x, y)$.

By symmetry, OF, BC, AD,... are lines of constant ϕ; let $\phi = 0$ on OF, $\phi = \phi_0$ on BC, so that $\phi = -\phi_0$ on AD. Also let the bed CFD and the free surface AOB, which are streamlines, be $\psi = \psi_1$ and $\psi = 0$ respectively. The wavelength AB is λ, the depth of the bed below a trough is $BC = h$, the amplitude $OE = a$, and the velocity of the liquid at F, relative to a fixed frame, is U.

The problem to be investigated can be stated as follows: knowing the values of U, a, h, and λ, to find c.

It is possible to establish two formulae of the form

$$E_0(a,h) = E(u,k), \qquad F_0(a,\lambda) = F(u,k), \tag{1.2}$$

together with one of the form

$$D_0(a,U,c) = D(u,k), \tag{1.3}$$

where u and k are two parameters; thus when U, a, h, and λ are given, u and k can be determined from (1.2) and we may calculate c by (1.3).

2. The complex potential

From (1.1) we have

$$dw = (u^*-iv^*)\,dz. \tag{2.1}$$

If q $(= ce^{\tau})$ is the velocity of a fluid particle relative to $O(x,y)$, and θ is the inclination to the x-axis, then

$$\frac{dw}{dz} = ce^{-\xi}, \qquad \xi = -\tau+i\theta. \tag{2.2}$$

Let the velocity at O be q_0, then Bernoulli's equation on the free surface gives

$$q^2 = q_0^2+2gy, \qquad \psi = 0; \tag{2.3}$$

this may be transformed, following Levi-Civita (**5**), into the form

$$\frac{\partial\theta}{\partial\psi} = -\frac{g}{c^3}e^{-3\tau}\sin\theta, \qquad \psi = 0.$$

In Part III this is replaced by the approximate condition

$$\frac{\partial\theta}{\partial\psi} = -\frac{gl}{c^3}e^{-3\tau}\sin 3\theta, \qquad \psi = 0, \tag{2.4}$$

where l takes a suitable numerical value, or by

$$\operatorname{im}\left\{i\frac{d\xi}{dw}+\frac{gl}{c^3}e^{3\xi}\right\} = 0, \qquad \psi = 0. \tag{2.5}$$

At the crest and on the bed of the channel the velocity is in a horizontal direction; thus we are required in this problem to find an analytic function ξ of w in $0 \leqslant \psi \leqslant \psi_1$ having a real period $2\phi_0$ and satisfying the following conditions:

(i) $\operatorname{im}\xi = 0$ when $\phi = 0$ or $\pm\phi_0$;

(ii) $\operatorname{im}\xi = 0$ when $\psi = \psi_1$;

(iii) $\operatorname{im}\left\{i\dfrac{d\xi}{dw}+\dfrac{gl}{c^3}e^{3\xi}\right\} = 0, \qquad \psi = 0.$

It is shown in Part III that the solution is given by

$$e^{-3\xi} = \frac{1}{c^3}\left(\frac{dw}{dz}\right)^3 = \left(\frac{U+c}{c}\right)^3\left\{1-k^2\,\mathrm{sn}^2\left(\frac{2iK\psi_1}{\phi_0}, k\right)\mathrm{sn}^2\left[\frac{K}{\phi_0}(w-i\psi_1), k\right]\right\}, \quad (2.6)$$

where $\mathrm{sn}(u,k)$ is one of the Jacobian elliptic functions with modulus k, $4K$ is the real period of these functions and, in order to satisfy (2.4), it is necessary that the following relation should hold between the parameters

$$A_0 \equiv \frac{3lg\psi_1}{(U+c)^3} = \frac{2u\,\mathrm{dn}(2u,k')}{\mathrm{sn}(2u,k')\mathrm{cn}(2u,k')} \equiv A(u,k), \quad (2.7)$$

where $u = K\psi_1/\phi_0$. In (2.7) the modulus k' is related to k by

$$k^2+k'^2 = 1 \quad (2.8)$$

and $2iK'$ is the so-called imaginary period for the Jacobian elliptic function $\mathrm{sn}(u,k)$. Furthermore, the wave exists in the range $0 \leqslant u \leqslant \frac{1}{3}K'$. When u is small the wave amplitude to wavelength ratio is small, and when $u = \frac{1}{3}K'$ the wave is on the point of breaking at the crest, possessing at this point an angle of 120 degrees.

3. Formulae obtained by integration of dw/dz

We may rewrite (2.6) in the form

$$(U+c)\frac{dz}{dw} = \left\{1-k^2\,\mathrm{sn}^2\left(\frac{2iK\psi_1}{\phi_0}\right)\mathrm{sn}^2\frac{K}{\phi_0}(w-i\psi_1)\right\}^{-\frac{1}{3}}, \quad (3.1)$$

each elliptic function having modulus k. If we integrate this along OF in Fig. 1 we obtain

$$(U+c)(a+h) = \int_0^{\psi_1}\left\{1-k^2\,\mathrm{sn}^2(2iu,k)\mathrm{sn}^2\left[\frac{iK}{\phi_0}(\psi-\psi_1), k\right]\right\}^{-\frac{1}{3}} d\psi,$$

where, as earlier, $u = K\psi_1/\phi_0$. By a change of variable, and by applying Jacobi's imaginary transformation, this relation can be written in the form

$$B_0 \equiv \frac{(U+c)(a+h)}{\psi_1}$$

$$= \frac{\mathrm{cn}^{\frac{2}{3}}(2u,k')}{u}\int_0^u\left\{1-\mathrm{sn}^2(2u,k')\frac{\mathrm{dn}^2(\xi,k')}{\mathrm{cn}^2(\xi,k')}\right\}^{-\frac{1}{3}} d\xi \equiv B(u,k). \quad (3.2)$$

Another formula can be obtained by integrating dz/dw along the bed FC in Fig. 1 and we obtain

$$\tfrac{1}{2}\lambda(U+c) = \int_0^{\phi_0}\{1-k^2\,\mathrm{sn}^2(2iu,k)\mathrm{sn}^2(K\phi/\phi_0,k)\}^{-\frac{1}{3}}\,d\phi.$$

By a change of variable and by applying again Jacobi's imaginary transformation this relation can be written in the form

$$C_0 \equiv \frac{(U+c)\lambda}{2\psi_1} = \frac{\mathrm{cn}^2(2u,k')}{u}\int_0^K \{1-\mathrm{sn}^2(2u,k')\mathrm{dn}^2(\xi,k)\}^{-\frac{1}{2}}\,d\xi \equiv C(u,k). \tag{3.3}$$

A fourth independent result follows from an integration along the free surface in which an integral expression may be obtained for the amplitude a of the wave. It is more convenient, however, to derive this result approximately, as in (1), by using Bernoulli's equation on the free surface (2.3). From (2.6) we obtain along the free surface

$$\frac{dw}{dz} = (U+c)\left\{1-k^2\,\mathrm{sn}^2(2iu,k)\mathrm{sn}^2\left[\frac{K}{\phi_0}(\phi-i\psi_1),k\right]\right\}^{\frac{1}{2}},$$

and thus at O, the crest, and B, the trough, we have

$$q_0 = (U+c)\{1-k^2\,\mathrm{sn}^2(2iu,k)\mathrm{sn}^2(iu,k)\}^{\frac{1}{2}},$$
$$q_B = (U+c)\{1-k^2\,\mathrm{sn}^2(2iu,k)\mathrm{sn}^2(K-iu,k)\}^{\frac{1}{2}}.$$

By applying the addition formula and the Jacobi imaginary transformation the above velocities may be written

$$q_0 = (U+c)\left\{1-k^2\frac{\mathrm{sn}^2(2u,k')\mathrm{sn}^2(u,k')}{\mathrm{cn}^2(2u,k')\mathrm{cn}^2(u,k')}\right\}^{\frac{1}{2}},$$

$$q_B = (U+c)\left\{1+\frac{k^2\,\mathrm{sn}^2(2u,k')}{\mathrm{cn}^2(2u,k')\mathrm{dn}^2(u,k')}\right\}^{\frac{1}{2}}.$$

If we specialize (2.3) to the point B we obtain

$$D_0 \equiv \frac{2ga}{(U+c)^2} = \left\{1+\frac{k^2\,\mathrm{sn}^2(2u,k')}{\mathrm{cn}^2(2u,k')\mathrm{dn}^2(u,k')}\right\}^{\frac{2}{3}} - \left\{1-k^2\frac{\mathrm{sn}^2(2u,k')\mathrm{sn}^2(u,k')}{\mathrm{cn}^2(2u,k')\mathrm{cn}^2(u,k')}\right\}^{\frac{2}{3}} \equiv D(u,k). \tag{3.4}$$

The four functions A, B, C, and D in (2.7), (3.2), (3.3), and (3.4) have been calculated for values of r and θ, where

$$u = \frac{rK'}{180}, \qquad k = \cos\theta,$$

$$0 \leqslant r(10) \leqslant 60, \qquad 0^\circ \leqslant \theta(15^\circ) \leqslant 90^\circ,$$

and the results are tabulated in the next section. It may be mentioned that the case $r = 60$, or $u = \frac{1}{3}K'$, is that of the limiting wave which is on the point of breaking at the crest. The limiting or breaking wave is of sufficient interest to warrant an analytical investigation and the present section will be concluded with a description of the breaking wave whose wavelength is

long compared with the depth of the liquid. In the case of infinite wavelength the value of the ratio $h:a$ for the limiting wave has been given by Packham to be 1·21 (**4**) and by McCowan to be 1·28 (**6**), and it is proposed here to derive the generalization of this property for large λ, which corresponds here to values of k which are near unity or to values of k' which are near zero. Accordingly it is necessary to obtain the expressions for A, B, C, D for small values of k'.

When $u = \frac{1}{3}K'$ and k' is small, the following results are obtained from (2.7), (3.2), (3.3), and (3.4)

$$\frac{3lg\psi_1}{(U+c)^3} = \frac{2K'\,\mathrm{dn}(\frac{2}{3}K', k')}{3\,\mathrm{sn}(\frac{2}{3}K', k')\mathrm{cn}(\frac{2}{3}K', k')} = \frac{4\pi}{3\sqrt{3}}\{1+O(k'^4)\}; \tag{3.5}$$

$$\frac{(U+c)(a+h)}{\psi_1} = \frac{3\,\mathrm{cn}^{\frac{2}{3}}(\frac{2}{3}K', k')}{K'}\int_0^{K'}\left\{1-\mathrm{sn}^2(\tfrac{2}{3}K', k')\frac{\mathrm{dn}^2(\xi, k')}{\mathrm{cn}^2(\xi, k')}\right\}^{-\frac{1}{3}} d\xi$$

$$= \frac{3.2^{\frac{1}{3}}}{\pi} I_0 + O(k'^4), \tag{3.6}$$

where

$$I_0 = \int_0^{\frac{1}{2}\pi} (1-\tfrac{3}{4}\sec^2 x)^{-\frac{1}{3}}\, dx; \tag{3.7}$$

$$\frac{(U+c)\lambda}{2\psi_1} = \frac{3\,\mathrm{cn}^{\frac{2}{3}}(\frac{2}{3}K', k')}{K'}\int_0^{K}\{1-\mathrm{sn}^2(\tfrac{2}{3}K', k')\mathrm{dn}^2(\xi, k)\}^{-\frac{1}{3}}\, d\xi$$

$$= -\frac{3.2^{\frac{1}{3}}}{\pi}\log\left(\frac{k'}{4}\right) + 1{\cdot}7306; \tag{3.8}$$

$$\frac{2ga}{(U+c)^2} = \left\{1+\frac{k^2\,\mathrm{sn}^2(\frac{2}{3}K', k')}{\mathrm{cn}^2(\frac{2}{3}K', k')\mathrm{dn}^2(\frac{2}{3}K', k')}\right\}^{\frac{2}{3}}$$

$$= 4^{\frac{2}{3}}\{1+\tfrac{1}{8}k'^2+O(k'^4)\}. \tag{3.9}$$

In deriving (3.8) considerable use has been made of some integrals given by Greenhill (**7**). Choosing $l = \frac{1}{3}$ in (3.5), as in Part I (**8**) of this series, it follows from (3.5), (3.6), and (3.9) that

$$\frac{a+h}{2a} = \frac{2I_0}{\sqrt{3}\{1+\frac{1}{8}k'^2+O(k'^4)\}}. \tag{3.10}$$

Similarly from (3.6) and (3.8) it follows that

$$\frac{2(a+h)}{\lambda} = \{-\log\tfrac{1}{4}k' + 1{\cdot}438\}^{-1}, \tag{3.11}$$

and thus by eliminating k' it follows that the lengths a, h, and λ are related, in a breaking wave, by the formula

$$1+\frac{h}{a} = \frac{4I_0}{\sqrt{3}\{1+35{\cdot}48\exp[-I_0\lambda/(a+h)]\}}. \tag{3.12}$$

Using numerical integration we find that $I_0 = 1{\cdot}066$ and thus

$$1+\frac{h}{a} = \frac{2{\cdot}46}{1+35{\cdot}48\exp[-1{\cdot}066\lambda/(a+h)]}. \tag{3.13}$$

As $\lambda \to \infty$ this gives $h/a = 1{\cdot}46$ which must be compared with the values 1·21 and 1·28 due to Packham (**4**) and McCowan (**6**) respectively. The difference in the value of this ratio will be discussed shortly, but it is important here to emphasize that the effect of a finite wavelength is to decrease the critical value of the ratio h/a. Since $h/a \geqslant 0$ it is necessary that $\lambda/(a+h) \geqslant 2{\cdot}99$ for the above formula to apply.

In Packham's derivation of the critical ratio $h/a = 1{\cdot}21$, the method of procedure is slightly different from that given above. Formulae (3.5) and (3.9) are used by Packham but, in place of the formula (3.6) a more exact formula is used which is derived from the condition that there is no absolute motion at infinity; this implies that $\psi_1 = ch$ and U satisfies

$$(U+c)^3 = c^3\cos^2\tfrac{1}{6}\pi.$$

Using these two results together with

$$\frac{g\psi_1}{(U+c)^3} = \frac{4\pi}{3\sqrt{3}}, \qquad \frac{2ga}{(U+c)^2} = 4^{\frac{1}{3}}$$

it follows that $h/a = 1{\cdot}21$. Similarly, in the present problem, we could postulate that the absolute velocity at a point on the horizontal bed beneath a trough is zero, but there would be no justification for such a procedure.

4. The determination of the velocity of propagation of the waves, given the physical dimensions

We have already introduced the four functions

$$\left.\begin{aligned} A_0 &\equiv \frac{3lg\psi_1}{(U+c)^3} = A(u,k) \\ B_0 &\equiv \frac{(U+c)(a+h)}{\psi_1} = B(u,k) \\ C_0 &\equiv \frac{(U+c)\lambda}{2\psi_1} = C(u,k) \\ D_0 &\equiv \frac{2ga}{(U+c)^2} = D(u,k) \end{aligned}\right\} \tag{4.1}$$

and we define two new functions E and F as follows:

$$\left.\begin{aligned} E(u,k) &= \frac{AB}{D} = \frac{3l(a+h)}{a} \equiv E_0 \\ F(u,k) &= \frac{AC}{D} = \frac{3l\lambda}{4a} \equiv F_0 \end{aligned}\right\}. \tag{4.2}$$

Knowing u and k, A and D are easily evaluated numerically using tables of elliptic functions, etc. The integral that occurs in B can be found by Simpson's rule in all cases except $r = 60$ or $u = \frac{1}{3}K'$, which is the breaking case. In this latter case the integrand is infinite at $\xi = u$ and the integral, which is convergent, has been found by expanding the integrand in ascending powers of $(\xi - u)$ over some suitable range $u - \epsilon$ to u and using Simpson's rule over the remainder of the range. It is most suitable in the integral of C to expand the integrand. For $k \geqslant \frac{1}{2}$ it can be expanded as a power series in $\mathrm{dn}^2(\xi, k)$, each term being integrable by a reduction formula. For $k < \frac{1}{2}$ the integrand can be expanded as a fairly rapidly converging power series in k^2.

Having found A, B, C, D for appropriate ranges of values of u and k, E and F can be found. The values of E and F for given values of u and k have been tabulated and graphs of $E =$ constant and $F =$ constant have been drawn in the (r, θ)-plane.

In a particular problem, if we know the physical quantities a, h, λ, the values of E and F, say E_0 and F_0 respectively, can be found from (4.2). The graphs of $E = E_0$ and $F = F_0$ are then superposed on the same (r, θ)-plane and their point of intersection, if any, determines the values of the parameters r and θ, or alternatively u and k for the problem. The value of D, that is $(U + c)$, may then be read from the tables.

TABLE 1

Values of the function A

r \ θ	0°	15°	30°	45°	60°	75°	90°
0	1·0000	1·0000	1·0000	1·0000	1·0000	1·0000	..
10	1·0206	1·0472	1·0207	1·0215	1·0241	1·0337	..
20	1·0861	1·0861	1·0867	1·0895	1·0994	1·1352	..
30	1·2092	1·2092	1·2104	1·2160	1·2361	1·3083	..
40	1·4178	1·4179	1·4196	1·4281	1·4586	1·5679	..
50	1·7723	1·7724	1·7745	1·7851	1·8232	1·9599	..
60	2·4184	2·4185	2·4207	2·4320	3·4722	2·6166	..

TABLE 2

Values of the function B

r \ θ	0°	15°	30°	45°	60°	75°	90°
0	1·0000	1·0000	1·0000	1·0000	1·0000	1·0000	1·0000
10	1·0002	1·0002	1·0002	1·0001	1·0001	1·0000	1·0000
20	1·0006	1·0006	1·0005	1·0005	1·0004	1·0000	1·0000
30	1·0026	1·0026	1·0025	1·0025	1·0024	1·0018	1·0000
40	1·0106	1·0106	1·0105	1·0102	1·0097	1·0082	1·0000
50	1·0374	1·0373	1·0372	1·0371	1·0358	1·0322	1·0000
60	1·2599	1·2587	1·2582	1·2579	1·2560	1·1629	1·0000

TABLE 3

Values of the function C

r \ θ	0°	15°	30°	45°	60°	75°	90°
0	..	..	..	..	..	..	..
10	∞	31·1969	22·9397	17·9303	14·0382	10·3807	..
20	∞	15·2900	11·3331	8·8559	6·9619	5·1708	..
30	∞	9·8367	7·3898	5·7725	4·5708	3·4235	..
40	∞	6·9446	5·3452	4·1740	3·3386	2·5276	..
50	∞	4·8551	4·0187	3·1527	2·5562	1·9648	..
60	∞	3·8429	3·0696	2·3966	1·9758	1·5509	..

TABLE 4

Values of the function D

r \ θ	0°	15°	30°	45°	60°	75°	90°
0	0·0000	0·0000	0·0000	0·0000	0·0000	0·0000	0·0000
10	0·0208	0·0201	0·0181	0·0147	0·0100	0·0046	0·0000
20	0·0892	0·0864	0·0782	0·0648	0·0528	0·0229	0·0000
30	0·2275	0·2264	0·2036	0·1731	0·1301	0·0734	0·0000
40	0·4899	0·4796	0·4483	0·3951	0·3175	0·2082	0·0000
50	1·0207	1·0054	0·9581	0·8772	0·7574	0·5807	0·0000
60	2·5198	2·4983	2·4332	2·3238	2·1674	1·9543	0·0000

TABLE 5

Values of E and $\log_{10} E$

r \ θ	0°	15°	30°	45°	60°	75°	90°
10	49·0771	52·1099	56·4035	69·4967	102·4202	224·7174	..
	1·6909	1·7169	1·7413	1·8420	2·0103	2·3516	..
20	12·1833	12·5781	13·9034	16·8217	20·8303	49·5721	..
	1·0869	1·0996	1·1421	1·2261	1·3187	1·6953	..
30	5·3279	5·3549	5·9657	7·0424	9·5239	17·8563	..
	0·7265	0·7287	0·7757	0·8477	0·9788	1·2518	..
40	2·9247	2·9878	3·1999	3·6514	4·6386	7·5925	..
	0·4661	0·4754	0·5051	0·5625	0·6664	0·8804	..
50	1·8013	1·8286	1·9210	2·1105	2·4294	3·4837	..
	0·2556	0·2621	0·2835	0·3244	0·3855	0·5420	..
60	1·2092	1·2185	1·2517	1·3165	1·4326	1·5570	..
	0·0824	0·0858	0·0975	0·1194	0·1561	0·1923	..

TABLE 6

Values of F and $\log_{10} F$

r \ θ	0°	15°	30°	45°	60°	75°	90°
10	..	1625·34	1293·62	1245·97	1437·65	2332·72	..
	..	3·2109	3·1119	3·0955	3·1576	3·3679	..
20	..	192·20	157·49	148·90	144·96	256·33	..
	..	2·2838	2·1973	2·1730	2·1612	2·4088	..
30	..	52·5377	43·9755	40·5509	42·7252	61·0213	..
	..	1·7205	1·6432	1·6080	1·6307	1·9855	..
40	..	20·5312	16·9263	15·0870	15·3376	19·0347	..
	..	1·3124	1·2285	1·1785	1·1857	1·2795	..
50	..	8·5590	7·4430	6·4157	6·1941	6·6313	..
	..	0·9324	0·8717	0·8073	0·7920	0·8216	..
60	..	3·7202	3·0538	2·5072	2·2537	2·0765	..
	..	0·5706	0·4848	0·3992	0·3529	0·3173	..

Applications and examples illustrating the use of the tables

In a particular case it may be found that the appropriate E and F curves do not meet: in this case the progressive wave of that description does not exist. Take, for example,

$$\frac{h}{a} = 0{\cdot}2, \qquad \frac{\lambda}{a} = 12{\cdot}6;$$

we then have $E_0 = 1{\cdot}2$, $F_0 = 3{\cdot}16$ (in numerical examples the value of l is taken to be $\frac{1}{3}$) and thus

$$\log_{10} E_0 = \tfrac{1}{12}, \qquad \log_{10} F_0 = \tfrac{1}{2}.$$

It will be found that these two curves do not meet and so there is no progressive wave with these dimensions.

It should be noted that the range of values of E and F give minimum values of h/a and λ/a. The minimum value of E is approximately 1·2 and so $h \geqslant \frac{1}{5}a$; hence using (3.13)

$$0{\cdot}68h \leqslant a \leqslant 5h.$$

Similarly, from the tables, the minimum value of F is greater than 2, hence $\lambda > 8a$. This result must be compared with the corresponding one in Part I (**8**), namely $a/\lambda = 0{\cdot}126$.

Consider now the case

$$\lambda/a = 40, \qquad h/a = 3{\cdot}6,$$

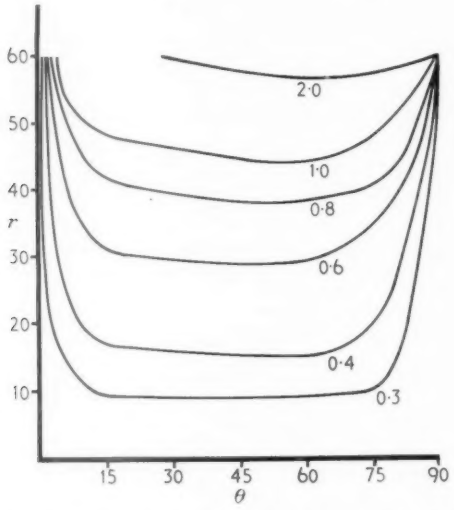

FIG. 2. Graphs of curves $1/\log_{10} F = J$ for $J = 0{\cdot}3,\ 0{\cdot}4,\ 0{\cdot}6,\ 0{\cdot}8,\ 1{\cdot}0,\ 2{\cdot}0$.

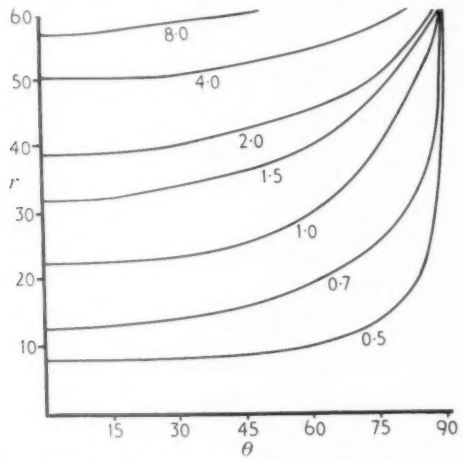

FIG. 3. Graphs of curves $1/\log_{10} E = J$ for $J = 0{\cdot}5,\ 0{\cdot}7,\ 1{\cdot}0,\ 1{\cdot}5,\ 2{\cdot}0,\ 4{\cdot}0,\ 8{\cdot}0$.

then $E_0 = 4{\cdot}6$, $F_0 = 10$ and thus

$$\frac{1}{\log_{10} E_0} = 1{\cdot}5, \qquad \frac{1}{\log_{10} F_0} = 1.$$

These curves meet at the point given by $\theta = 75°$, $r = 48$. Then, either by interpolation between the tabulated values, or by direct calculation,

we find that $D = 0{\cdot}525$. Hence the velocity of propagation is given by the formula

$$\frac{2ga}{(U+c)^2} = 0{\cdot}525.$$

The velocity of propagation may be determined only when a and U are given. If the wave amplitude is 1 inch, so that $a = \frac{1}{12}$, we have

$$U+c = 3{\cdot}2 \text{ feet per second.}$$

The fact that c is indeterminate as long as U is unknown in this finite depth problem was pointed out originally by Stokes, and it is clear that this difficulty will remain as long as the liquid is assumed to be non-viscous.

REFERENCES

1. T. V. Davies, *Quart. of Appl. Math.* **10** (1952), 57 (Part III).
2. D. J. Korteweg and G. De Vries, *Phil. Mag.* (5) **39** (1895), 422.
3. H. Lamb, *Hydrodynamics*, 3rd edition (1906), 399–403.
4. B. A. Packham, *Proc. Roy. Soc.* A, **213** (1952), 238 (Part II).
5. T. Levi-Civita, *Math. Ann.* **93** (1925), 264.
6. J. McCowan, *Phil. Mag.* (5) **32** (1891), 45.
7. A. G. Greenhill, *The Applications of Elliptic Functions* (1892), 245–51.
8. T. V. Davies, *Proc. Roy. Soc.* A, **208** (1951), 475 (Part I).

FLOW WITH VARIABLE SHEAR PAST CIRCULAR CYLINDERS

By J. D. MURRAY (*King's College, University of Durham*) *and*
A. R. MITCHELL (*United College, University of St. Andrews*)

[Received 15 March 1956]

SUMMARY

Stream functions are obtained for two variable shear flows past a circular cylinder. The shear distributions in the free stream are of the 'linear' and 'boundary layer' type respectively. In both flows, the stagnation streamline is displaced in the free stream towards a region of higher velocity. This is in agreement with the results obtained by the present authors (**1**) in the case of constant shear flow past a cylinder and with the experimental results of Young and Maas (**2**) for a pitot tube of circular cross-section in a low-speed shear flow. The displacements in both variable shear flows are comparable in magnitude to the values obtained in the constant shear case but are considerably smaller than the experimental values of Young and Maas.

List of notation

J	Bessel function of the first kind
I	modified Bessel function of the first kind
Y	Bessel function of the second kind
K	modified Bessel function of the second kind
l	typical linear dimension
L	perimeter of cylinder
N	rotational flow parameter ($= U/\omega_0 l$)
x, y	cartesian coordinates
q_x, q_y	velocity components in the x- and y-directions
r, θ	polar coordinates
q_r, q_θ	radial and transverse velocity components
q	velocity
U	standard velocity
y_s	deflexion of the stagnation streamline in the free stream
Γ	circulation
δ	thickness of the incompressible boundary layer
ψ	stream function
Ψ	disturbance stream function
ω	vorticity

1. Introduction

THE stream function ψ for the steady rotational two-dimensional flow of an incompressible inviscid fluid satisfies the equation

$$\frac{\partial^2\psi}{\partial x^2}+\frac{\partial^2\psi}{\partial y^2}+\omega = 0, \tag{1}$$

where the vorticity ω, given by

$$\omega = \frac{\partial q_y}{\partial x}-\frac{\partial q_x}{\partial y}, \tag{2}$$

satisfies the equation

$$q_x\frac{\partial\omega}{\partial x}+q_y\frac{\partial\omega}{\partial y} = 0, \tag{3}$$

and

$$q_x = \frac{\partial\psi}{\partial y}, \qquad q_y = -\frac{\partial\psi}{\partial x}$$

are the velocity components parallel to the x- and y-axes respectively.

As far as the present authors are aware, no exact solutions of (1) and (3) exist except in the case of constant rotation, although several investigations using approximate methods have been carried out. In the present paper, the stream functions for some variable shear flows past a circular cylinder are obtained, and certain aspects of these flows compared with experimental results.

2. The 'linear' shear distribution

The general solution of (3) is

$$\omega = f(\psi),$$

and so the vorticity is constant along a streamline. In the particular case

$$f(\psi) = -\frac{\psi}{r_0^2},$$

where r_0 is an arbitrary length, (1) becomes

$$\frac{\partial^2\psi}{\partial x^2}+\frac{\partial^2\psi}{\partial y^2} = \frac{\psi}{r_0^2}. \tag{4}$$

A vorticity distribution in the free stream near $x = -\infty$, consistent with (4), is

$$\omega = -\left[\frac{a}{r_0^2}e^{y/r_0}+\frac{b}{r_0^2}e^{-y/r_0}\right], \tag{5}$$

which on integration gives the velocity distribution

$$q_x = \frac{a}{r_0}e^{y/r_0}-\frac{b}{r_0}e^{-y/r_0}, \tag{6}$$

where the constants a and b are arbitrary. If a standard rotation ω_0 and

a standard velocity U are introduced as the values of ω and q_x where $y = 0$, it follows from (5) and (6) that

$$a = \tfrac{1}{2}r_0(U-\omega_0 r_0), \qquad b = -\tfrac{1}{2}r_0(U+\omega_0 r_0).$$

If these values are substituted in (5) and (6), the vorticity and velocity distributions in the free stream near $x = -\infty$ become

$$\frac{\omega}{\omega_0} = \cosh\frac{y}{r_0} - N\sinh\frac{y}{r_0}, \tag{7}$$

and

$$\frac{q_x}{U} = \cosh\frac{y}{r_0} - \frac{1}{N}\sinh\frac{y}{r_0}, \tag{8}$$

respectively, where $N = U/(\omega_0 r_0)$. In order to keep the velocity positive everywhere the parameter N must satisfy the inequality $N > 1$. The above distributions are now expanded in powers of y/r_0. If higher powers of y/r_0 are neglected, the expansions become

$$\frac{\omega}{\omega_0} = 1 - N\left(\frac{y}{r_0}\right), \tag{9}$$

and

$$\frac{q_x}{U} = 1 - \frac{1}{N}\left(\frac{y}{r_0}\right) + \frac{1}{2}\left(\frac{y}{r_0}\right)^2, \tag{10}$$

respectively, and so the free stream shear distribution (7) is approximately linear in the vicinity of the x-axis. In Fig. 1 the similarity of the velocity profiles given by (8) and (10) in the vicinity of the x-axis is shown for the case $N = 2$.

A circular cylinder of radius r_0 is now introduced at the origin and it is required to find a stream function which satisfies (4) and takes a constant value on the cylinder. For convenience, introduce the function Ψ where

$$\psi = ae^{y/r_0} + be^{-y/r_0} + \Psi, \tag{11}$$

and from (4), Ψ, which tends to zero as x tends to $-\infty$, satisfies the equation

$$\frac{\partial^2\Psi}{\partial x^2} + \frac{\partial^2\Psi}{\partial y^2} = \frac{\Psi}{r_0^2}. \tag{12}$$

Using polar coordinates r, θ, and the method of separation of variables, (12) is solved to give

$$\Psi = B_0\theta K_0(r') + \sum_{m=0}^{\infty}(A_m\cos m\theta + B_m\sin m\theta)K_m(r'), \tag{13}$$

where A_m, B_m are constants, K_m is the modified Bessel function of the second kind of order m, and $r' = r/r_0$. Thus from (11) the required stream function ψ is given by

$$\psi = ae^{y/r_0} + be^{-y/r_0} + B_0\theta K_0(r') + \sum_{m=0}^{\infty}(A_m\cos m\theta + B_m\sin m\theta)K_m(r'),$$

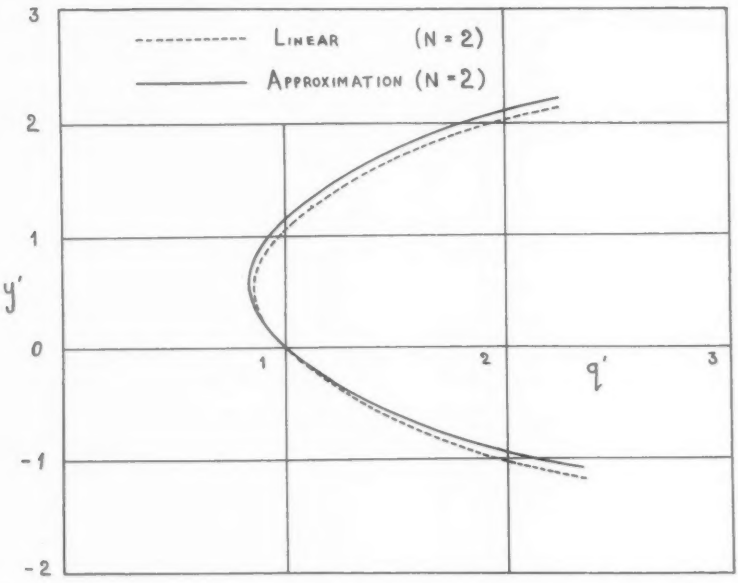

FIG. 1

where $y' = y/r_0$. Now ψ must take a constant value, say c, on the circular cylinder $r = r_0$, and so

$$c = ae^{\sin\theta} + be^{-\sin\theta} + B_0\theta K_0(1) + \sum_{m=0}^{\infty} (A_m \cos m\theta + B_m \sin m\theta) K_m(1). \quad (14)$$

The Fourier expansion of $e^{\pm\sin\theta}$ is

$$e^{\pm\sin\theta} = I_0(1) + 2\sum_{m=1}^{\infty} (-1)^m I_{2m}(1)\cos 2m\theta \pm 2\sum_{m=0}^{\infty} (-1)^m I_{2m+1}(1)\sin(2m+1)\theta.$$

The above values are substituted into (14) and the coefficients of corresponding sine and cosine terms equated. With the values of a and b found previously, the stream function becomes

$$\frac{\psi}{Ur_0} = \sinh y' - \frac{1}{N}\cosh y' + \left[\frac{c}{Ur_0} + \frac{1}{N} I_0(1)\right] \frac{K_0(r')}{K_0(1)} +$$

$$+ \frac{2}{N} \sum_{m=1}^{\infty} (-1)^m \frac{I_{2m}(1)}{K_{2m}(1)} K_{2m}(r')\cos 2m\theta +$$

$$+ 2 \sum_{m=0}^{\infty} (-1)^{m+1} \frac{I_{2m+1}(1)}{K_{2m+1}(1)} K_{2m+1}(r')\sin(2m+1)\theta. \quad (15)$$

The velocity components in polar coordinates are

$$q_r = \frac{1}{r}\frac{\partial \psi}{\partial \theta} \quad \text{and} \quad q_\theta = -\frac{\partial \psi}{\partial r}.$$

Round the circumference L of the circular cylinder, $q_r = 0$, and the circulation Γ in an anticlockwise direction is given by

$$\Gamma = \oint_L q_\theta r_0 \, d\theta = \Gamma_0 + \Gamma_1,$$

where Γ_0 and Γ_1 are the circulations arising from the undisturbed flow and the disturbance flow respectively. Using (15),

$$\frac{\Gamma_0}{2\pi U r_0} = \frac{1}{N} I_1(1),$$

and

$$\frac{\Gamma_1}{2\pi U r_0} = -\frac{K_0'(1)}{K_0(1)}\left[\frac{1}{N} I_0(1) + \frac{c}{U r_0}\right],$$

where $K_0'(1) = [dK_0(r')/dr']_{r'=1}$. Now in the case of constant shear flow past a circular cylinder, Tsien (**3**) (see also Richardson (**4**)) uses the hypothesis that the introduction of a cylinder into an inviscid incompressible rotational flow does not alter the circulation round the path L, which coincides with the perimeter of the cylinder. In the present problem this leads to the result $\Gamma_1 = 0$ and so

$$c = -\omega_0 r_0^2 I_0(1).$$

If this value is substituted into (15), the stream function becomes

$$\frac{\psi}{U r_0} = \sinh y' - \frac{1}{N}\cosh y' + \frac{2}{N}\sum_{m=1}^{\infty} (-1)^m \frac{I_{2m}(1)}{K_{2m}(1)} K_{2m}(r') \cos 2m\theta +$$

$$+ 2\sum_{m=0}^{\infty} (-1)^{m+1} \frac{I_{2m+1}(1)}{K_{2m+1}(1)} K_{2m+1}(r') \sin(2m+1)\theta, \quad (16)$$

resulting in a velocity on the cylinder of

$$(q_\theta')_{r'=1} = -\left[\sin\theta\left\{\cosh(\sin\theta) - \frac{1}{N}\sinh(\sin\theta)\right\} + \right.$$

$$+ \frac{2}{N}\sum_{m=1}^{\infty} (-1)^m \frac{I_{2m}(1)}{K_{2m}(1)} K_{2m}'(1) \cos 2m\theta +$$

$$\left. + 2\sum_{m=0}^{\infty} (-1)^{m+1} \frac{I_{2m+1}(1)}{K_{2m+1}(1)} K_{2m+1}'(1) \sin(2m+1)\theta\right], \quad (17)$$

where

$$K_{2m}'(1) = \left[\frac{dK_{2m}(r')}{dr'}\right]_{r'=1}, \qquad K_{2m+1}'(1) = \left[\frac{dK_{2m+1}(r')}{dr'}\right]_{r'=1}$$

and $q_\theta' = q_\theta / U$. The stagnation points on the cylinder are given by

$(q'_\theta)_{r'=1} = 0$, and the stagnation streamline, given by $\psi/Ur_0 = -I_0(1)/N$, starts in the free stream near $x = -\infty$ at the position y'_s given by

$$y'_s = \log_e \frac{[I_0^2(1)+(N^2-1)]^{\frac{1}{2}} - I_0(1)}{N-1} \qquad (N > 1). \tag{18}$$

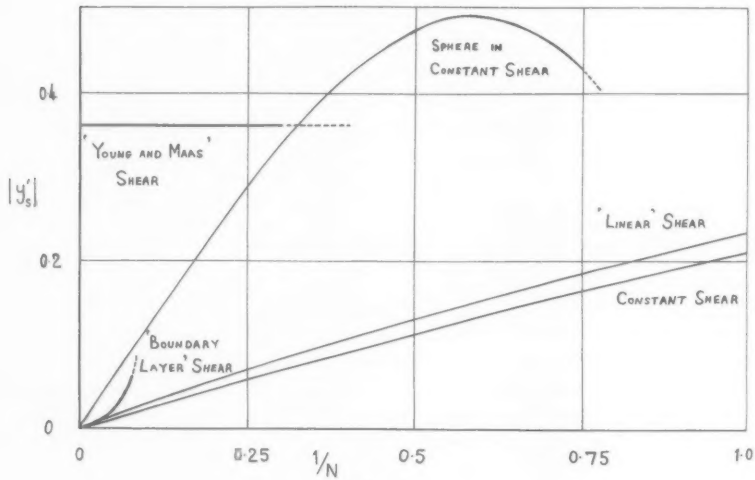

FIG. 2

The deflexion of the stagnation streamline is shown in Fig. 2. It should be noted that the convergence of the series in (16) and (17) is extremely rapid and the series may be terminated at $m = 4$ for all practical purposes.

3. The 'boundary layer' shear distribution

Another particular solution of (3) is

$$\omega = \frac{\psi}{l^2},$$

where l is an arbitrary length. On substitution into (1) this leads to the equation

$$\frac{\partial^2\psi}{\partial x^2} + \frac{\partial^2\psi}{\partial y^2} = -\frac{\psi}{l^2}. \tag{19}$$

Vorticity and velocity distributions in the free stream near $x = -\infty$ consistent with (19) are

$$\omega = \frac{a}{l^2}\cos\left(\frac{y}{l}\right) + \frac{b}{l^2}\sin\left(\frac{y}{l}\right), \tag{20}$$

and

$$q_x = \frac{b}{l}\cos\left(\frac{y}{l}\right) - \frac{a}{l}\sin\left(\frac{y}{l}\right), \tag{21}$$

respectively, where a and b are arbitrary constants. If a standard rotation ω_0 and a standard velocity U are introduced as the values of $-\omega$ and q_x, where $y = 0$ and $y = \delta - y_0$ respectively, it follows from (20) and (21) that

$$a = -\omega_0 l^2, \qquad b = \frac{N' - \sin\{(\delta - y_0)/l\}}{\cos\{(\delta - y_0)/l\}} \omega_0 l^2,$$

where $N' = U/(\omega_0 l)$, and y_0 is a variable parameter lying in the range $0 \leqslant y_0 \leqslant \delta$. If

$$\cos\frac{y_0}{l} = \frac{1}{N'},$$

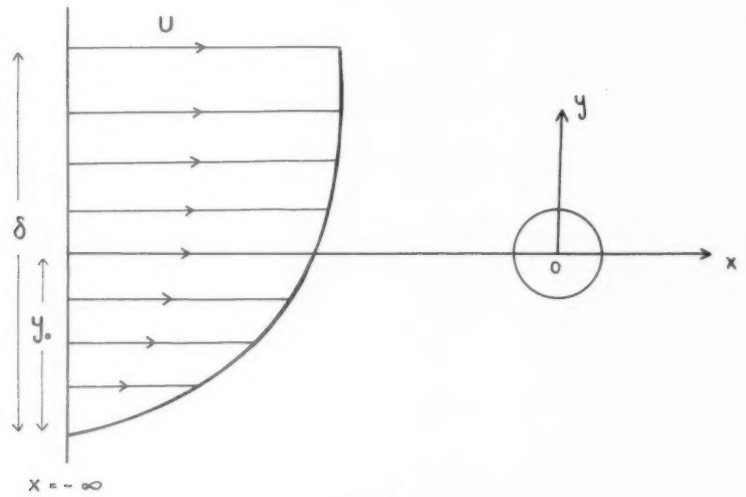

FIG. 3

and the arbitrary length l is chosen to be

$$l = \frac{2}{\pi}\delta,$$

the vorticity and velocity distributions in the free stream near $x = -\infty$ become

$$\frac{\omega}{\omega_0} = -N' \cos\left(\frac{\pi(y+y_0)}{2\delta}\right), \tag{22}$$

and

$$\frac{q_x}{U} = \sin\left(\frac{\pi(y+y_0)}{2\delta}\right), \tag{23}$$

respectively. In the range $0 \leqslant y + y_0 \leqslant \delta$, the free stream velocity distribution (23) is Lamb's approximation for the flow in an incompressible boundary layer of thickness δ (**5**).

A circular cylinder of radius r_0 is now introduced at the origin, and the stream function required which satisfies (19) and takes a constant value on the cylinder. Introduce Ψ where

$$\psi = a\cos\frac{y}{l} + b\sin\frac{y}{l} + \Psi, \tag{24}$$

then from (19), Ψ, which tends to zero as x tends to $-\infty$, satisfies the equation

$$\frac{\partial^2\Psi}{\partial x^2} + \frac{\partial^2\Psi}{\partial y^2} = -\frac{\Psi}{l^2}. \tag{25}$$

An appropriate solution of (25) is

$$\Psi = B_0\,\theta Y_0(r') + \sum_{m=0}^{\infty}(A_m\cos m\theta + B_m\sin m\theta)Y_m(r'),$$

where A_m, B_m are constants, Y is the Bessel function of the second kind, and $r' = r/l$. Thus from (24) the required stream function ψ is given by

$$\psi = a\cos y' + b\sin y' + B_0\,\theta Y_0(r') + \sum_{m=0}^{\infty}(A_m\cos m\theta + B_m\sin m\theta)Y_m(r'),$$

and since ψ takes a constant value, say c, on the circular cylinder $r = r_0$, it follows that

$$c = a\cos(k\sin\theta) + b\sin(k\sin\theta) + B_0\,\theta Y_0(1) + \\ + \sum_{m=0}^{\infty}(A_m\cos m\theta + B_m\sin m\theta)Y_m(1), \tag{26}$$

where $k = \pi r_0/2\delta$. The Fourier expansions of $\cos(k\sin\theta)$ and $\sin(k\sin\theta)$ are

$$\cos(k\sin\theta) = J_0(k) + 2\sum_{m=1}^{\infty} J_{2m}(k)\cos 2m\theta$$

and

$$\sin(k\sin\theta) = 2\sum_{m=0}^{\infty} J_{2m+1}(k)\sin(2m+1)\theta,$$

respectively, where J is the Bessel function of the first kind. The above series are substituted into (26) and the coefficients of corresponding sine and cosine terms equated. Following the method of the previous section, and with the present values of a and b, the stream function becomes

$$\frac{\psi}{Ul} = -\cos(y' + y_0') + 2\cos y_0' \sum_{m=1}^{\infty}\frac{J_{2m}(k)}{Y_{2m}(k)}Y_{2m}(r')\cos 2m\theta - \\ - 2\sin y_0' \sum_{m=0}^{\infty}\frac{J_{2m+1}(k)}{Y_{2m+1}(k)}Y_{2m+1}(r')\sin(2m+1)\theta, \tag{27}$$

where $y' = y/l$, $y_0' = y_0/l$, and the constant value taken by ψ on the cylinder is

$$c = -\omega_0 l^2 J_0(k). \tag{28}$$

The stagnation points on the cylinder are again given by $(\partial\psi'/\partial r')_{r'=k} = 0$ with $\psi' = \psi/Ul$, and the stagnation streamline starts in the free stream near $x = -\infty$ at the position y_s given by

$$y_s' = \cos^{-1}\left[\frac{J_0(k)}{N'}\right] - \cos^{-1}\left[\frac{1}{N'}\right], \tag{29}$$

where $y_s' = y_s/l$.

The field of flow represented by the stream function (27) is a good approximation to the flow past a circular cylinder situated in a two-dimensional boundary layer provided r_0/δ is small and y_0/δ has a value not too near the end values of its allowable range $0 \leqslant y_0/\delta \leqslant 1$. The problem is illustrated in Fig. 3. The deflexion of the stagnation streamline is shown in Fig. 2 for $r_0/\delta = \frac{1}{20}$ $(k = \pi/40)$ over the range $\frac{1}{5} \leqslant y_0/\delta \leqslant \frac{4}{5}$, where $N\ (\equiv U/\omega_0 r_0)$ is equal to $(40/\pi)\,N'$.

4. Comparison with experimental results

In measuring the profile drag of a wing-section by the pitot traverse method, there is a considerable velocity gradient across the wake traversed by the pitot and so it cannot be assumed that the pressure registered by the tube is the total pressure of the stream opposite the geometric centre of the face of the pitot. Accordingly, Young and Maas (**2**) carried out tests which showed that when a pitot tube of circular cross-section is placed at zero incidence in a low speed flow with a constant total pressure gradient, the stagnation streamline comes from a region where the velocity is higher than the velocity upstream on the pitot axis. If d is the upstream displacement of the stagnation streamline and r_0 is the outside radius of the pitot tube, Young and Maas found that d/r_0 is approximately constant for a variety of conditions and equal to 0·36. In terms of N defined by

$$N = U/\omega_0 r_0,$$

the range covered by the experiments was $0 < 1/N < 0{\cdot}3$, where U and ω_0 are the values of the velocity and rotation at the geometric centre of the face of the pitot tube.

This displacement of the stagnation streamline when a pitot is placed in a flow across which there is a constant total pressure gradient is shown in Fig. 2, together with the magnitudes of the displacements previously obtained from theoretical considerations of inviscid incompressible shear flows past a circular cylinder. The types of free stream shear distribution considered are constant, 'linear', and 'boundary layer' respectively. In the constant shear case (**1**), with the usual notation, the displacement of the stagnation streamline is given by

$$y_s' = N - (N^2+1)^{\frac{1}{2}}, \tag{30}$$

where $N > 0$, and U is the free stream velocity at $y = 0$. Also shown in Fig. 2 is the displacement obtained using theoretical methods by Hall (**6**) for constant shear flow past a sphere.

In drawing conclusions from Fig. 2 it must be kept in mind that in Young and Maas's experiments the shear distribution in the wake, across which the total pressure gradient is constant, does not correspond directly to any of the theoretical models, although it is closest to the 'boundary layer' distribution of shear. Also, in the theoretical models the fluid is assumed to be inviscid, incompressible, and two-dimensional. Despite the above differences between theory and experiment, the following broad conclusions can be reached by comparing the experimental with the theoretical results in Fig. 2:

(1) The contention of Young and Maas that the stagnation streamline is displaced towards a region of higher velocity is supported by all the theoretical results.

(2) It seems probable that the curve obtained from experiment by Young and Maas should pass through the origin of the coordinate system.

(3) In view of the small range of $1/N$ ($0 < 1/N < 0{\cdot}3$) covered by Young and Maas's experiments it seems rather premature to assume that d/r_0 will equal 0·36 at values of $1/N$ considerably in excess of 0·3. Recently, however, MacMillan (**7**) using a circular pitot has traversed the turbulent boundary layers adjacent to a circular pipe and a flat plate. For a variety of positions of the pitot, he found that d/r_0 was substantially constant and never in excess of 0·32.

(4) The stagnation streamline displacements obtained from the 'linear' and 'boundary layer' type shear flows past a circular cylinder are comparable in magnitude to the displacement obtained in the constant shear case. This suggests that in two-dimensional shear flow problems the magnitude of the displacement is not greatly influenced by the type of shear distribution in the free stream.

(5) At small values of $1/N$ the experimental displacement of Young and Maas is much greater than the displacements obtained from the theoretical solutions of two-dimensional shear flow problems. It is, however, comparable in magnitude to the theoretical value obtained by Hall for constant shear flow past a sphere, and so despite the difference in free stream conditions between Young and Maas's experiments and Hall's theoretical problem, it does appear that the Young and Maas displacement is essentially a three-dimensional effect. An additional verification of this might be obtained from experimental displacement measurements using flat 'two-dimensional' pitots.

Finally, mention must be made of some recent experimental work by Davies (**8**), where the boundary layers on a flat plate and a cone in supersonic flow are traversed by a pitot with circular cross-section. In all cases the stagnation streamline has a comparatively small deflexion towards a region of lower velocity. So far no theoretical verification or otherwise of this result has been obtained.

REFERENCES

1. A. R. Mitchell and J. D. Murray, *Z. angew. Math. Phys.* **6** (1955), 223.
2. A. D. Young and J. N. Maas, A.R.C. R. and M., 1770 (1936).
3. H. S. Tsien, *Quart. J. App. Math.* **1** (1943), 130.
4. M. Richardson, ibid. **3** (1945), 175.
5. H. Lamb, *Hydrodynamics* (Cambridge, 1932).
6. I. M. Hall, *J. Fluid Mech.* **1** (1956), 142.
7. F. A. MacMillan, *Cambridge Engineering Laboratory Report* (1955).
8. F. V. Davies, R.A.E. Technical Note, Aero. 2179 (1952).

TWO-DIMENSIONAL CONTRACTING DUCT FLOW

By J. C. GIBBINGS† *and* J. R. DIXON‡

[Received 12 September 1955. Revise received 31 May 1956]

SUMMARY

This paper deals with the incompressible potential flow through two-dimensional contracting channels of finite length. These channel flows are obtained by first specifying flow patterns in the logarithmic hodograph plane. It is shown that certain of these patterns can result in infinite values, at points on the channel wall, of both the velocity gradient and wall curvature. A method of avoiding these undesirable features is given which alters the contraction boundary so as to replace them by wall portions along which the velocity gradient is constant. A numerical example is given.

1. Introduction

DESPITE a general increase in the velocity of a fluid stream on passing through contracting ducts in a potential flow, it is possible for the velocity to decrease along portions of the boundary. These adverse gradients can, in a real flow, cause boundary layer separation. In wind-tunnels this can seriously disturb the working section flow (**1**) which follows a contraction.

Many methods are available for designing two-dimensional and axially symmetric contractions that have no adverse velocity gradients in the potential incompressible flow through them. It seems that all such contractions must necessarily have boundaries that are infinite in length. Goldstein (**2**) appears to have first provided a method of designing contractions having finite length boundaries. In his paper and in papers by Whitehead, Wu, and Waters (**3**), and by Lighthill (**4**), it is shown that adverse velocity gradients exist all along the upstream and downstream parallel walls. Goldstein further showed that these gradients could become infinite at points where the parallel walls joined the contraction curves, and for his particular design method he showed how these infinite gradients could be removed.

It can be shown, by a proof similar to that in section 2 of this paper, that these infinite adverse gradients occur at each end of the contraction described by Whitehead, Wu, and Waters.

Discussion of the relative lengths of different contraction shapes is of limited value if only the boundary shape is considered. For the velocity distribution across each end of a contraction only becomes exactly uniform at infinity up- and down-stream. In many real cases a desirable degree of uniformity can be specified and then the stations at each end of the

† Royal Aircraft Establishment. ‡ The Bristol Aeroplane Company.

contraction where these distributions occur can be found. Then the contraction length that is of interest is the distance between these stations. Thus both the centre line and wall velocity distributions are of interest. Unfortunately both Lighthill and Goldstein discuss only the wall distributions, as they were largely concerned with the length of boundary wall.

The design method used in this paper avoids these defects. It differs from Goldstein's, and so, the occurrence of infinite velocity gradients is reconsidered more generally for applications using the present method.

2. Preliminary general analysis

In the present design method a flow pattern is specified in the logarithmic hodograph plane and certain features of these patterns are now considered.

Writing

$$\Omega \equiv \log \frac{dw}{dz} = \log q - i\theta, \tag{1}$$

where

$w = \phi + i\psi$,
$z = x + iy$,
ϕ = velocity potential,
ψ = stream function,
x, y = coordinates in the physical plane,
q, θ = respectively scale and direction of the velocity vector in the physical plane,
$\bar{q} = +\text{grad}\,\phi$.

Conditions in the z-plane at points corresponding to points of zero 'velocity' in the flow pattern in the $\log dw/dz$-plane are now discussed. We have

$$\frac{dw}{d\Omega} = U - iV, \tag{2}$$

where U and V are the 'velocity components' in the Ω-plane.

From equation (1) we have

$$\Omega + \overline{\Omega} = 2 \log q,$$

hence
$$dq = \tfrac{1}{2} q \, (d\Omega + d\overline{\Omega}); \tag{3}$$

and also
$$\overline{\Omega} - \Omega = 2i\theta,$$

hence
$$d\theta = \frac{1}{2i} (d\overline{\Omega} - d\Omega). \tag{4}$$

On the boundary where $d\psi = 0$,

$$ds = \frac{d\phi}{q} = \frac{dw}{q} = \frac{U - iV}{q} \, d\Omega \tag{5}$$

$$= \frac{U + iV}{q} \, d\overline{\Omega}, \tag{6}$$

where s is distance along the boundary. Then from equations (3), (5), and (6) the velocity gradient is

$$\frac{dq}{ds} = \frac{q}{2}\left(\frac{d\Omega}{ds} + \frac{d\overline{\Omega}}{ds}\right) = \frac{q^2 U}{U^2+V^2}. \tag{7}$$

Similarly from equations (4), (5), and (6) the radius of curvature ρ is

$$\frac{1}{\rho} = \frac{d\theta}{ds} = -\frac{qV}{U^2+V^2}. \tag{8}$$

At stagnation points in the Ω-plane, $U = V = 0$, and in this limiting case,

$$\frac{U}{U^2+V^2} \to \infty \quad \text{if } \frac{dU}{dV} \neq 0 \quad \text{or} \quad \to \frac{1}{2}\frac{d^2U}{dV^2} \quad \text{if } \frac{dU}{dV} = 0,$$

and also

$$\frac{V}{U^2+V^2} \to \infty \quad \text{if } \frac{dV}{dU} \neq 0 \quad \text{or} \quad \to \frac{1}{2}\frac{d^2V}{dU^2} \quad \text{if } \frac{dV}{dU} = 0.$$

Thus at all points in the z-plane that correspond to stagnation points in the Ω-plane, the wall velocity gradient is infinite except when $dU/dV = 0$ whilst the curvature is infinite except when $dV/dU = 0$.

3. Numerical solution in the Ω-plane for special boundary conditions

The flow in the Ω-plane is governed by either of the Laplace equations

$$\nabla^2\phi = 0 \quad \text{or} \quad \nabla^2\psi = 0.$$

The solution to be presented was obtained numerically and, as a consequence, it was found more convenient to solve the second of these two equations. This was done by using Relaxation methods which, for a flow past specified boundaries, are well known (**5**).

The following method was used to obtain boundaries in the Ω-plane, which corresponded to boundaries in the z-plane along which the velocity gradient had specified values.

The two boundary conditions are

$$\psi = \text{constant}, \tag{9}$$

$$\frac{dq}{ds} = \text{constant}. \tag{10}$$

Writing the boundary slope in the Ω-plane as Y' we have

$$Y' = \frac{V}{U}, \tag{11}$$

and thus using equation (7) the boundary condition of equation (10) becomes either

$$\frac{\partial\psi}{\partial(-\theta)} = U = \frac{q^2}{(1+Y'^2)(dq/ds)}, \tag{12}$$

or

$$\frac{\partial\psi}{\partial(\log q)} = -V = -\frac{Y'q^2}{(1+Y'^2)(dq/ds)}. \tag{13}$$

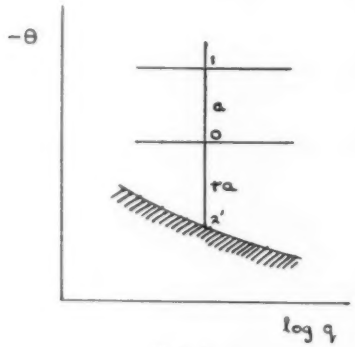

FIG. 1

Numerical differentiation formulae provide a relation between the boundary coordinates and the boundary values of $\frac{\partial\psi}{\partial(-\theta)}$ or $\frac{\partial\psi}{\partial(\log q)}$. For instance, with the mesh system illustrated in Fig. 1 and using one of the formulae given in (**6**),

$$\frac{\partial\psi}{\partial(-\theta)} = \frac{1}{ar(1+r)}[-(1+2r)\psi_{2'}+(1+r)^2\psi_0-r^2\psi_1]. \tag{14}$$

The method of relaxation employed was to

(*a*) Specify a boundary shape in the Ω-plane.

(*b*) Solve $\nabla^2\psi = 0$, for the boundary condition (9).

(*c*) Numerically differentiate the specified boundary curve to obtain Y' and substitute this together with the specified value of dq/ds into equations (12) and (13) to give $\frac{\partial\psi}{\partial(-\theta)}$ and $\frac{\partial\psi}{\partial(\log q)}$.†

(*d*) Compute a corrected boundary shape from equation (14), which is a quadratic in r.

(*e*) Continue the process until successive boundary shapes coincide to the desired degree of accuracy.

† Alternatively one can obtain a boundary shape in the physical plane having a specified radius of curvature. This ability will be used in a future paper on aerofoil design.

4. Numerical integration to obtain the physical plane

Numerical differentiation of the values of ψ obtained from the relaxation solution, substituted into the Cauchy–Reimann equations

$$\frac{\partial\phi}{\partial(\log q)} = \frac{\partial\psi}{\partial(-\theta)},$$

$$\frac{\partial\phi}{\partial(-\theta)} = -\frac{\partial\psi}{\partial(\log q)},$$

followed by a numerical integration will give values of ϕ. From equation (1),

$$dz = \frac{1}{q}e^{i\theta}\,dw$$

$$= \frac{1}{q}[(\cos\theta\,d\phi - \sin\theta\,d\psi) + i(\sin\theta\,d\phi + \cos\theta\,d\psi)].$$

Thus,

$$dx = \frac{1}{q}(\cos\theta\,d\phi - \sin\theta\,d\psi), \tag{15}$$

$$dy = \frac{1}{q}(\sin\theta\,d\phi + \cos\theta\,d\psi). \tag{16}$$

Numerical integration is conveniently performed along lines for which either $\log q$ = constant or θ = constant. But even when computed values of ϕ and ψ are known at regular intervals of $\log q$ and $-\theta$, equations (15) and (16) are still unsuitable for numerical integration. A simple integration by parts makes them suitable. For instance, when $\log q$ = constant,

$$dx = \frac{1}{q}[d(\phi\cos\theta) - d(\psi\sin\theta) - \{\phi\sin\theta + \psi\cos\theta\}d(-\theta)],$$

$$dy = \frac{1}{q}[d(\phi\sin\theta) + d(\psi\cos\theta) + \{\phi\cos\theta - \psi\sin\theta\}d(-\theta)].$$

Or, when $-\theta$ = constant,

$$dx = \cos\theta\,d\left(\frac{\phi}{q}\right) - \sin\theta\,d\left(\frac{\psi}{q}\right) - \{\psi\sin\theta - \phi\cos\theta\}\frac{1}{q}\,d(\log q),$$

$$dy = \sin\theta\,d\left(\frac{\phi}{q}\right) + \cos\theta\,d\left(\frac{\psi}{q}\right) + \{\phi\sin\theta + \psi\cos\theta\}\frac{1}{q}\,d(\log q).$$

Simplification when also either ψ = constant or ϕ = constant is evident.

5. A particular contraction example

Consider first the contraction as sketched in Fig. 2 where AB and EF are straight lines parallel to the centre line $A'F'$, A and F being the points at infinity; BC and DE are curved boundaries along which the velocity is specified as constant; and CD is a straight line along which the velocity is to increase monotonically from C to D.

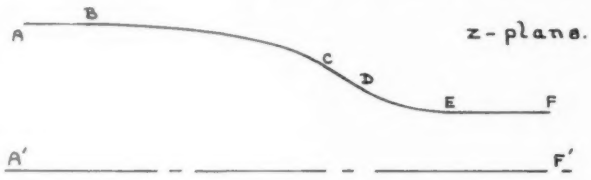

FIG. 2

With this specification the corresponding flow pattern in the Ω-plane is readily sketched as illustrated in Fig. 3, there being a source at A and a sink of equal strength at F.

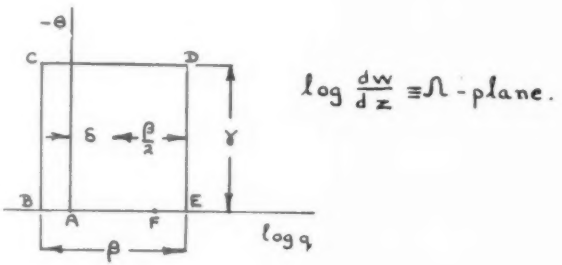

FIG. 3

Flows through similar contractions have previously been obtained by Hughes (7) and Waters (8).

In Hughes's chosen pattern in the Ω-plane, both C and D were at $-\theta = \infty$ and the source and sink were situated at B and E respectively. Thus the contraction obtained was of infinite length and had a singularity consisting of a spiral at the point corresponding to C and D. Waters is understood to have obtained the contraction shape of infinite length corresponding to the pattern of Fig. 3, except that the source and sink were at B and E respectively.

From the preceding results it is now known that along AB and EF in Fig. 2 the adverse velocity gradients will be infinite in value at B and E.

As a first step towards a solution that avoids these infinite adverse gradients, the flow within a boundary of the type of Fig. 3 was obtained by the relaxation method.† The rectangular boundary is convenient for

† The solution of this pattern, given in Appendix I, requires less labour of computation than did the relaxation method. However, a later, modified pattern could only be solved by the relaxation method, and it was thus more convenient to solve by relaxation from the start.

this method, hence the choice of the Ω-plane in which to specify a flow pattern. Relaxation is also made easier by making the velocity drop from A to B the same percentage of the velocity at A as the drop from E to F is of the velocity at F. Then $AB = EF$ and the pattern has an added symmetry.

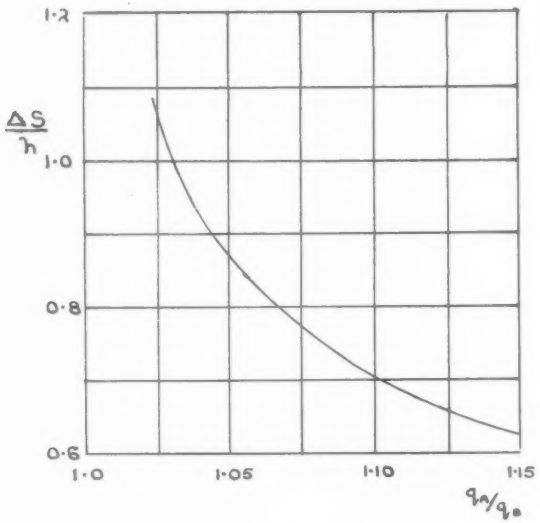

FIG. 4

For this numerical example, the value of $-\theta$ at the points C and D was arbitrarily chosen as 1·0,† and the contraction ratio was specified as $\exp(0{\cdot}95) = 2{\cdot}58$, in order to fit a particular application, and to simplify the relaxation mesh.

The solution given in Appendix I enabled a graph to be drawn illustrating the change in contraction length with change in value of the percentage velocity drops. This graph is given in Fig. 4, where the change in length is expressed as a fraction of the contraction width at the low speed end. From inspection of this, and again to suit the relaxation mesh, velocity drops in the ratio of $\exp(-0{\cdot}05) = 0{\cdot}951$ were chosen.

In order that the ordinates of the contraction shape should give a curve of sufficient smoothness a fair degree of accuracy was required of the relaxation solution. This accuracy was conveniently obtained using the definition of the relaxation residual as given by Woods (**9**). Relaxation in

† It was thought that the success mentioned in the last paragraph of section 6 might not be achieved if this maximum slope was much greater.

the region of point A was carried out according to Woods' technique for this type of singularity (**10**).†

The contraction shape obtained is shown plotted in Fig. 5 and the corresponding velocity distributions along both the wall and the centre line are given in Fig. 6. The four infinite velocity gradients, two favourable and two adverse, can be seen.

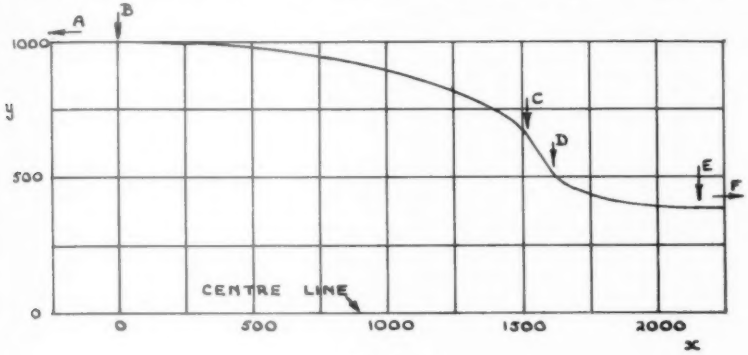

FIG. 5

To obtain a contraction shape along which the adverse gradients are finite, the relaxation method of section 3 was used to modify the boundary at the points B and E of Fig. 3. The modified portions then corresponded to portions in the z-plane along which the adverse gradient had a constant and specific value.

The method of Appendix II provided an approximation to the modified boundary shape required and also enabled an estimate of the change in contraction length resulting from this modification to be obtained. This estimate is shown graphically in Fig. 7 in the form of the change in length at either end, ΔS, as a fraction of the contraction width h at that end, plotted against the non-dimensional adverse gradient,

$$\frac{h}{q}\frac{dq}{ds}.$$

There is difficulty in specifying a value of the adverse gradient so that the boundary layer in a real flow will not separate. Batchelor and Shaw were unable (**1**) to compute successfully the boundary layer development along a contraction where separation was occurring. In order that the significance of the scale of gradients in Fig. 7 can be visualized there is added an auxiliary scale of cone angles of diffusers having corresponding

† There appears to be a slight error in this paper at the foot of p. 182. The expression there should read

$$R_5 = \tfrac{1}{6}(4\Delta'\phi_5 + \Delta''\phi_5) - a^2 k_5 - \tfrac{1}{24}\, m\pi.$$

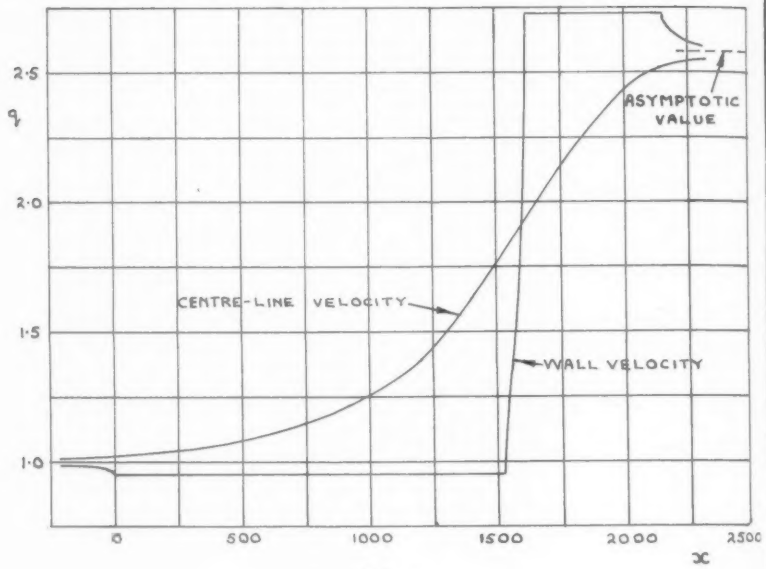

FIG. 6

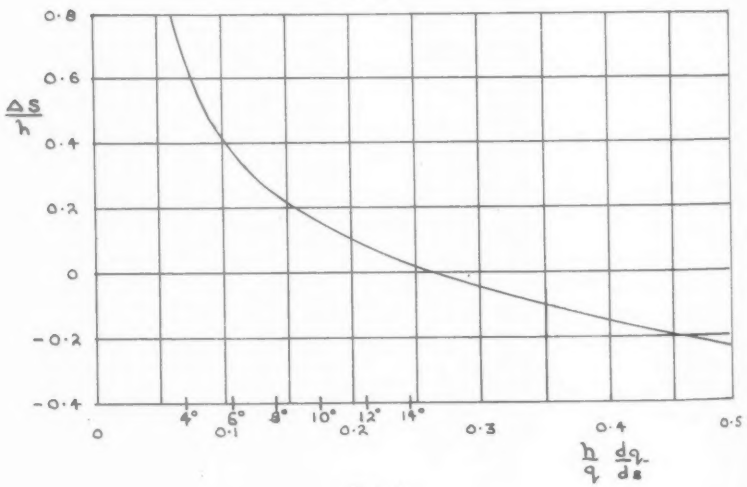

FIG. 7

velocity gradients. Hence there was only slight justification for the choice of a value of

$$\frac{h}{q}\frac{dq}{ds} = -0{\cdot}15$$

in the numerical example.

The resulting approximate shape of the modified boundary in the Ω-plane is plotted in Fig. 8. It is of interest in that an infinite adverse gradient is avoided, whilst there is still a stagnation point at H. As shown in Appendix II the slope is infinite at H. On moving away from H it diminishes from

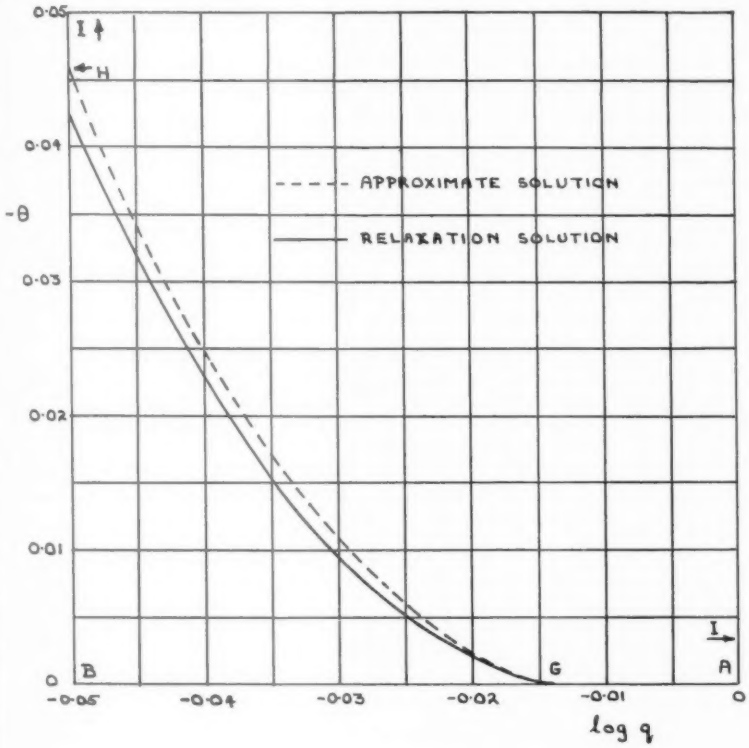

FIG. 8

this value with extreme rapidity, and as a consequence the relaxation solution was unable to distinguish, in the similar shape that was obtained, between the true shape and the more common form of stagnation point that exists at a point of discontinuity in the boundary slope. No difficulty was, however, experienced with the relaxation solution and the final boundary shape was obtained quite rapidly after three successive approximations from the shape given by the method of Appendix II. Fig. 8 provides a comparison between these first and final curves.

The changed velocity distribution at the high speed end of the contraction is compared with the original one, having the infinite gradient,

in Fig. 9. This figure also illustrates the increase in length at this end of

$$\frac{\Delta S}{h} = 0{\cdot}165,$$

compared with the approximate value from Fig. 7 of

$$\frac{\Delta S}{h} = 0{\cdot}21.$$

The discrepancy is not surprising, for the velocity potential at G in Fig. 8 can change quite rapidly with small movements of G along AB.

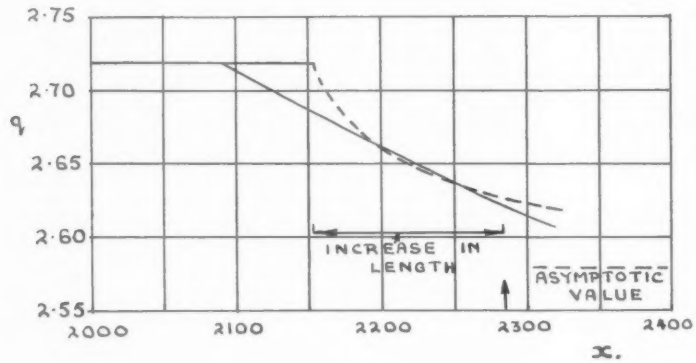

FIG. 9

Though the change in the velocity distribution is seen to be appreciable, the corresponding differences in the contraction boundary shape were found to be not large. This thus suggests that in the potential flow the velocity gradients at the ends of the contraction are particularly sensitive to small changes in boundary shape.

The total length of the modified contraction is 1·28 times the width at the low speed end.

6. Practical application

Whitehead, Wu, and Waters have shown (**3**) that a contraction shape obtained by two-dimensional flow analysis can be used as the shape for an axi-symmetric contraction. They showed that gradients that were favourable in two-dimensional flow became more so in the axi-symmetric flow whilst adverse gradients were lessened. Analysis of the flow in square contractions (**11**) has shown that adverse gradients, when they appear, do so firstly along the corners. A comparison has been made (**12**) of the gradients along the walls of a two-dimensional, an axi-symmetric, and the corner of a square contraction, all having the same boundary shape. This

showed that the gradients were favourable in all three cases, those at each end of the square contraction being slightly less so than the corresponding ones for the axi-symmetric contraction.

Though these are specific examples and not general results it seems that a suitably designed two-dimensional contraction shape can be successfully used for axi-symmetric and square contractions.

The difficulty discussed by Batchelor and Shaw (**1**), in predicting the boundary layer development along a contraction where separation was present, has already been mentioned. Present practice is to allow for viscous effects by adjusting the boundary coordinates, as obtained from the potential flow solution, by an empirical boundary layer displacement thickness. It is suggested that this can be more readily done with the present method where all velocity gradients can be made finite and of any desired value than with one in which infinite gradients are obtained.

7. Conclusions

The present paper has shown that a contraction of finite length must be carefully designed so as to avoid, in the potential flow through it, the infinite adverse wall velocity gradients that occur in Whitehead, Wu, and Waters' design (**3**). The elimination of these gradients is considered in greater detail here than in Goldstein's paper (**2**) and a method is given whereby the value of the gradient can be more readily controlled than can be done using his or Lighthill's (**4**) method.

Acknowledgements

Both authors are extremely grateful to Dr. G. M. Roper for her most thorough reading of this paper and for her many criticisms and suggested improvements in mathematical technique.

One of the authors (J. C. G.) is in addition indebted to Mr. D. E. Morris, for his practical encouragement without which the work reported herein could not have been done.

APPENDIX I

Solution giving the flow in the rectangular boundary in the Ω-plane

The origin in the Ω-plane, as illustrated in Fig. 3, is shifted to the centre of the rectangle by putting

$$L = \Omega - \delta - \tfrac{1}{2}i\gamma = m + in \quad \text{(say)}.$$

The rectangular boundary in this L-plane, as illustrated in Fig. 10, is transformed to a unit circle, as illustrated in Fig. 11 by (**13**)

$$\zeta = \frac{\mathrm{sn}(\tfrac{1}{2}\lambda L)\mathrm{dn}(\tfrac{1}{2}\lambda L)}{\mathrm{cn}(\tfrac{1}{2}\lambda L)}, \tag{A1}$$

where the quarter periods $K(k)$ and $iK'(k)$ of modulus k and k' respectively of the Jacobian elliptic functions satisfy the relations

$$\frac{K(k)}{\beta} = \frac{K'(k)}{\gamma} = \frac{\lambda}{2}. \tag{A2}$$

From equation (A1) $$\zeta^2 = \frac{1-\mathrm{cn}(\lambda L)}{1+\mathrm{cn}(\lambda L)},$$

whence $$\mathrm{cn}(\lambda L) = \frac{1-\zeta^2}{1+\zeta^2},$$

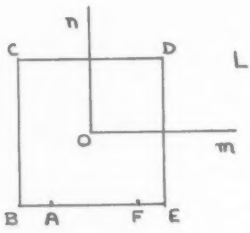

FIG. 10

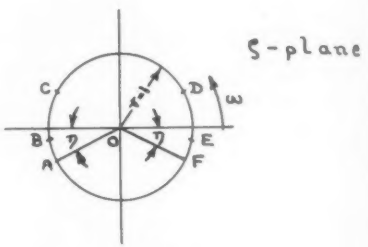

FIG. 11

and on the circle $$\zeta = e^{i\omega}, \tag{A3}$$

whence $$\mathrm{cn}(\lambda L) = -i\tan\omega. \tag{A4}$$

Along BE, $L = m - \frac{i\gamma}{2}$. Hence

$$\begin{aligned}\mathrm{cn}(\lambda L) &= \mathrm{cn}(\lambda m - iK', k)\\ &= \mathrm{cn}(iK' - \lambda m, k)\\ &= -\frac{i\,\mathrm{ds}(-\lambda m, k)}{k},\end{aligned}$$

and substituting into equation (A4) gives

$$\omega = \tan^{-1}\left[\frac{1}{k}\,\mathrm{ds}(-\lambda m, k)\right] \tag{A5}$$

and in particular at B, $$\omega_B = \tan^{-1}\left(\frac{k'}{k}\right).$$

The flow pattern in the ζ-plane, consisting of a source at A and a sink at F, is given by $$w = \log[\zeta - e^{i(\pi+\eta)}] - \log[\zeta - e^{i(-\eta)}], \tag{A6}$$

and substituting from equation (A3) this leads to the velocity potential ϕ as

$$\phi = \tfrac{1}{2}\log\frac{1+\cos(\omega-\eta)}{1-\cos(\omega+\eta)}. \tag{A7}$$

Specification of β and γ enables K, K' and k, k' and λ to be obtained from equations (A2). Then successive use of equations (A5) and (A7) gives the velocity potential

around the boundary in Fig. 3. Using suffixes to denote values at the correspondingly lettered points in Fig. 3, the contraction boundary length s_{total} is

$$s_{\text{total}} = \frac{1}{q_B}(\phi_C-\phi_B)+\int_C^D \frac{1}{q}\,d\phi+\frac{1}{q_E}(\phi_E-\phi_D)$$

$$\doteq \frac{1}{q_B}(\phi_C-\phi_B)+\frac{2}{q_D+q_C}(\phi_D-\phi_C)+\frac{1}{q_E}(\phi_E-\phi_D)$$

$$= \left(\frac{1}{q_B}+\frac{1}{q_E}\right)(\phi_C-\phi_B)+\frac{2}{q_D+q_C}(\phi_D-\phi_C).$$

From equation (A6) it is readily shown that by putting $\psi = 0$ along AF, then $\psi = \pi$ along $ABCDEF$, thus showing that the contraction widths at either end are $2\pi/q_A$ and $2\pi/q_F$. By arbitrarily placing A at the origin, then $q_A = 1{\cdot}0$.

Then the change of the contraction length, in terms of its width, with variation in q_A/q_B, is indicated by

$$\frac{\Delta S}{2\pi} = \frac{1}{q_B}(\phi_C-\phi_B)$$

and is plotted in Fig. 4.

APPENDIX II

An approximate solution giving the modified boundary shape in the Ω-plane

The boundary shape in the Ω-plane, when the corners B and E (Fig. 3) are modified, is shown in Fig. 8. An approximation is now obtained for the boundary shape HG, along which, at corresponding points in the z-plane, the velocity gradient is constant. The flow at this corner is approximated to by the flow due to a source at A, the two arms of the corner extending to infinity.

From equation (2)

$$\frac{d\Omega}{dw} = \frac{U}{Q^2}+i\frac{V}{Q^2},$$

where Q is the 'resultant velocity' in the Ω-plane. Substituting from equations (7) and (8)

$$\frac{d\Omega}{dw} = \frac{1}{q^2}\frac{dq}{ds}-i\frac{1}{q}\frac{1}{\rho}.$$

Along GH, q will vary by only a few per cent. and so if this portion of the boundary is a line on which $U/Q^2 =$ constant, it will be approximately a line on which $dq/ds =$ constant.

The $d\Omega/dw$-plane is as shown in Fig. 12, the points H and I being at infinity. It is noted in passing, that point H corresponds to a stagnation point in the Ω-plane, yet $\frac{1}{q^2}\frac{dq}{ds}$ is finite there. Writing $p = d\Omega/dw$, the p-plane is transformed to the upper half of the t-plane (Fig. 13) by the Schwarz–Christoffel transformation, which gives

$$\frac{dp}{dt} = Ct^{-\frac{1}{2}}(t+a)^{-1}(t+b).$$

Writing $\sqrt{(b/a)} = c$ and substituting $r = \sqrt{t}$ this integrates to

$$p = C[2r+i\sqrt{a}(1-c^2)\{\log(r-i\sqrt{a})-\log(r+i\sqrt{a})\}]+C_1, \qquad \text{(B1)}$$

C_1 being the constant of integration.

Along the line from G to I, $0 < r < +\infty$, and it is found that

$$p = C\left[2r+2\sqrt{a}(1-c^2)\tan^{-1}\frac{\sqrt{a}}{r}\right]+C_1.$$

Thus C and C_1 are real, and hence at G

$$\frac{p-C_1}{C} = -\pi\sqrt{a}(c^2-1) \tag{B2}$$

and also at A where $p = 0$ and $r = r_0$ (say)

$$2r_0+2\sqrt{a}(1-c^2)\tan^{-1}\frac{\sqrt{a}}{r_0}+C_1 = 0. \tag{B3}$$

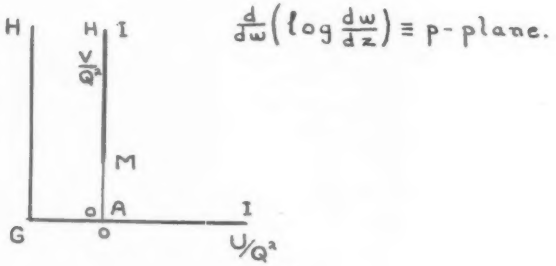

FIG. 12

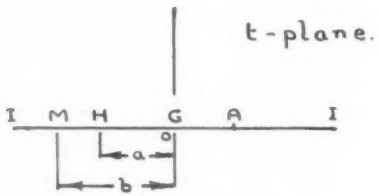

FIG. 13

Along the line from H to M, $i\sqrt{a} < r < i\sqrt{b}$ and writing $r = ir'$,

$$\frac{p-C_1}{C} = 2ir'+i\sqrt{a}(1-c^2)\log\frac{r'-\sqrt{a}}{r'+\sqrt{a}}. \tag{B4}$$

Thus $C_1 = 0$ and at M $\quad \dfrac{p}{C} = i\sqrt{a}\left[2c+(1-c^2)\log\dfrac{c-1}{c+1}\right]$.

Comparing this equation with equation (B2) shows that the ratio of the values of p at G and M is independent of a and C, depending only upon c. As only this ratio and the value of p at G will be varied, the value of a can arbitrarily be put equal to 1·0. Thus equation (B1) becomes

$$\frac{p}{C} = 2r+i(1-c^2)\log\frac{r-i}{r+i}. \tag{B5}$$

The flow in the t-plane is that given by a source at A, thus

$$w = \log(r^2-r_0^2);$$

hence

$$\frac{dr}{dw} = \frac{r^2-r_0^2}{2r}, \tag{B6}$$

and

$$p \equiv \frac{d}{dw}\left(\log\frac{dw}{dz}\right) = \frac{r^2-r_0^2}{2r}\frac{d}{dr}\left(\log\frac{dw}{dz}\right).$$

Substitution into equation (B5) gives

$$\frac{1}{2C}\frac{d}{dr}\left(\log\frac{dw}{dz}\right)=\frac{2r^2}{r^2-r_0^2}+i\frac{r}{r^2-r_0^2}(1-c^2)\log\frac{r-i}{r+i}. \tag{B7}$$

The integral of the first term on the right-hand side is

$$2\left[r+\tfrac{1}{2}r_0\log\frac{r-r_0}{r+r_0}\right] \tag{B8}$$

but integration of the second term leads to an integral of the type

$$-\int_0^x\frac{\log(1-j)}{j}\,dj,$$

that is, Euler's dilogarithmic integral. So equation (B7) is integrated numerically. Along the boundaries to be considered r is either wholly real, when

$$\log\frac{r-i}{r+i}=-2i\tan^{-1}\frac{1}{r}, \tag{B9}$$

or is wholly imaginary, when

$$\log\frac{ir'-i}{ir'+i}=i\pi+\log\frac{1-r'}{1+r'}. \tag{B10}$$

The value of (B8) becomes infinite at A, thus in integrating from G to A, the whole of equation (B7) is integrated numerically; thus, noting equation (B9),

$$\frac{1}{2C}[\log q_A-\log q_G]=\int_0^{r_0}\frac{r}{r^2-r_0^2}\left[2r+2(1-c^2)\tan^{-1}\frac{1}{r}\right]dr. \tag{B11}$$

The limit of the integrand at A as $r\to r_0$ is

$$1+\frac{r_0}{1+r_0^2}\frac{1}{\tan^{-1}(1/r_0)}.$$

Substituting equation (B10) into equation (B7) gives the ordinates of the curve GH as

$$\frac{1}{2C}\left[\log\frac{dw}{dz}\right]_G=\int_0^{r'}\frac{r}{r^2-r_0^2}\left[2r+i(1-c^2)\left\{\log\frac{1-r'}{1+r'}+i\pi\right\}\right]dr.$$

This reduces to

$$\frac{1}{2C}\log q=-\tfrac{1}{2}\pi(1-c^2)\log(r'^2+r_0^2)+\text{constant}, \tag{B12}$$

$$\frac{1}{2C}(-\theta)=2\left[r'+r_0\tan^{-1}\frac{r_0}{t'}\right]+(1-c^2)\int_0^{r'}\frac{r'}{r_0^2+r'^2}\log\frac{1-r'}{1+r'}\,dr'+\text{constant}. \tag{B13}$$

Specifying values of r_0, equation (B3) gives corresponding values of c. Use of equations (B11) and (B12) gives $(1/C)[\log q_A-\log q_H]$, then specifying $\log q_H$ and putting $q_A=1{\cdot}0$ gives C. In the present case $\psi=0$ on the contraction centre line, and π on one wall, so that the contraction width at the low speed end is 2π and equation (B2) then gives $\left(\frac{h}{q}\frac{dq}{ds}\right)_G$. Values obtained when $q_H=0{\cdot}95$ were

$r_0=$	0·1	0·2	0·5	1·0	2·0
$\left[\frac{h}{q}\frac{dq}{ds}\right]_G=$	−0·06126	−0·08258	−0·1439	−0·2548	−0·4912

A difficulty arises in computing the coordinates of the curve GH, for the integrand in equation (B13) tends to infinity as $r' \to 1{\cdot}0$ at H. This is avoided by computing from the following series expansion the integral

$$\int \frac{r'}{r_0^2+r'^2}\log(1-r')\,dr' = \frac{1-r'}{1+r_0^2}\left[\left\{1+\frac{1-r_0^2}{1+r_0^2}\frac{1-r'}{4}+\frac{1-3r_0^2}{(1+r_0^2)^2}\frac{(1-r')^2}{9}+\ldots\right\}\right]-$$

$$-\log(1-r')\left[\left\{1+\frac{1-r_0^2}{1+r_0^2}\frac{1-r'}{2}+\frac{1-3r_0^2}{(1+r_0^2)^2}\frac{(1-r')^2}{4}+\ldots\right\}\right]. \quad \text{(B14)}$$

As $r' \to 1{\cdot}0$ the right-hand side tends to zero.

To investigate in more detail the shape of the curve GH near to H, equations (B12) and (B13) are, noting equation (B14), expanded in the series form

$$\frac{1}{2C}(\log q - \log q_H) = \tfrac{1}{2}\pi(1-c^2)\left[\frac{2}{1+r_0^2}(1-r')+\ldots\right],$$

$$\frac{1}{2C}(-\theta+\theta_H) = \left[\frac{(1-c^2)(1+\log 2)-2}{1+r_0^2}(1-r')+\ldots\right]+$$

$$+\log(1-r')\left[\frac{1-c^2}{1+r_0^2}(1-r')+\ldots\right].$$

Including only the terms in $(1-r')$,

$$\frac{-\theta+\theta_H}{\log q-\log q_H} \simeq \frac{1}{\pi}\left[1+\log 2-\frac{2}{1-c^2}+\log(1-r')\right].$$

This illustrates the extreme rapidity with which the slope of the curve changes from its value of $-\infty$ as a point moves away from H.

The effect, on contraction length, of the modified boundary

To obtain an approximate value for the change in contraction length due to rounding the corner B in the logarithmic hodograph plane consider the two flow boundaries of Fig. 14, that of case II being the present approximate one.

In case II, on going from H towards I, the influence of the rounded corner GH will have a lessening effect and the flow will tend to that in case I.

Thus the difference in contraction boundary length between case I and case II will be

$$\Delta S = \int_I^{B_I} \frac{1}{q}\,d\phi - \int_I^{G_{II}} \frac{1}{q}\,d\phi \simeq \frac{1}{q_B}[\phi_{B_I}-\phi_{G_{II}}].$$

In case I the flow in the $\Omega = \log(dw/dz)$-plane is given by

$$w = \log(\Omega-a) - \log(\Omega+a).$$

Hence

$$e^w = \frac{\Omega-a}{\Omega+a}.$$

At B where $\Omega = 0$, $e^w = -1$, $\psi = \pi$,

$$\phi_{B_I} = 0.$$

In case II, from equation (B6),

$$e^w = r^2-r_0^2.$$

At G where $r = 0$, $e^w = -r_0^2$, $\psi = \pi$,

and hence

$$\phi_{G_{II}} = 2\log r_0.$$

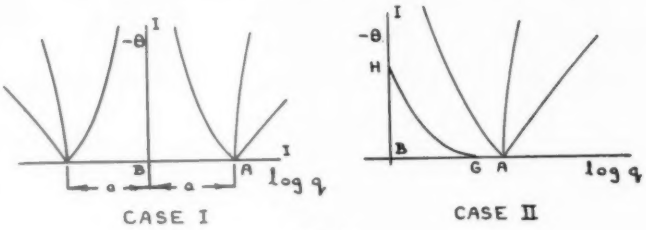

FIG. 14

Putting $q_H = 0{\cdot}95$, $$\Delta S = \frac{2}{0{\cdot}95}\log r_0.$$

Writing h = contraction width at low speed end,

$$\frac{\Delta S}{h} = \frac{\log r_0}{0{\cdot}95\pi}.$$

Values obtained are plotted against $\frac{h}{q}\frac{dq}{ds}$ in Fig. 7.

REFERENCES

1. G. K. BATCHELOR and F. SHAW, 'A consideration of the design of wind tunnel contractions', Australian Council for Aer. Rep. ACA–4 (1944).
2. S. GOLDSTEIN, 'Notes on the design of converging channels', A.R.C. Rep. and Mem. 2643 (1945).
3. L. G. WHITEHEAD, L. Y. WU, and M. H. L. WATERS, 'Contracting ducts of finite length', *Aero. Quart.* **2**, Feb. 1951.
4. M. J. LIGHTHILL, 'A new method of two-dimensional aerodynamic design', A.R.C. Rep. and Mem. 2112 (1945).
5. R. V. SOUTHWELL, *Relaxation Methods in Theoretical Physics* (Oxford, 1946).
6. C. H. WU, 'Formulas and tables of coefficients for numerical differentiation with function values given at unequally spaced points and application to solution of partial differential equations', N.A.C.A. T.N. 2214.
7. H. J. S. HUGHES, 'Stream expansion with discontinuity in velocity on the boundary', A.R.C. Rep. and Mem. 1978 (1944).
8. M. H. L. WATERS, Ph.D. Thesis. Faculty of Engineering, University of London, 1951.
9. L. C. WOODS, 'Improvements to the accuracy of arithmetical solutions to certain two-dimensional field problems', *Quart. J. Mech. and App. Math.* **3** (1950), 352, equation (11).
10. —— 'The relaxation of singular points in Poisson's equation', ibid. **6** (1953), 182.
11. J. C. GIBBINGS, Ph.D. Thesis. Faculty of Engineering, University of London, 1951.
12. —— 'Aerodynamics of wind-tunnel design', unpublished lecture before Grad. and Stud. Sec. R.Ae.S. (1952).
13. L. M. MILNE-THOMPSON, *Theoretical Aerodynamics*, p. 259 (London, 1948).

A NEW EXACT SOLUTION OF THE EQUATIONS OF VISCOUS MOTION WITH AXIAL SYMMETRY

By H. L. AGRAWAL

(*Muir Central College, Allahabad University, Allahabad*)

[Received 16 December 1955]

SUMMARY

An exact solution for the motion of viscous fluid flow for axially symmetric motion has been found by Squire (**1**) in the form $\psi = \nu r f(\mu)$, where (r, θ, ϕ) are spherical polar coordinates, $\mu = \cos\theta$, and ν is the kinematic viscosity. Squire has shown that a special case of his solution gives the flow for a jet emerging from a hole in an infinite plane wall. In the present paper, another exact solution of the Navier–Stokes equations is obtained for the steady flow of a viscous incompressible fluid for the case of axial symmetry in the form $\psi = \nu r^n f(\theta)$ provided that $n = 1$, 2, or 4. For $n = 1$ the solution becomes that of Squire. For $n = 2$ we obtain the solution $\psi = \nu r^2 C_1 \sin^2\theta$ (C_1 being a constant) which is well known. The case $n = 4$ appears to be new.

1. The equations of motion

We take spherical polar coordinates (r, θ, ϕ) with θ measured from the axis of symmetry. The velocity components are $(u, v, 0)$ measured in the directions (r, θ, ϕ) respectively, and all the quantities are independent of ϕ. The equation of continuity is (**2**, § 41)

$$\frac{1}{r^2}\frac{\partial}{\partial r}(r^2 u) + \frac{1}{r\sin\theta}\frac{\partial}{\partial\theta}(v\sin\theta) = 0,$$

and the equations of motion are

$$u\frac{\partial u}{\partial r} + \frac{v}{r}\frac{\partial u}{\partial\theta} - \frac{v^2}{r} = -\frac{1}{\rho}\frac{\partial p}{\partial r} + \nu\left(\nabla^2 u - \frac{2u}{r^2} - \frac{2}{r^2}\frac{\partial v}{\partial\theta} - \frac{2v\cot\theta}{r^2}\right),$$

$$u\frac{\partial v}{\partial r} + \frac{v}{r}\frac{\partial v}{\partial\theta} + \frac{uv}{r} = -\frac{1}{\rho}\frac{\partial p}{r\,\partial\theta} + \nu\left(\nabla^2 v + \frac{2}{r^2}\frac{\partial u}{\partial\theta} - \frac{v}{r^2\sin^2\theta}\right),$$

where p is the pressure, ρ is the density, ν is the kinematic viscosity, and

$$\nabla^2 = \frac{1}{r^2}\frac{\partial}{\partial r}\left(r^2\frac{\partial}{\partial r}\right) + \frac{1}{r^2\sin\theta}\frac{\partial}{\partial\theta}\left(\sin\theta\frac{\partial}{\partial\theta}\right).$$

We shall assume that ψ (the Stokes's stream function) has the form

$$\psi = \nu r^n f(\theta), \tag{1}$$

so that

$$\left.\begin{aligned} u &= -\frac{1}{r\sin\theta}\frac{\partial\psi}{r\,\partial\theta} = -\frac{\nu r^{n-2}}{\sin\theta}f'(\theta) \\ v &= \frac{1}{r\sin\theta}\frac{\partial\psi}{\partial r} = \frac{\nu n\, r^{n-2}}{\sin\theta}f(\theta) \end{aligned}\right\}. \tag{2}$$

The equation for the stream function ψ is (**2**)

$$\frac{1}{r^2\sin\theta}\frac{\partial(\psi, D^2\psi)}{\partial(r,\theta)} - \frac{2D^2\psi}{r^2\sin^2\theta}\left\{\cos\theta\frac{\partial\psi}{\partial r} - \frac{\sin\theta}{r}\frac{\partial\psi}{\partial\theta}\right\} = \nu D^4\psi, \tag{3}$$

where

$$D^2 \equiv \frac{\partial^2}{\partial r^2} + \frac{\sin\theta}{r^2}\frac{\partial}{\partial\theta}\left(\frac{1}{\sin\theta}\frac{\partial}{\partial\theta}\right).$$

Substituting the assumed form (1) for ψ,

$$D^2\psi = \nu r^{n-2}(f'' - \cot\theta f' + n(n-1)f); \tag{4}$$

and hence from (3) we get, after some simplification,

$$\begin{aligned} r^{n-1}[&-2n^2(n-1)\cot\theta f^2 + n\{4n-3+3\cot^2\theta\}ff' - \\ &-3n\cot\theta ff'' + (n-4)\cot\theta f'^2 - (n-4)f'f'' + nff'''] \\ &= \sin\theta[n(n-1)(n-2)(n-3)f - (2n^2-6n+9+3\cot^2\theta)\cot\theta f' + \\ &\quad + (2n^2-6n+8+3\cot^2\theta)f'' - 2\cot\theta f''' + f^{\mathrm{iv}}], \end{aligned} \tag{5}$$

where dashes denote differentiation with respect to θ.

2. Equation (5) is the differential equation which $f(\theta)$ must satisfy in order that $\nu r^n f(\theta)$ may be a possible form for the Stokes's stream-function. Putting $n = 1$ in equation (5), we can show that it has a solution

$$f = \frac{2\sin^2\theta}{C + 1 - \cos\theta}.$$

The corresponding stream-function is $\psi = \nu r f(\theta)$. This is the case investigated by Squire (**1**, **3**).

If $n \neq 1$ the presence of the term r^{n-1} in (5) shows that the two sides of this equation must separately vanish. We shall find a solution which is common to the two differential equations thus obtained.

We find by actual substitution and simplification that the left-hand side of (5) equated to zero is satisfied by $f(\theta) = C_2\sin^n\theta$, where C_2 is a constant. However, when we substitute this value of $f(\theta)$ in the right-hand side of (5), the latter reduces to

$$n(n-2)^2(n-4)C_2\sin^{n-3}\theta.$$

It appears, therefore, that n must be 0, 2, or 4 in order that $C_2\sin^n\theta$ may be a possible value of $f(\theta)$. As $n = 0$ is trivial and $n = 2$ gives a well-known solution, we consider here only the case $n = 4$. Putting $n = 4$ in (5) the equation becomes

$$\begin{aligned} &4r^3f[f''' - 3\cot\theta f'' + (13+3\cot^2\theta)f' - 24\cot\theta f] \\ &\quad = \sin\theta[f^{\mathrm{iv}} - 2\cot\theta f''' + (16+3\cot^2\theta)f'' - (17+3\cot^2\theta)\cot\theta f' + 24f] \end{aligned}$$

or

$$\left[4r^3f - \sin\theta\left(\frac{d}{d\theta} + \cot\theta\right)\right][f''' - 3\cot\theta f'' + (13+3\cot^2\theta)f' - 24f\cot\theta] = 0.$$

Hence any solution of

$$f'''-3f''\cot\theta+(13+3\cot^2\theta)f'-24f\cot\theta=0$$

gives a possible stream function. Now

$$f'''-3f''\cot\theta+(13+3\cot^2\theta)f'-24f\cot\theta \equiv \left(\frac{d}{d\theta}-2\cot\theta\right)(f''-f'\cot\theta+12f).$$

Hence we require a solution of

$$f''-\cot\theta f'+12f=A\sin^2\theta,$$

where A is a constant. Now the general solution† is

$$f(\theta)=\sin^2\theta[\tfrac{1}{10}A+BP_3'(\mu)+CQ_3'(\mu)],$$

where P_3', Q_3' are the derivatives of the Legendre functions P_3 and Q_3, $\mu=\cos\theta$ and B and C are constants.

A particular case of the above solution is obtained by putting $C=0$ and $A/B=15$; we thus get

$$\psi=kr^4\sin^2\theta\cos^2\theta,$$

where k is a constant.

This solution is of interest since it makes $u=v=0$ for $\theta=\frac{1}{2}\pi$, and this represents a motion with a plane boundary. The stream lines are rectangular hyperbolas in this case.

This may be regarded as the motion in a slightly divergent jet striking a distant wall at right angles, but as in the case considered by Squire, the boundary conditions are not satisfied at the outer surface of the jet.

It is easy to show that in this case, at any point (r,θ,ϕ), the components of vorticity are

$$\xi=\eta=0, \qquad \zeta=2kr\sin\theta,$$

and

$$q^2=4k^2r^4\cos^2\theta,$$

where q is the resultant velocity.

In conclusion I thank Dr. Gorakh Prasad, Allahabad University, Allahabad, under whose guidance this investigation was carried out.

REFERENCES

1. H. B. Squire, *Quart. J. Mech. Appl. Math.* **4** (1951), 321.
2. S. Goldstein (ed.), *Modern Development in Fluid Dynamics* (Oxford, 1938).
3. H. B. Squire, *Phil. Mag.* **43** (1952), 942.

† I am indebted to one of the referees for this general solution.

THE LAUNCHING AND PROPAGATION OF ELASTIC WAVES IN PLATES

By H. PURSEY (*National Physical Laboratory, Teddington, Middlesex*)

[Received 16 February 1956]

SUMMARY

Integral representations are derived for the displacement at an arbitrary point in an isotropic plate due to a stress distribution on the free surfaces which varies sinusoidally with time. It is shown that evaluation of the integrals leads to secular equations identical with those originally obtained by Lamb, and the solutions of these equations have been investigated for the symmetric and antisymmetric wave types in plates up to $8/\pi$ compressional wavelengths thick. New tables of solutions are provided for the two principal waves and graphical representations of the solutions corresponding to complementary waves are given in Figs. 1–6. Difficulties which arise in the use of Lamb's tables have been avoided by the method of normalization adopted in the present paper.

Formulae are derived from which the amplitude and group velocity of a given wave may be calculated, and their application is illustrated by means of a worked example.

1. Introduction

THE first rigorous analysis of wave propagation in an isotropic plate was given by Lamb (**1**) for the two-dimensional problem of a harmonic wave travelling in a direction parallel to the medial plane. He considered two types of wave, one symmetric and the other antisymmetric with respect to the medial plane, and derived equations relating their phase velocities to the thickness of the plate. It is apparent from these equations that the phase velocities are many-branched functions of plate thickness, and with the exception of one branch in each case their values are complex when the plate thickness is small compared with the length of a plane transverse wave in the material. Hence, only waves corresponding to one symmetric and one antisymmetric branch can propagate in a thin plate. These are referred to as 'principal waves', and corresponding solutions of the secular equation are tabulated by Lamb.

The symmetric modes of propagation have been studied by Holden (**2**), who shows how the approximate form of the solutions may be deduced from Lamb's secular equation without undertaking a detailed numerical analysis. Holden also considers the case of symmetric waves propagated in cylinders, while the principal antisymmetric branch has been studied by Osborne and Hart (**3**) for plates, and by Hudson (**4**) for cylinders.

The purpose of the present paper is to show how the amplitude of the disturbance is related to a given stress distribution on the free surfaces of the plate, varying harmonically with time. Two types of source are con-

sidered, one giving a two-dimensional field, as in Lamb's paper, and the other having circular symmetry about an axis normal to the surface of the plate. The method of solution follows that used in the analysis of the field from a radiator on the free surface of a semi-infinite solid by Miller and Pursey (**5**),† leading to definite-integral representations of the field components at an arbitrary point in the plate. The value of the integrals is shown to be the sum of the residues at the poles of the integrand lying in the upper half-plane or on the negative portion of the real axis, and investigation of the positions of the poles leads to the secular equations originally obtained by Lamb. New tables are provided, showing the velocity of propagation as a function of plate thickness for the two principal modes in materials with Poisson's ratios of $\frac{1}{4}$ and $\frac{1}{3}$. The parameters are normalized by comparison with the velocity and wavelength of a plane compressional wave in the material. This avoids difficulties which arise in the use of Lamb's tables, where the plate thickness is measured in terms of the length of the appropriate principal wave—a quantity which is itself a function of plate thickness.

Consideration is given to the complementary modes of propagation (that is, modes other than principal modes) in both the symmetric and antisymmetric cases, and Figs. 1–6 show the relationship between phase velocity and plate thickness for propagating waves in plates whose thickness does not exceed three compressional wavelengths.

Formulae are derived from which the amplitudes and group velocities of the normal surface components of all propagating waves may be obtained, and their application is illustrated in a worked example in which the plate is assumed to have a Poisson's ratio of $\frac{1}{3}$ and a thickness equal to $2/\pi$ compressional wavelengths.

2. Derivation of integral representations for the displacement components

It is convenient to reproduce here the equations of displacement, stress, and propagation derived in section 2 of Paper I, which also find application in the problems considered in the present paper. Cartesian and cylindrical polar coordinate systems are used, the z-axis being in both cases normal to the medial plane, which also contains the coordinate origin. The relevant equations are

$$u_{zF} = -\frac{c_{44}}{\rho\omega^2}\left(\mu^2\frac{d\Delta_F}{dz} - i\zeta W_F\right), \qquad u_{xF} = -\frac{c_{44}}{\rho\omega^2}\left(\frac{dW_F}{dz} + i\mu^2\zeta\Delta_F\right), \tag{1}$$

$$\frac{d^2\Delta_F}{dz^2} - (\zeta^2 - k_1^2)\Delta_F = 0, \qquad \frac{d^2W_F}{dz^2} - (\zeta^2 - k_2^2)W_F = 0, \tag{2}$$

† Subsequently referred to as 'Paper I'.

$$\frac{\rho\omega^2}{c_{44}^2}\widehat{zz}_F = -\mu^4\frac{d^2\Delta_F}{dz^2} + 2i\zeta\frac{dW_F}{dz} + \mu^2(\mu^2-2)\zeta^2\Delta_F, \tag{3}$$

$$\frac{\rho\omega^2}{c_{44}^2}\widehat{zx}_F = -\left(\frac{d^2W_F}{dz^2} + 2i\mu^2\zeta\frac{d\Delta_F}{dz} + \zeta^2 W_F\right), \tag{4}$$

$$u_{zB_0} = -\frac{c_{44}}{\rho\omega^2}\left(\mu^2\frac{d\Delta_{B_0}}{dz} - \zeta W_{B_1}\right), \qquad u_{rB_1} = -\frac{c_{44}}{\rho\omega^2}\left(\frac{dW_{B_1}}{dz} - \mu^2\zeta\Delta_{B_0}\right), \tag{5}$$

$$\frac{d^2\Delta_{B_0}}{dz^2} - (\zeta^2-k_1^2)\Delta_{B_0} = 0, \qquad \frac{d^2W_{B_1}}{dz^2} - (\zeta^2-k_2^2)W_{B_1} = 0, \tag{6}$$

$$\frac{\rho\omega^2}{c_{44}^2}\widehat{zz}_{B_0} = -\mu^4\frac{d^2\Delta_{B_0}}{dz^2} + 2\zeta\frac{dW_{B_1}}{dz} + \mu^2(\mu^2-2)\zeta^2\Delta_{B_0}, \tag{7}$$

$$\frac{\rho\omega^2}{c_{44}^2}\widehat{zr}_{B_1} = -\left(\frac{d^2W_{B_1}}{dz^2} - 2\mu^2\zeta\frac{d\Delta_{B_0}}{dz} + \zeta^2 W_{B_1}\right), \tag{8}$$

where

u_x, u_r, and u_z are components of displacement,

$\widehat{zx}$, $\widehat{zr}$, and $\widehat{zz}$ are components of stress (Pearson's notation),

ρ is the density of the plate,

ω is the pulsatance of the vibration,

c_{11} and c_{44} are respectively the compressional and shear elastic constants of the plate,

and
$$k_1 = \omega\sqrt{(\rho/c_{11})}, \qquad k_2 = \omega\sqrt{(\rho/c_{44})}, \tag{9}$$

$$\Delta = \boldsymbol{\nabla}.\mathbf{U}, \qquad W = |\boldsymbol{\nabla}\times\mathbf{U}|, \tag{10}$$

$$\mu = \sqrt{(c_{11}/c_{44})} = k_2/k_1 = \sqrt{\{2(1-\sigma)/(1-2\sigma)\}}, \tag{11}$$

σ is the Poisson's ratio of the plate.

The suffix F, B_0, or B_1 indicates that a variable has been transformed by the Fourier or Hankel integral transform, defined respectively by the equations

$$\phi_F(\zeta) = \int_{-\infty}^{\infty}\phi(x)e^{-i\zeta x}\,dx, \qquad \phi_{B_m}(\zeta) = \int_0^{\infty}\phi(r)rJ_m(\zeta r)\,dr. \tag{12}$$

As in Paper I, it will be convenient to normalize the equations by measuring lengths in units of $1/k_1$. Equations (2) and (6) then become

$$\frac{d^2\Delta_F}{dz^2} - (\zeta^2-1)\Delta_F = 0, \qquad \frac{d^2W_F}{dz^2} - (\zeta^2-\mu^2)W_F = 0, \tag{13}$$

$$\frac{d^2\Delta_{B_0}}{dz^2} - (\zeta^2-1)\Delta_{B_0} = 0, \qquad \frac{d^2W_{B_1}}{dz^2} - (\zeta^2-\mu^2)W_{B_1} = 0, \tag{14}$$

the remainder of equations (1) to (8) being unchanged, provided that all symbols are now regarded as denoting quantities measured in normalized units.

Case (a) Field invariant with y

SYMMETRIC WAVES

It is convenient to introduce here the notation

$$S_z^m = \sinh\{z\sqrt{(\zeta^2-m^2)}\}, \qquad C_z^m = \cosh\{z\sqrt{(\zeta^2-m^2)}\}. \tag{15}$$

The appropriate solutions of equations (13) for waves having symmetry with respect to the medial plane are then

$$\Delta_F = A_1 C_z^1, \qquad W_F = B_1 S_z^\mu. \tag{16}$$

Substitution in equations (3) and (4) leads to the following expressions for the transformed components of stress:

$$-\frac{\rho\omega^2}{c_{44}^2}\widehat{zz}_F = A_1\mu^2(2\zeta^2-\mu^2)C_z^1 - 2iB_1\zeta\sqrt{(\zeta^2-\mu^2)}C_z^\mu, \tag{17}$$

$$-\frac{\rho\omega^2}{c_{44}^2}\widehat{zx}_F = 2iA_1\mu^2\zeta\sqrt{(\zeta^2-1)}S_z^1 + B_1(2\zeta^2-\mu^2)S_z^\mu. \tag{18}$$

If we now write for the transforms of the symmetric components of stress on the free surface

$$f_1(\zeta) = (\widehat{zz}_F)_{z=a}, \qquad g_1(\zeta) = (\widehat{zx}_F)_{z=a}, \tag{19}$$

where a is the half-thickness of the plate, we obtain for A_1 and B_1

$$A_1 = \frac{-\rho\omega^2}{\mu^2 c_{44}^2 D_1(\zeta;a,\mu)}\{(2\zeta^2-\mu^2)f_1(\zeta)S_a^\mu + 2i\zeta\sqrt{(\zeta^2-\mu^2)}g_1(\zeta)C_a^\mu\},$$

$$B_1 = \frac{-\rho\omega^2}{c_{44}^2 D_1(\zeta;a,\mu)}\{(2\zeta^2-\mu^2)g_1(\zeta)C_a^1 - 2i\zeta\sqrt{(\zeta^2-1)}f_1(\zeta)S_a^1\},$$

where

$$D_1(\zeta;a,\mu) = (2\zeta^2-\mu^2)^2 S_a^\mu C_a^1 - 4\zeta^2\sqrt{(\zeta^2-\mu^2)}\sqrt{(\zeta^2-1)}S_a^1 C_a^\mu. \tag{20}$$

Using equations (1) and (16), we then find for the transforms of the field components

$$u_{zF} = \frac{1}{c_{44} D_1(\zeta;a,\mu)}[\sqrt{(\zeta^2-1)}f_1(\zeta)\{(2\zeta^2-\mu^2)S_a^\mu S_z^1 - 2\zeta^2 S_a^1 S_z^\mu\} + \\ + i\zeta g_1(\zeta)\{2\sqrt{(\zeta^2-\mu^2)}\sqrt{(\zeta^2-1)}C_a^\mu S_z^1 - (2\zeta^2-\mu^2)C_a^1 S_z^\mu\}], \tag{21}$$

$$u_{xF} = \frac{1}{c_{44} D_1(\zeta;a,\mu)}[i\zeta f_1(\zeta)\{(2\zeta^2-\mu^2)S_a^\mu C_z^1 - 2\sqrt{(\zeta^2-\mu^2)}\sqrt{(\zeta^2-1)}S_a^1 C_z^\mu\} - \\ - \sqrt{(\zeta^2-\mu^2)}g_1(\zeta)\{2\zeta^2 C_a^\mu C_z^1 - (2\zeta^2-\mu^2)C_a^1 C_z^\mu\}]. \tag{22}$$

ANTISYMMETRIC WAVES

The appropriate solutions of equations (13) for waves antisymmetric with respect to the medial plane are

$$\Delta_F = A_2 S_z^1, \qquad W_F = B_2 C_z^\mu. \tag{23}$$

If we write for the transforms of the antisymmetric components of stress on the free surface

$$f_2(\zeta) = (\widehat{zz}_F)_{z=a}, \qquad g_2(\zeta) = (\widehat{zx}_F)_{z=a}, \tag{24}$$

and proceed as in the case of symmetric waves, we obtain for the transforms of the field components

$$u_{zF} = \frac{1}{c_{44}\, D_2(\zeta; a, \mu)} [\sqrt{(\zeta^2-1)} f_2(\zeta)\{(2\zeta^2-\mu^2) C_a^\mu C_z^1 - 2\zeta^2 C_a^1 C_z^\mu\} + \\ + i\zeta g_2(\zeta)\{2\sqrt{(\zeta^2-\mu^2)}\sqrt{(\zeta^2-1)} S_a^\mu C_z^1 - (2\zeta^2-\mu^2) S_a^1 C_z^\mu\}]. \tag{25}$$

$$u_{xF} = \frac{1}{c_{44}\, D_2(\zeta; a, \mu)} [i\zeta f_2(\zeta)\{(2\zeta^2-\mu^2) C_a^\mu S_z^1 - 2\sqrt{(\zeta^2-\mu^2)}\sqrt{(\zeta^2-1)} C_a^1 S_z^\mu\} - \\ - \sqrt{(\zeta^2-\mu^2)} g_2(\zeta)\{2\zeta^2 S_a^\mu S_z^1 - (2\zeta^2-\mu^2) S_a^1 S_z^\mu\}], \tag{26}$$

where

$$D_2(\zeta; a, \mu) = (2\zeta^2-\mu^2)^2 S_a^1 C_a^\mu - 4\zeta^2\sqrt{(\zeta^2-\mu^2)}\sqrt{(\zeta^2-1)} S_a^\mu C_a^1. \tag{27}$$

Case (b) Axially symmetric field

SYMMETRIC WAVES

The solutions of equations (14) corresponding to waves having symmetry with respect to the medial plane are

$$\Delta_{B_0} = A_3 C_z^1, \qquad W_{B_1} = B_3 S_z^\mu. \tag{28}$$

If we write for the transforms of the symmetric components of stress on the free surface

$$f_3(\zeta) = (\widehat{zz}_{B_0})_{z=a}, \qquad g_3(\zeta) = (\widehat{zr}_{B_1})_{z=a}, \tag{29}$$

and proceed as before, we obtain for the transforms of the field components

$$u_{zB_0} = \frac{1}{c_{44}\, D_1(\zeta; a, \mu)} [\sqrt{(\zeta^2-1)} f_3(\zeta)\{(2\zeta^2-\mu^2) S_a^\mu S_z^1 - 2\zeta^2 S_a^1 S_z^\mu\} + \\ + \zeta g_3(\zeta)\{2\sqrt{(\zeta^2-\mu^2)}\sqrt{(\zeta^2-1)} C_a^\mu S_z^1 - (2\zeta^2-\mu^2) C_a^1 S_z^\mu\}], \tag{30}$$

$$u_{rB_1} = \frac{1}{c_{44}\, D_1(\zeta; a, \mu)} [\zeta f_3(\zeta)\{2\sqrt{(\zeta^2-\mu^2)}\sqrt{(\zeta^2-1)} S_a^1 C_z^\mu - (2\zeta^2-\mu^2) S_a^\mu C_z^1\} + \\ + \sqrt{(\zeta^2-\mu^2)} g_3(\zeta)\{(2\zeta^2-\mu^2) C_a^1 C_z^\mu - 2\zeta^2 C_a^\mu C_z^1\}]. \tag{31}$$

ANTISYMMETRIC WAVES

The solutions of equations (14) corresponding to waves antisymmetric with respect to the medial plane are

$$\Delta_{B_0} = A_4 S_z^1, \qquad W_{B_1} = B_4 C_z^\mu. \tag{32}$$

Writing for the transforms of the antisymmetric components of stress on the free surface

$$f_4(\zeta) = (\widehat{zz}_{B_0})_{z=a}, \qquad g_4(\zeta) = (\widehat{zr}_{B_1})_{z=a}, \tag{33}$$

and proceeding as before, we obtain for the transforms of the field components

$$u_{zB_0} = \frac{1}{c_{44}\, D_2(\zeta; a, \mu)} [\sqrt{(\zeta^2-1)} f_4(\zeta)\{(2\zeta^2-\mu^2) C_a^\mu C_z^1 - 2\zeta^2 C_a^1 C_z^\mu\} + \\ + \zeta g_4(\zeta)\{2\sqrt{(\zeta^2-\mu^2)}\sqrt{(\zeta^2-1)} S_a^\mu C_z^1 - (2\zeta^2-\mu^2) S_a^1 C_z^\mu\}], \tag{34}$$

$$u_{rB_1} = \frac{1}{c_{44}\, D_2(\zeta; a, \mu)} [\zeta f_4(\zeta)\{2\sqrt{(\zeta^2-\mu^2)}\sqrt{(\zeta^2-1)} C_a^1 S_z^\mu - (2\zeta^2-\mu^2) C_a^\mu S_z^1\} + \\ + \sqrt{(\zeta^2-\mu^2)} g_4(\zeta)\{(2\zeta^2-\mu^2) S_a^1 S_z^\mu - 2\zeta^2 S_a^\mu S_z^1\}]. \tag{35}$$

The displacement components are obtained by application of the appropriate inverse transform formulae.

Case (a)

SYMMETRIC WAVES

$$u_z = \frac{1}{2\pi c_{44}} \int_{-\infty}^{\infty} [\sqrt{(\zeta^2-1)} f_1(\zeta)\{(2\zeta^2-\mu^2) S_a^\mu S_z^1 - 2\zeta^2 S_a^1 S_z^\mu\} + \\ + i\zeta g_1(\zeta)\{2\sqrt{(\zeta^2-\mu^2)}\sqrt{(\zeta^2-1)} C_a^\mu S_z^1 - (2\zeta^2-\mu^2) C_a^1 S_z^\mu\}] \frac{e^{i\zeta x}\, d\zeta}{D_1(\zeta; a, \mu)}, \tag{36}$$

$$u_x = \frac{1}{2\pi c_{44}} \int_{-\infty}^{\infty} [i\zeta f_1(\zeta)\{(2\zeta^2-\mu^2) S_a^\mu C_z^1 - 2\sqrt{(\zeta^2-\mu^2)}\sqrt{(\zeta^2-1)} S_a^1 C_z^\mu\} - \\ - \sqrt{(\zeta^2-\mu^2)} g_1(\zeta)\{2\zeta^2 C_a^\mu C_z^1 - (2\zeta^2-\mu^2) C_a^1 C_z^\mu\}] \frac{e^{i\zeta x}\, d\zeta}{D_1(\zeta; a, \mu)}. \tag{37}$$

ANTISYMMETRIC WAVES

$$u_z = \frac{1}{2\pi c_{44}} \int_{-\infty}^{\infty} [\sqrt{(\zeta^2-1)} f_2(\zeta)\{(2\zeta^2-\mu^2) C_a^\mu C_z^1 - 2\zeta^2 C_a^1 C_z^\mu\} + \\ + i\zeta g_2(\zeta)\{2\sqrt{(\zeta^2-\mu^2)}\sqrt{(\zeta^2-1)} S_a^\mu C_z^1 - (2\zeta^2-\mu^2) S_a^1 C_z^\mu\}] \frac{e^{i\zeta x}\, d\zeta}{D_2(\zeta; a, \mu)}, \tag{38}$$

$$u_x = \frac{1}{2\pi c_{44}} \int_{-\infty}^{\infty} [i\zeta f_2(\zeta)\{(2\zeta^2-\mu^2) C_a^\mu S_z^1 - 2\sqrt{(\zeta^2-\mu^2)}\sqrt{(\zeta^2-1)} C_a^1 S_z^\mu\} - \\ - \sqrt{(\zeta^2-\mu^2)} g_2(\zeta)\{2\zeta^2 S_a^\mu S_z^1 - (2\zeta^2-\mu^2) S_a^1 S_z^\mu\}] \frac{e^{i\zeta x}\, d\zeta}{D_2(\zeta; a, \mu)}. \tag{39}$$

Case (b)

SYMMETRIC WAVES

$$u_z = \frac{1}{c_{44}} \int_0^\infty [\sqrt{(\zeta^2-1)} f_3(\zeta)\{(2\zeta^2-\mu^2) S_a^\mu S_z^1 - 2\zeta^2 S_a^1 S_z^\mu\} + \\ + \zeta g_3(\zeta)\{2\sqrt{(\zeta^2-\mu^2)}\sqrt{(\zeta^2-1)} C_a^\mu S_z^1 - (2\zeta^2-\mu^2) C_a^1 S_z^\mu\}] \frac{\zeta J_0(\zeta r)\, d\zeta}{D_1(\zeta; a, \mu)}, \quad (40)$$

$$u_r = \frac{1}{c_{44}} \int_0^\infty [\zeta f_3(\zeta)\{2\sqrt{(\zeta^2-\mu^2)}\sqrt{(\zeta^2-1)} S_a^1 C_z^\mu - (2\zeta^2-\mu^2) S_a^\mu C_z^1\} + \\ + \sqrt{(\zeta^2-\mu^2)} g_3(\zeta)\{(2\zeta^2-\mu^2) C_a^1 C_z^\mu - 2\zeta^2 C_a^\mu C_z^1\} \frac{\zeta J_1(\zeta r)\, d\zeta}{D_1(\zeta; a, \mu)}. \quad (41)$$

ANTISYMMETRIC WAVES

$$u_z = \frac{1}{c_{44}} \int_0^\infty [\sqrt{(\zeta^2-1)} f_4(\zeta)\{(2\zeta^2-\mu^2) C_a^\mu C_z^1 - 2\zeta^2 C_a^1 C_z^\mu\} + \\ + \zeta g_4(\zeta)\{2\sqrt{(\zeta^2-\mu^2)}\sqrt{(\zeta^2-1)} S_a^\mu C_z^1 - (2\zeta^2-\mu^2) S_a^1 C_z^\mu\}] \frac{\zeta J_0(\zeta r)\, d\zeta}{D_2(\zeta; a, \mu)}, \quad (42)$$

$$u_r = \frac{1}{c_{44}} \int_0^\infty [\zeta f_4(\zeta)\{2\sqrt{(\zeta^2-\mu^2)}\sqrt{(\zeta^2-1)} C_a^1 S_z^\mu - (2\zeta^2-\mu^2) C_a^\mu S_z^1\} + \\ + \sqrt{(\zeta^2-\mu^2)} g_4(\zeta)\{(2\zeta^2-\mu^2) S_a^1 S_z^\mu - 2\zeta^2 S_a^\mu S_z^1\}] \frac{\zeta J_1(\zeta r)\, d\zeta}{D_2(\zeta; a, \mu)}. \quad (43)$$

The integrands in the above expressions can be rearranged so as to involve only even functions of the radicals $\sqrt{(\zeta^2-\mu^2)}$ and $\sqrt{(\zeta^2-1)}$, and therefore have no branch-points. However, zeros of $D_1(\zeta; a, \mu)$ and $D_2(\zeta; a, \mu)$ give rise to poles on the real axis, and consideration of the effect of finite dissipation in the medium on the positions of the poles leads us to introduce indentations of the contour, as described in Paper I, section 3, passing above the positive and below the negative poles.

The integrals corresponding to case (*a*) are convergent at infinity in the upper half-plane, and are therefore readily evaluated by the theory of residues. To evaluate the semi-infinite integrals which arise in case (*b*), we make use of the following results from the theory of Bessel functions:

$$J_0(z) = \tfrac{1}{2}\{H_0^{(1)}(z) - H_0^{(1)}(z \exp i\pi)\}, \\ J_1(z) = \tfrac{1}{2}\{H_1^{(1)}(z) + H_1^{(1)}(z \exp i\pi)\}, \quad (44)$$

where $H_0^{(1)}$ and $H_1^{(1)}$ are Hankel functions of the first kind (see **6**, ch. 3). The integrals have one of the following two forms:

$$I_1 = \int_0^\infty \chi_1(\zeta) J_0(\zeta r)\, d\zeta, \qquad I_2 = \int_0^\infty \chi_2(\zeta) J_1(\zeta r)\, d\zeta,$$

where χ_1 and χ_2 are respectively odd and even functions of ζ. Applying the formulae (44) above, and changing to a new variable of integration, $-z$, in the second term of each integrand, we readily obtain the results

$$I_1 = \tfrac{1}{2}\int_{-\infty}^{\infty} \chi_1(\zeta) H_0^{(1)}(\zeta r)\, d\zeta, \qquad I_2 = \tfrac{1}{2}\int_{-\infty}^{\infty} \chi_2(\zeta) H_1^{(1)}(\zeta r)\, d\zeta, \tag{45}$$

the contour passing above the branch-point at the origin in each case. The integrals may now be evaluated by the theory of residues, as in case (*a*).

3. Determination of velocities of the principal waves

The affixes of the poles of the integrands in expressions (36) to (43) are determined by the equations

$$D_n(\zeta; a, \mu) = 0 \quad (n = 1, 2). \tag{46}$$

We exclude the solutions $\zeta = \mu$, $n = 1$, and $\zeta = 1$, $n = 2$, inspection of the integral formulae showing that these do not correspond to poles of the integrand. Since (46) is an equation in ζ^2, the poles are distributed symmetrically about the origin, but only the negative poles are enclosed by the contour of integration. If the positive poles, arranged in increasing order of magnitude, are denoted by $p_{nm}, m = 1, 2, \ldots$, then the corresponding phase velocities are given by

$$V_{nm} = V_c/p_{nm}, \tag{47}$$

where V_c is the velocity of a plane compressional wave in the medium. Rearrangement of the expressions (20) and (27) for $D_n(\zeta; a, \mu)$ leads to the following secular equations:

Symmetric waves

$$\frac{(2p^2-\mu^2)^2}{4p^2} = \frac{\sqrt{(p^2-\mu^2)}\sqrt{(p^2-1)}S_a^1(p)C_a^\mu(p)}{S_a^\mu(p)C_a^1(p)}. \tag{48}$$

Antisymmetric waves

$$\frac{(2p^2-\mu^2)^2}{4p^2} = \frac{\sqrt{(p^2-\mu^2)}\sqrt{(p^2-1)}S_a^\mu(p)C_a^1(p)}{S_a^1(p)C_a^\mu(p)}. \tag{49}$$

We next consider the asymptotic solutions of equations (48) and (49) as $a \to \infty$ and as $a \to 0$. Provided $|\zeta| > \mu$, we have

$$\lim_{a\to\infty} \frac{S_a^1 C_a^\mu}{S_a^\mu C_a^1} = \lim_{a\to\infty} \frac{S_a^\mu C_a^1}{S_a^1 C_a^\mu} = 1. \tag{50}$$

The limiting equation for both symmetric and antisymmetric waves with $|\zeta| > \mu$ is therefore

$$(2p^2-\mu^2)^2 = 4p^2\sqrt{(p^2-\mu^2)}\sqrt{(p^2-1)}, \tag{51}$$

which is the secular equation for surface waves propagating in a semi-infinite medium.

When $|\zeta| < \mu$ the limiting formulae (50) are no longer valid, and solutions of the secular equations exist which correspond physically to waves reflected from side to side across the plate. The path lengths of such waves will be long in comparison with the distance travelled along the plate axis, and hence they will in practice be attenuated rapidly.

For small a we may make the following approximations:

$$(2p_{1m}^2-\mu^2)^2 \doteq 4p_{1m}^2(p_{1m}^2-1),$$
$$(2p_{2m}^2-\mu^2)^2 \doteq 4p_{2m}^2(p_{2m}^2-\mu^2)\{1+\tfrac{1}{3}a^2(\mu^2-1)\}.$$

Hence,
$$p_{11}^2 \doteq \frac{\mu^4}{4(\mu^2-1)}, \qquad p_{21}^4 \doteq \frac{3\mu^4}{4a^2(\mu^2-1)},$$

there being only one real solution in each case. Therefore, for small a,

$$V_{11}^2 \doteq \frac{4(\mu^2-1)}{\mu^4}V_c^2, \qquad V_{21}^4 \doteq \frac{4a^2(\mu^2-1)}{3\mu^4}V_c^4. \tag{52}$$

Equations (46) have been solved numerically for values of a between 0 and 3·2, and for $\mu = \sqrt{3}$ and 2, corresponding to plates having Poisson ratios equal to $\frac{1}{4}$ and $\frac{1}{3}$ respectively. The results are presented in Table 1, which includes an auxiliary table of $p_{21}\sqrt{a}$ for $0 \leqslant a \leqslant 1{\cdot}2$, to assist interpolation in this range.

4. Propagation of complementary waves

It is readily established that equations (46) have only one solution in the range $\mu < |\zeta| < \infty$, corresponding to the principal symmetric and antisymmetric waves discussed in section 3. However, in the range $0 < |\zeta| < \mu$ the arguments of some or all of the hyperbolic functions are imaginary quantities, and the behaviour of the functions is oscillatory. It is clear from the limiting expressions in section 3 that no solutions are possible in this range when a is small, but as a approaches the length of a compressional wave in the plate, solutions arise which correspond to complementary waves, characterized by high phase velocity and dispersion. A. N. Holden (**2**) has investigated the behaviour of symmetric complementary waves in considerable detail, and has found confining lines for each branch of the solution of the secular equation, thereby demonstrating that the branches do not intersect. It is also evident from Holden's work that the curves representing each branch are very irregular, particularly in the region near $p = 1$. To provide an interpolable table of solutions would therefore entail a large amount of computation, and this is not attempted either by Holden or, except for the principal waves, in the present paper. Instead, Holden has studied the symmetric branches by finding a set of smoother curves about which the branches oscillate, and locating the points where the branches intersect these curves. In the present

TABLE 1

Variation of wave number with normalized plate thickness for principal waves

	p_{11}			p_{11}			p_{21}	$p_{21}\sqrt{a}$	p_{21}	$p_{21}\sqrt{a}$
a	$\mu=\sqrt{3}$	$\mu=2$	a	$\mu=\sqrt{3}$	$\mu=2$	a	$\mu=\sqrt{3}$	$\mu=\sqrt{3}$	$\mu=2$	$\mu=2$
0·00	1·061	1·155	1·75	1·684	2·009	0·0	∞	1·355	∞	1·414
0·05	1·061	1·155	1·80	1·707	2·024	0·1	4·549	1·438	4·795	1·516
0·10	1·061	1·155	1·85	1·726	2·037	0·2	3·397	1·519	3·612	1·615
0·15	1·061	1·156	1·90	1·743	2·048	0·3	2·917	1·598	3·126	1·712
0·20	1·062	1·157	1·95	1·758	2·058	0·4	2·648	1·675	2·856	1·807
0·25	1·062	1·159	2·00	1·771	2·066	0·5	2·475	1·750	2·686	1·899
0·30	1·063	1·161	2·05	1·782	2·074	0·6	2·354	1·824	2·569	1·990
0·35	1·064	1·163	2·10	1·792	2·081	0·7	2·266	1·896	2·484	2·078
0·40	1·065	1·166	2·15	1·801	2·087	0·8	2·199	1·967	2·421	2·165
0·45	1·066	1·169	2·20	1·809	2·093	0·9	2·147	2·037	2·373	2·251
0·50	1·067	1·174	2·25	1·816	2·098	1·0	2·106	2·106	2·334	2·334
0·55	1·069	1·178	2·30	1·822	2·102	1·1	2·072	2·173	2·304	2·417
0·60	1·070	1·184	2·35	1·828	2·106	1·2	2·045	2·240	2·279	2·497
0·65	1·072	1·191	2·40	1·833	2·109	1·3	2·022		2·259	
0·70	1·075	1·199	2·45	1·837	2·112	1·4	2·003		2·243	
0·75	1·078	1·208	2·50	1·841	2·115	1·5	1·987		2·229	
0·80	1·081	1·220	2·55	1·845	2·118	1·6	1·973		2·217	
0·85	1·085	1·235	2·60	1·848	2·120	1·7	1·961		2·207	
0·90	1·090	1·253	2·65	1·851	2·122	1·8	1·951		2·198	
0·95	1·096	1·276	2·70	1·854	2·124	1·9	1·943		2·191	
1·00	1·104	1·307	2·75	1·857	2·126	2·0	1·935		2·185	
1·05	1·113	1·348	2·80	1·859	2·128	2·1	1·929		2·180	
1·10	1·126	1·401	2·85	1·861	2·129	2·2	1·923		2·175	
1·15	1·142	1·468	2·90	1·863	2·130	2·3	1·918		2·171	
1·20	1·165	1·546	2·95	1·865	2·132	2·4	1·914		2·167	
1·25	1·197	1·624	3·00	1·866	2·133	2·5	1·910		2·164	
1·30	1·242	1·695	3·05	1·868	2·134	2·6	1·907		2·162	
1·35	1·303	1·757	3·10	1·869	2·135	2·7	1·904		2·160	
1·40	1·371	1·810	3·15	1·870	2·135	2·8	1·901		2·158	
1·45	1·438	1·854	3·20	1·871	2·136	2·9	1·899		2·156	
1·50	1·498	1·891				3·0	1·897		2·154	
1·55	1·549	1·923				3·1	1·896		2·153	
1·60	1·591	1·949				3·2	1·894		2·152	
1·65	1·628	1·972								
1·70	1·658	1·992								
1·75	1·684	2·009								

paper numerical solutions of both the symmetric and antisymmetric secular equations have been obtained at a sufficient number of points to enable approximate graphs of p against a to be drawn.

It is convenient to express the secular equations in the following forms:

$0 \leqslant p \leqslant 1$: *Symmetric waves:*

$$\frac{\tan a\sqrt{(\mu^2-p^2)}}{\tan a\sqrt{(1-p^2)}} = -\frac{4p^2\sqrt{(\mu^2-p^2)}\sqrt{(1-p^2)}}{(2p^2-\mu^2)^2}. \tag{53}$$

Antisymmetric waves:

$$\frac{\tan a\sqrt{(1-p^2)}}{\tan a\sqrt{(\mu^2-p^2)}} = -\frac{4p^2\sqrt{(\mu^2-p^2)}\sqrt{(1-p^2)}}{(2p^2-\mu^2)^2}. \tag{54}$$

$1 \leqslant p \leqslant \mu$: *Symmetric waves:*

$$\frac{\tan a\sqrt{(\mu^2-p^2)}}{\tanh a\sqrt{(p^2-1)}} = \frac{4p^2\sqrt{(\mu^2-p^2)}\sqrt{(p^2-1)}}{(2p^2-\mu^2)^2}. \tag{55}$$

Antisymmetric waves:

$$\frac{\tanh a\sqrt{(p^2-1)}}{\tan a\sqrt{(\mu^2-p^2)}} = \frac{4p^2\sqrt{(\mu^2-p^2)}\sqrt{(p^2-1)}}{(2p^2-\mu^2)^2}. \tag{56}$$

For the numerical solution of equations (53) and (54) we make the change of variables

$$x = a\sqrt{(1-p^2)}, \qquad m = \sqrt{(\mu^2-p^2)}/\sqrt{(1-p^2)}$$

and express the right-hand sides as functions of m and μ, so that, for example, (53) becomes

$$\frac{\tan mx}{\tan x} = F(m, \mu), \tag{57}$$

where F is independent of x. For any given m we can calculate F and hence solve (57) for x. In particular, if m is an integer $\tan mx/\tan x$ reduces to a polynomial in $\tan x$.

Similarly, when $1 \leqslant p \leqslant \mu$ we may first transform equations (55) and (56) by changing to variables $x' = a\sqrt{(p^2-1)}$ and $m' = \sqrt{(\mu^2-p^2)}/\sqrt{(p^2-1)}$, and solve for x' in terms of m'. When x' is large a good first approximation is obtained by replacing $\tanh x'$ by unity.

Figs. 1–6 illustrate the symmetric and antisymmetric branches for values of a between 0 and 8, and for $\mu = \sqrt{3}$, 2, and $\sqrt{5}$.

5. Calculation of the group velocity

The rapid variation of p with a indicates that the plate is a highly dispersive medium, and therefore in order to calculate the time of travel of a pulse of energy between two points on the surface we need to know the 'group velocity', which is the velocity at which the pulse envelope travels, as distinct from the phase velocity calculated above. A detailed analysis of propagation in a dispersive medium has been given by Sommerfeld (**7**) and Brillouin (**8**), and is summarized by Stratton (**9**). A rigorous treatment of a given problem would involve a formidable amount of numerical

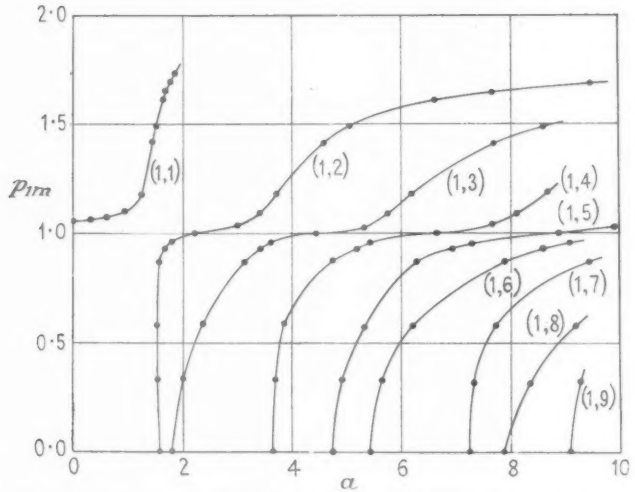

FIG. 1. Variation of wave number with normalized plate thickness for principal and complementary waves. Symmetric case, $\mu = \sqrt{3}$.

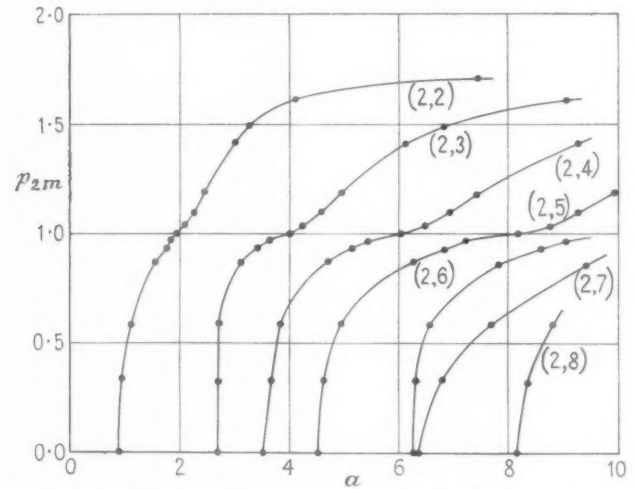

FIG. 2. Variation of wave number with normalized plate thickness for complementary waves. Antisymmetric case, $\mu = \sqrt{3}$.

computation, but if the signal is such that its Fourier representation is confined to a narrow band of the frequency spectrum, the phase velocity may be represented in terms of frequency over this range by the first two

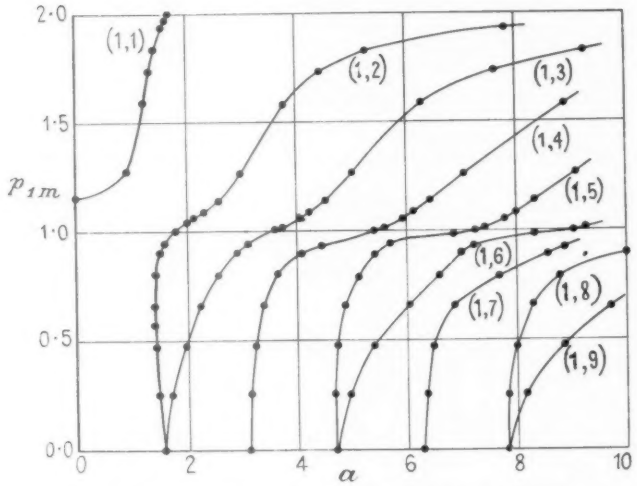

FIG. 3. Variation of wave number with normalized plate thickness for principal and complementary waves. Symmetric case, $\mu = 2$.

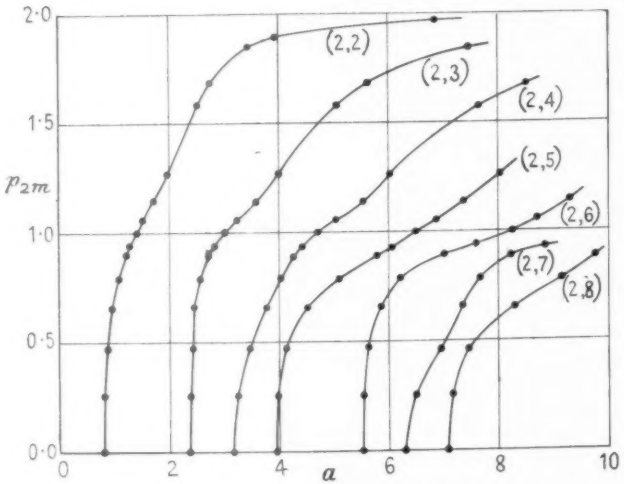

FIG. 4. Variation of wave number with normalized plate thickness for complementary waves. Antisymmetric case, $\mu = 2$.

terms of a Taylor series, and the group velocity is then given by the formula

$$U = \frac{V}{1-(\omega/V)(dV/d\omega)}, \tag{58}$$

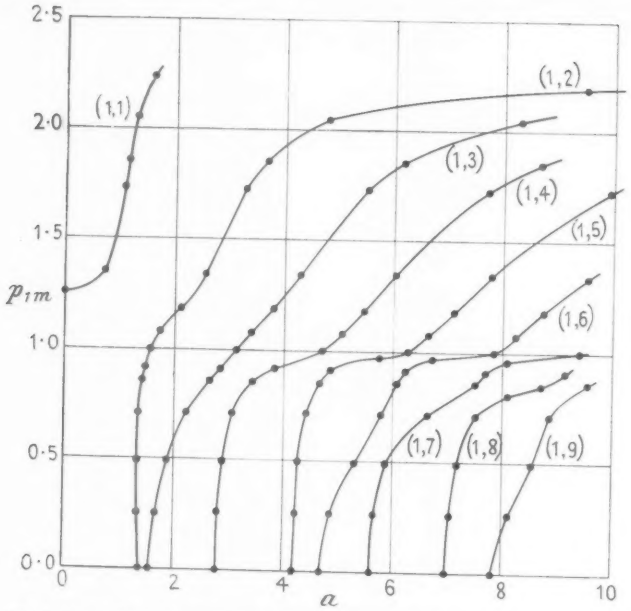

FIG. 5. Variation of wave number with normalized plate thickness for principal and complementary waves. Symmetric case, $\mu = \sqrt{5}$.

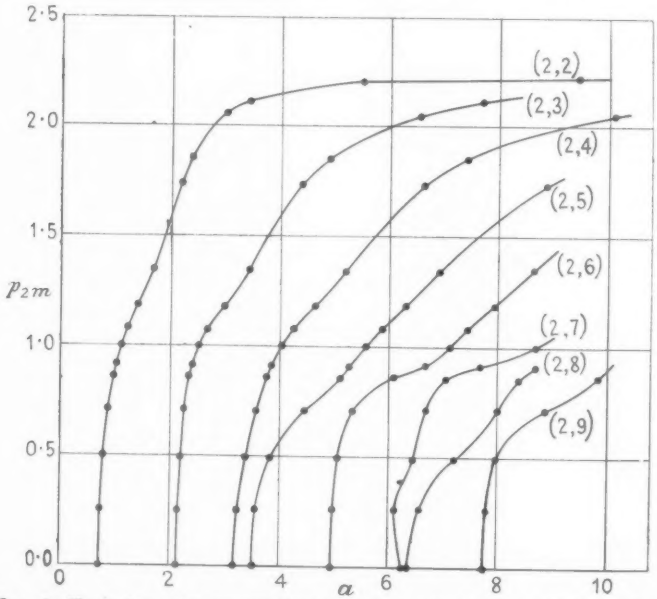

FIG. 6. Variation of wave number with normalized plate thickness for complementary waves. Antisymmetric case, $\mu = \sqrt{5}$.

where U is the group velocity, V is the phase velocity, and ω is the angular frequency. This formula cannot be applied in the neighbourhood of a cut-off frequency, where the Taylor-series representation ceases to be valid. In such a region the pulse shape would be greatly distorted, and the concept of group velocity would no longer be meaningful.

Now if a_0 is the thickness of the plate in unnormalized units, we have

$$a = k_1 a_0,$$

and hence

$$\omega = k_1 V_c = a V_c / a_0.$$

Using equation (47) we obtain

$$\frac{\omega}{V} = \frac{ap}{a_0}, \qquad \frac{dV}{d\omega} = -\frac{a_0\, dp}{p^2\, da},$$

and

$$U = \frac{V}{1+(a/p)(dp/da)} = \frac{V_c}{d(ap)/da}. \tag{59}$$

The equations relating p and a are of the form

$$\phi(p) = \psi_n(p, a), \tag{60}$$

where

$$\phi(p) = \frac{4p^2\sqrt{(p^2-\mu^2)}\sqrt{(p^2-1)}}{(2p^2-\mu^2)^2}, \tag{61}$$

$$\psi_1(p,a) = \frac{S_a^\mu(p) C_a^1(p)}{S_a^1(p) C_a^1(p)} \quad \text{for symmetric waves,} \tag{62}$$

and

$$\psi_2(p,a) = \frac{S_a^1(p) C_a^\mu(p)}{S_a^\mu(p) C_a^1(p)} \quad \text{for antisymmetric waves.} \tag{63}$$

On differentiating we obtain

$$\frac{dp}{da} = \frac{\partial\psi_n/\partial a}{d\phi/dp - \partial\psi_n/\partial p}. \tag{64}$$

We deduce the following formulae from equations (61), (62), and (63):

$$\frac{d\phi}{dp} = \frac{8(1-\mu^2)p^5 + 4\mu^2(3\mu^2-1)p^3 - 8\mu^4 p}{(2p^2-\mu^2)^3\sqrt{(p^2-\mu^2)}\sqrt{(p^2-1)}}, \tag{65}$$

$$\frac{\partial\psi_1}{\partial a} = \frac{1}{S_a^1(p) C_a^\mu(p)}\left\{\frac{\sqrt{(p^2-\mu^2)}\, C_a^1(p)}{C_a^\mu(p)} - \frac{\sqrt{(p^2-1)}\, S_a^\mu(p)}{S_a^1(p)}\right\}, \tag{66}$$

$$\frac{\partial\psi_1}{\partial p} = \frac{ap}{S_a^1(p) C_a^\mu(p)}\left\{\frac{C_a^1(p)}{\sqrt{(p^2-\mu^2)}\, C_a^\mu(p)} - \frac{S_a^\mu(p)}{\sqrt{(p^2-1)}\, S_a^1(p)}\right\}, \tag{67}$$

$$\frac{\partial\psi_2}{\partial a} = \frac{1}{C_a^1(p) S_a^\mu(p)}\left\{\frac{\sqrt{(p^2-\mu^2)}\, S_a^1(p)}{S_a^\mu(p)} - \frac{\sqrt{(p^2-1)}\, C_a^\mu(p)}{C_a^1(p)}\right\}, \tag{68}$$

$$\frac{\partial\psi_2}{\partial p} = \frac{ap}{C_a^1(p) S_a^\mu(p)}\left\{\frac{S_a^1(p)}{\sqrt{(p^2-\mu^2)}\, S_a^\mu(p)} - \frac{C_a^\mu(p)}{\sqrt{(p^2-1)}\, C_a^1(p)}\right\}. \tag{69}$$

Values of the group velocity U may be calculated once equations (48) and (49) have been solved for p.

A curve showing the variation of group velocity with plate thickness for the principal symmetric mode in a plate having a Poisson ratio of 0·29 (corresponding to $\mu = 1{\cdot}839$) is given by H. Kolsky (**10**), and a set of curves showing the phase and group velocities of the first five symmetric and antisymmetric modes in aluminium sheet as functions of the product of frequency and plate thickness is given by Firestone (**11**). In the next section of the present paper a more detailed analysis is given of a single case, and both phase and group velocities are evaluated for all propagating modes, as well as the amplitudes of the waves at a point distant from the source.

6. Investigation of the modes generated in a plate whose thickness is of the order of a wavelength

To illustrate the way in which the theory developed in the preceding sections may be applied to a practical case, we consider the normal surface displacement due to a small circular source of radius r_0 on one side of the plate. We shall assume the stress on the portion of the surface under the source to be unity, and the plate to have a thickness of $2\lambda_c/\pi$ and a Poisson's ratio of $\frac{1}{3}$, so that $a = k_1\lambda_c/\pi = 2$ and $\mu = 2$.

The boundary conditions on the free surface are therefore:

$$z = a: \quad \widehat{zr} = 0 \text{ (for all } r), \quad \widehat{zz} = 1 \ (r < r_0), \quad \widehat{zz} = 0 \ (r > r_0), \tag{70}$$

$$z = -a: \quad \widehat{zr} = \widehat{zz} = 0 \text{ (for all } r). \tag{71}$$

If we denote the symmetric and antisymmetric components of stress by $\widehat{zz}^{(1)}$ and $\widehat{zz}^{(2)}$ respectively, it follows that

$$\widehat{zz}^{(1)} = \widehat{zz}^{(2)} = \tfrac{1}{2} \quad (r < r_0), \tag{72}$$

$$\widehat{zz}^{(1)} = \widehat{zz}^{(2)} = 0 \quad (r > r_0), \tag{73}$$

and from equations (12), (29), and (33) we find for the transforms of the stress components

$$f_3(\zeta) = f_4(\zeta) = \frac{r_0 J_1(\zeta r_0)}{2\zeta}, \tag{74}$$

$$g_3(\zeta) = g_4(\zeta) = 0. \tag{75}$$

We therefore derive from equations (40)–(43) the following expressions for the normal displacement components on the surface of the plate:

Symmetric component:

$$u_z^{(1)} = -\frac{\mu^2 r_0}{4c_{44}} \int_{-\infty}^{\infty} \sqrt{(\zeta^2-1)} S_a^{\mu} S_a^1 \frac{J_1(\zeta r_0) H_0^{(1)}(\zeta r)\, d\zeta}{D_1(\zeta; a, \mu)}. \tag{76}$$

Antisymmetric component:

$$u_z^{(2)} = -\frac{\mu^2 r_0}{4c_{44}} \int_{-\infty}^{\infty} \sqrt{(\zeta^2-1)} C_a^\mu C_a^1 \frac{J_1(\zeta r_0) H_0^{(1)}(\zeta r)\, d\zeta}{D_2(\zeta; a, \mu)}. \tag{77}$$

For small values of r_0 we may put $J_1(\zeta r_0) \sim \frac{1}{2}\zeta r_0$, and equations (76) and (77) then become:

$$u_z^{(1)} \sim -\frac{\mu^2 r_0^2}{8c_{44}} \int_{-\infty}^{\infty} \sqrt{(\zeta^2-1)} S_a^\mu S_a^1 \frac{H_0^{(1)}(\zeta r)\zeta\, d\zeta}{D_1(\zeta; a, \mu)}, \tag{78}$$

$$u_z^{(2)} \sim -\frac{\mu^2 r_0^2}{8c_{44}} \int_{-\infty}^{\infty} \sqrt{(\zeta^2-1)} C_a^\mu C_a^1 \frac{H_0^{(1)}(\zeta r)\zeta\, d\zeta}{D_2(\zeta; a, \mu)}, \tag{79}$$

and on evaluating the integrals we obtain

$$u_z^{(1)} \sim -\frac{\pi i \mu^2 r_0^2}{4c_{44}} \sum_m \sqrt{(p^2-1)} S_a^\mu(p) S_a^1(p) \frac{H_0^{(1)}(e^{i\pi} rp)p}{D_1'(p; a, \mu)}, \tag{80}$$

$$u_z^{(2)} \sim -\frac{\pi i \mu^2 r_0^2}{4c_{44}} \sum_m \sqrt{(p^2-1)} C_a^\mu(p) C_a^1(p) \frac{H_0^{(1)}(e^{i\pi} rp)p}{D_2'(p; a, \mu)}, \tag{81}$$

the primes denoting differentiation with respect to p. For large values of r the Hankel function may be represented by the first term of its asymptotic expansion, namely,

$$H_0^{(1)}(z) \sim \left(\frac{2}{\pi z}\right)^{\frac{1}{2}} e^{i(z-\frac{1}{4}\pi)},$$

and we then find for the displacement components

$$u_z^{(1)} \sim \frac{\sqrt{(2\pi)}\mu^2 r_0^2 e^{\frac{1}{4}i\pi}}{4c_{44}\sqrt{r}} \sum_m \sqrt{\{p(p^2-1)\}} S_a^\mu(p) S_a^1(p) \frac{e^{-ipr}}{D_1'(p; a, \mu)}, \tag{82}$$

$$u_z^{(2)} \sim \frac{\sqrt{(2\pi)}\mu^2 r_0^2 e^{\frac{1}{4}i\pi}}{4c_{44}\sqrt{r}} \sum_m \sqrt{\{p(p^2-1)\}} C_a^\mu(p) C_a^1(p) \frac{e^{-ipr}}{D_2'(p; a, \mu)}. \tag{83}$$

If we introduce the notation

$$\Phi_1(p) = \sqrt{\{2\pi p(p^2-1)\}} \frac{S_a^\mu(p) S_a^1(p)}{D_1'(p; a, \mu)}, \tag{84}$$

$$\Phi_2(p) = \sqrt{\{2\pi p(p^2-1)\}} \frac{C_a^\mu(p) C_a^1(p)}{D_2'(p; a, \mu)}, \tag{85}$$

(82) and (83) become

$$u_z^{(1)} \sim \frac{\mu^2 r_0^2}{4c_{44}} \sum_m \Phi_1 \frac{e^{i(\frac{1}{4}\pi - pr)}}{\sqrt{r}}, \tag{86}$$

$$u_z^{(2)} \sim \frac{\mu^2 r_0^2}{4c_{44}} \sum_m \Phi_2 \frac{e^{i(\frac{1}{4}\pi - pr)}}{\sqrt{r}}. \tag{87}$$

Inspection of Figs. 3 and 4 shows that three symmetric and two antisymmetric waves are propagated, and corresponding values of the phase velocity, group velocity, and relative amplitudes of the waves are given in Table 2.

TABLE 2

n	m	p_{nm}	dp/da	V/V_c	U/V_c	$D_n(p;2,2)$	$\Phi_n(p)$
1	1	2·0665	0·1645	0·4839	0·4175	8576	0·01748
1	2	1·0361	0·1659	0·9651	0·7310	130·3	$-0{\cdot}0008207i$
1	3	0·5050	0·7331	1·9802	0·5073	$-14{\cdot}25i$	$0{\cdot}07101i$
2	1	2·1849	0·1739	0·4577	0·3949	−13590	−0·03856
2	2	1·2768	2·7211	0·7832	0·1488	102·0	$-0{\cdot}05610$

The ratio of phase velocity to group velocity for a given wave is a measure of the degree of dispersion of the wave, and it will be seen from the table above that the values of this ratio for the (1, 3) and (2, 2) waves are approximately four and five. This well illustrates the need for calculating the group velocity in determining the travel time of a pulse of energy along the plate and, conversely, provides a warning against facile interpretation of travel time measurements in elasticity determination.

Acknowledgements

The author wishes to acknowledge the contribution of Mr. G. F. Miller and Mrs. O. E. Taylor, who carried out most of the computation involved in the preparation of Table 1 and Figs. 1–6. Acknowledgement is also due to Mr. Miller for much helpful criticism and advice, and for assistance in checking the equations and the numerical results presented in Table 2.

The work described above has been carried out as part of the research programme of the National Physical Laboratory, and this paper is published by permission of the Director of the Laboratory.

REFERENCES

1. H. LAMB, *Proc. Roy. Soc.* A, **93** (1917), 114.
2. A. N. HOLDEN, *B.S.T.J.* **30** (1951), 956.
3. M. F. M. OSBORNE and S. D. HART, *J. Acoust. Soc. Amer.* **17** (1945), 1.
4. G. E. HUDSON, *Phys. Rev.* **63** (1943), 46.
5. G. F. MILLER and H. PURSEY, *Proc. Roy. Soc.* A, **223** (1954), 521.
6. G. N. WATSON, *A Treatise on the Theory of Bessel Functions* (Cambridge, 1922).
7. A. SOMMERFELD, *Ann. d. Phys.* **44** (1914), 177.
8. L. BRILLOUIN, ibid. 203.
9. J. A. STRATTON, *Electromagnetic Theory* (McGraw Hill, 1941).
10. H. KOLSKY, *Stress Waves in Solids* (Oxford, 1953).
11. F. A. FIRESTONE, *Non-destructive Testing*, **7** (1948), 5.

VIBRATIONS OF BEAMS

I. LONGITUDINAL MODES

By G. J. KYNCH *and* W. A. GREEN

(*University College of Wales, Aberystwyth*)

[Received 9 February 1956]

SUMMARY

Second-order perturbation theory, using known solutions for a circular cylinder, is applied to the exact elasticity equations to determine the wavelength frequency curves for the longitudinal vibrations of a non-circular cylinder. General formulae are given and applied to elliptic, square, and rectangular beams. Owing to resonance, the simplest technique is inadequate at certain wavelengths for elliptical and rectangular beams, and this makes the method rather cumbersome. It is also clear that such sections as a square deviate sufficiently from a circle as to demand the inclusion of third-order terms.

1. Introduction

THE velocity of longitudinal stress waves along uniform beams has been calculated for sections which are circular and rectangular using the exact elasticity equations, assuming Hooke's law for an isotropic material (cf. R. M. Davies (**1**), for references). In this paper and a later one we seek the solution of the same problem for a beam with a general section whose boundary, in polar coordinates, has the form

$$r = a(1 + \sum b_s \cos s\theta), \tag{1.1}$$

where the coefficients b_s are small. We do this using a perturbation theory based on the solutions in polar coordinates used to solve the problem for a circular cylinder $r = a$. In other words, for a given wavelength, we expand the phase velocity as a power series in the coefficients b_s.

In this way we hoped not only to obtain more general results than those obtained previously and to observe the effect on the dispersion curve of various changes in the shape of the cross-section, but also to explore the possibilities of perturbation theory in this type of problem and to see if it could be used to derive other approximations which might give better results. Moreover, by using a series of type (1.1) as an approximation to sections with sharp corners, it may be possible to estimate the effect on the velocity of rubbing off the corners.

The construction of a second-order perturbation theory was straightforward, but an extension to third-order is very elaborate. It is easy to include what seem to be the main third-order terms, but the magnitude of the residue could not be determined. This meant that the limits of validity

of the second-order theory, which fixes bounds on the magnitude of the coefficients b_s, could not be determined by an examination of higher-order terms. We therefore apply our results to a square cross-section, for which experimental results are available (**2**). Although this comparison was rather inadequate, it made two things clear. First, that the second-order theory is not adequate for such a section, and higher-order terms should be included, a result not unexpected, as a square is appreciably different from a circle. Secondly, the effect of the higher coefficients b_s with $s > 8$ was quite negligible, i.e. less than 1 in 10^5, for all frequencies corresponding to velocities greater than the shear wave velocity, and possibly for higher frequencies.

As the work is in part exploratory, and the calculations lengthy, they were not made for many frequencies, and the frequencies chosen were near crucial points in the dispersion curve. For example, a value giving a phase velocity approximately $\sqrt{2}$ times the shear wave velocity was chosen because of a limitation on the perturbation theory which was not suspected when the calculations began. This limitation is due to a degeneracy of two distinct modes of vibration of a circular cylinder in this region, and needs a little explanation.

As the basis of our theory we use solutions of the elasticity equations in polar coordinates, which can be classified according to the number (n) of nodal planes intersecting the axis. The fundamental modes of vibration of the circular cylinder are then classified by the solutions needed to describe them. For the longitudinal and torsional modes $n = 0$, for the flexural modes $n = 1$, for the screw modes $n = 2$, and so on (the existence of higher modes is not yet certain). Using an approximate theory it was discovered that the longitudinal and another mode, which was later described as a screw mode, had dispersion curves which intersect in the region $c^2 = 2c_s^2$, and that the torsional and screw modes intersect where the latter crosses $c^2 = c_s^2$. Now the perturbation theory breaks down whenever the boundary conditions couple two solutions which describe degenerate modes of the circular cylinder. Hence it breaks down for the present calculation of the longitudinal mode near $c^2 = 2c_s^2$ and gives poor results in the neighbourhood of this value.

This difficulty does not arise for a square cylinder, where the solutions needed are those for $n = 0, 4, 8, \ldots$ and there is no coupling between the longitudinal and screw modes, nor does it arise for sections such as an equilateral triangle. It does arise for an elliptical or rectangular cross-section, where values of n differing by 2 are needed, and as a result, the dispersion curves for the longitudinal and screw modes, $n = 0$ and 2 respectively, are replaced by two adjacent branches which do not intersect. This is in agreement with the experimental results obtained by Morse.

The results of our calculations are summarized in section 3 and Table 1. Using this table it is possible to calculate the change in phase velocity at various wavelengths, due to changes in the cross-section due to terms b_{2s} $(s < 6)$.

2. Method of calculation

To find the oscillations of a circular cylinder it is appropriate to use cylindrical coordinates (r, θ, z) and to set up the elasticity equations for the components (u, v, w) of the displacement in the radial, transverse, and longitudinal directions, respectively.

The axis of the cylinder is along the z-axis, and we look for solutions where the components are proportional to $e^{i(n\theta+kz-\omega t)}$, where n is an integer, $k(=2\pi/\lambda)$ the wave number, $\omega\,(=2\pi\nu)$ the angular frequency, and $c\,(=\omega/k)$ the phase velocity. Thus ka is the number of wavelengths in the perimeter of the cylinder.

There are three solutions of the equations for each value of n, which are labelled $i = 1, 2, 3$:

$$\left.\begin{aligned} u &= u_{ni}(A_{ni}\cos n\theta + B_{ni}\sin n\theta)\cos(kz-\omega t) \\ v &= v_{ni}(A_{ni}\sin n\theta - B_{ni}\cos n\theta)\cos(kz-\omega t) \\ w &= w_{ni}(A_{ni}\cos n\theta + B_{ni}\sin n\theta)\sin(kz-\omega t) \end{aligned}\right\}. \tag{2.1}$$

The expressions for u_{ni}, v_{ni}, w_{ni} are given in the Appendix. The general solution is a linear combination of these solutions, and the stress components p_{rz}, etc., are determined by the formulae given by Love (**3**).

In the case of a circular cylinder, the boundary conditions,

$$p_{zr} = p_{r\theta} = p_{rr} = 0 \quad \text{at } r = a,$$

are satisfied by combinations of the solutions for *each* value of n. In fact, we only need the solution $n = 0$, $i = 1$ for the torsional mode and its harmonics, and a mixture of the solutions $n = 0$, $i = 2$ and 3, for the longitudinal mode of vibration and its harmonics. The two flexural oscillations A_1 and B_1 are determined by the solutions with $n = 1$, one needing the solutions with coefficients A (cf. (2.1)) and the other solutions with the coefficients B. The two screw vibrations A_2 and B_2 require solutions with $n = 2$, and so on. The equations which determine the phase velocities are the Pochhammer equations, which have been solved numerically by R. M. Davies (**4**), and Bancroft (**5**) for $n = 0$, and by Hudson (**6**) for $n = 1$.

By plotting phase velocity against wavelength or frequency for each mode, a branch of the dispersion curve is obtained. These branches and their relative positions are shown in Fig. 1, for long waves. This diagram, which does not include the harmonics, shows that the number of inter-

sections, or cross-overs, of the branches is small in this range of wavelengths. There may be more when the wavelength is small compared with the mean diameter. These cross-overs are important because any small change in the boundary which mixes two modes of vibration, causes a separation of their dispersion curves at the cross-over, as indicated by the dotted lines, at

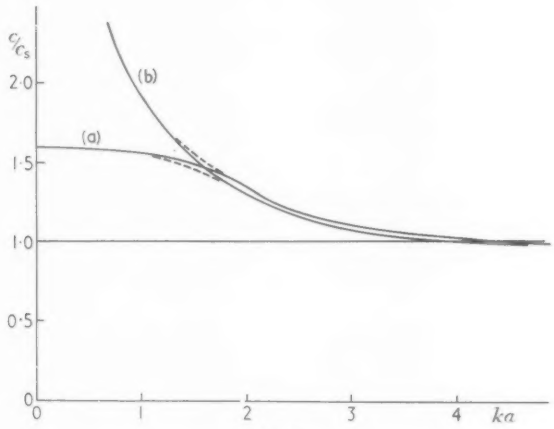

FIG. 1

some points in the figure, which cannot be dealt with by simple perturbation theory. In fact, our calculations break down near such points, although this type of degeneracy can be dealt with easily in principle, because the amount of numerical work is excessive. If we include harmonics of the different modes there are further cross-overs with the screw branch and its harmonics.

As we see later, the solutions for a normal oscillation with the perturbed boundary (1.1), which only involves terms in cosines and therefore has one plane of symmetry, divide into two groups containing, respectively, the solutions (2.1) with coefficients A and with coefficients B. The first includes the longitudinal mode and the second the torsional mode. Detailed considerations depend on the symmetry of the cross-section and the coefficients b_s which occur in its equation. In general a non-zero coefficient b_s mixes the elementary solutions with values of n differing by a multiple of s.

For example, a square boundary only requires terms in $b_4, b_8, \ldots$. Consequently the solutions are mixed in the four groups $n = (0, 4, 8, \ldots), (1, 5, 9, \ldots), (2, 6, \ldots)$, and $(3, 7, \ldots)$. Thus, not only are the torsional and longitudinal vibrations, $n = 0$, never mixed, as explained above, but they never mix with the flexural vibrations $n = 1$ or the screw vibrations $n = 2$. Thus

the cross-overs with the screw vibrations for the circular cylinder are unimportant for our calculations, but are retained in the dispersion curves for an exactly square beam. The same is true for a beam whose section is an equilateral triangle, whose motion is described by mixtures of solutions with values of n differing by multiples of three.

This is not true for a rectangular or elliptical beam, where terms in b_2 occur. There are now only two groups of solution, n even or n odd, for either A or B, so that the longitudinal and screw mode A are mixed, and the torsional and screw mode B (**7**). The flexural mode ($n = 1$) is mixed with higher orders. The low-frequency cross-overs are now relevant, since the separation of the dispersion curves means that the low-frequency part of the longitudinal branch joins up smoothly with the high-frequency screw branch, and vice versa, together with a similar effect on the torsion branch.

The calculations for non-circular beams proceed as follows. The boundary conditions for a uniform infinite beam, on the curved surface, are

$$p_{jr}\, r\, d\theta - p_{j\theta}\, dr = 0, \tag{2.2}$$

where the suffix j has the values 1, 2, 3 corresponding to suffixes r, θ, z. Both r and the stress components on the boundary are periodic functions of θ with period 2π, so that these equations can be expanded as Fourier series, and become

$$\sum_m (F_{jm} \cos m\theta + F'_{jm} \sin m\theta) = 0 \quad (j = 1, 2, 3)$$

where
$$\left.\begin{aligned} \pi F_{jm} &= \int_0^{2\pi} \cos m\theta \{r p_{jr} - (dr/d\theta) p_{j\theta}\}\, d\theta \quad (m \neq 0) \\ 2\pi F_{j0} &= \int_0^{2\pi} \{r p_{jr} - (dr/d\theta) p_{j\theta}\}\, d\theta \qquad\quad (m = 0) \end{aligned}\right\}. \tag{2.3}$$

The equations for F'_{jm} are similar to those for F_{jm}. Then the orthogonal property of the circular functions enables us to replace these by the equations

$$F_{jm} = 0, \qquad F'_{jm} = 0 \quad (\text{all } m, j). \tag{2.4}$$

Now the stress components and the Fourier coefficients are linear functions of the displacements and the coefficients A_{in}, B_{in} in the displacements. Moreover, it is easily shown that the coefficients B do not appear in F_{jm} nor the coefficients A in F'_{jm} when r is an even function of θ on the boundary. Hence these equations form two sets of linear simultaneous equations

$$F_{jm} = \sum_{i,n} P^{in}_{jm} A_{in} = 0, \qquad F'_{jm} = \sum_{i,n} Q^{in}_{jm} B_{in} = 0 \quad (\text{all } j, m) \tag{2.5}$$

which have non-zero solutions only when the determinants of the coefficients vanish,

$$\|P^{in}_{jm}\| = 0, \qquad \|Q^{in}_{jm}\| = 0. \tag{2.6}$$

The determinant P includes the solutions $n = 0$, $i = 2$ and 3 which appear in the longitudinal vibration of a circular cylinder, so that it has one solution corresponding to the longitudinal oscillation of the given beam. The determinant Q includes the solution $n = 0$, $i = 1$ for the torsional oscillation of a circular cylinder, so that it has one solution corresponding to a torsional oscillation of the given beam. We can also deduce from

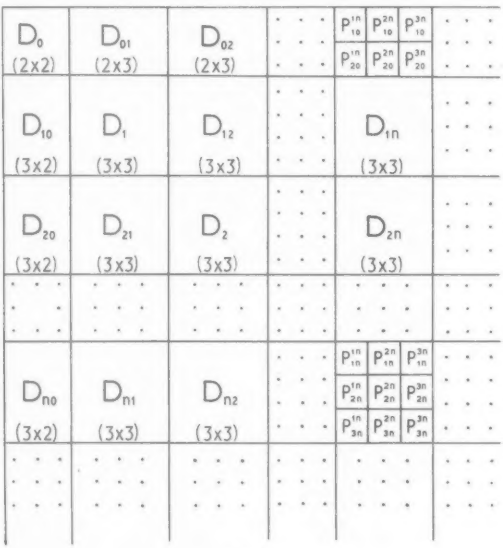

FIG. 2

equations (2.3) and (2.5) the earlier statement on the mixing of the various solutions, for example that, when r contains only terms in 2θ, 4θ,..., then the elements P^{in}_{jm}, Q^{in}_{jm} of the determinants are zero unless m and n are both even or both odd, so that the determinants factorize into two smaller determinants.

The solution of (2.6) by perturbation theory begins with the expansion of the elements in powers of the small quantities b_s, which we may assume to be of the same order of magnitude. The determinant P has the form shown in Fig. 2.

When the b_s are all zero, this determinant reduces to a product of small determinants $D_0 D_1 D_2$..., where D_0 is constructed from elements with $m = n = 0$ and has two rows and columns, D_n is constructed from elements $m = n$ $(n > 0)$ and has three rows and columns. When the b_s are not zero, there are further terms of order b_s or higher order in the off-diagonal positions D_{mn} $(m \neq n)$.

For a complete solution, the determinant should first be transformed so that all the off-diagonal elements D_{mn} $(m \neq n)$ become zero. In particular, to find the longitudinal vibration, we should transform it so that the terms D_{0n} and D_{m0} are zero, whereupon the determinant factorizes into two parts, one corresponding to D_0 which gives the longitudinal frequencies, and the other including all remaining motions. Such a solution is not possible, but it is possible to obtain answers correct to the second order by removing the terms in b_s from the elements D_{0n}. This can be done fairly easily, by subtracting from these two rows, multiples of the three rows of D_n, i.e. by subtracting multiples p, q, r of the three rows $m = n$, chosen so that

$$\left.\begin{aligned} P^{in}_{1n}\,p_n + P^{in}_{2n}\,q_n + P^{in}_{3n}\,r_n &= P^{in}_{10} \quad (i = 1, 2, 3) \\ P^{in}_{1n}\,p'_n + P^{in}_{2n}\,q'_n + P^{in}_{3n}\,r'_n &= P^{in}_{20} \quad (i = 1, 2, 3) \end{aligned}\right\}. \tag{2.7}$$

In these equations the terms P^{in}_{jn} are needed only to order zero, so that they have solutions, unless $D_n = 0$, without any limitations on the right-hand sides. The subtraction is performed for every value of n (except zero), with the result that the terms in the position of the matrix D_{0n} are of order b_s^2 and the determinant D_0 has become, with revised elements,

$$D'_0 = \begin{vmatrix} \overline{P^{10}_{10}} & \overline{P^{10}_{20}} \\ \overline{P^{20}_{10}} & \overline{P^{20}_{20}} \end{vmatrix}. \tag{2.8}$$

Since the elements D_{m0} $(m > 0)$ are at most of order b_s, the whole determinant can be expanded in the form

$$D'_0 \times \{D_1\,D_2 \ldots + \text{terms due to } b_s\} + \text{terms of order } b_s^3 = 0.$$

Provided the determinants D_1, D_2,... are not too small, this equation has one solution,

$$D'_0 = 0 \quad (\text{to order } b_s^2).$$

In the evaluation of the correction terms we assume that the phase velocity differs little from the solution of $D_0 = 0$ for the longitudinal mode of a circular cylinder of the same wavelength. Our perturbation theory therefore breaks down either for large values of the coefficients b_s, or when one of the determinants D_n becomes small for this velocity and wavelength, i.e. the two dispersion curves come close together, for two different branches of a circular cylinder corresponding to zero values of D_0 and D_n. In fact, for wavelengths which are not much smaller than the lateral dimensions of the beam, only one determinant becomes small in this way, namely D_2. This does not matter in calculations for beams with fourfold symmetry such as a square, as explained above, but it does upset those for a rectangle or ellipse where $n = 2$ is also required. For such beams calculations by our present method are inaccurate in the range of

wavelengths where D_2 is zero or small. Points are obtained for both smaller and larger wavelengths, but the former are probably not very good, and although they describe essentially longitudinal vibrations, they do not lie on the same (continuous) branch of the dispersion curve as the latter.

The various elements of the determinant used in these calculations are given in the Appendix.

3. Results

In view of the numerical work involved, the calculations were made for only one value of Poisson's ratio, $\sigma = 0{\cdot}3$, for the limit of long wavelengths and four other frequencies, one of them the frequency such that the phase velocity c equals the shear wave velocity. The results are summarized in Table 1.

The final determinant D_0' is expanded and expressed in the form

$$-D_0' = \Delta + \sum \tfrac{1}{4} b_s^2 \Gamma_s, \tag{3.1}$$

where

$$\Delta = \{1+\phi_0(\beta a)\} - \tfrac{1}{2}(1-\beta^2/k^2)(1+K\phi_0(\alpha a)),$$

$$K = 1+\lambda(k^2+\alpha^2)/2\mu a^2, \quad \text{and} \quad \phi_0(x) = xJ_0(x)/J_0'(x).$$

The coefficients Γ_s are functions of the wavelength. The phase velocity is now determined from the equation $D_0' = 0$, or

$$\Delta = -\sum \tfrac{1}{4} b_s^2 \Gamma_s. \tag{3.2}$$

The phase velocity can be expressed as a function of Δ in the form

$$c^2\,(\text{section}) - c^2\,(\text{circle}) = -c_s^2\{A\Delta + B\Delta^2 + C\Delta^3 + \ldots\}. \tag{3.3}$$

The coefficients A, B, C are given in Table 1. This table includes, therefore,

TABLE 1

Values of Γ_s

$c^2/c_s^2(circle)$	(*a*) 2·6	(*b*) 49/19	(*c*) 7/3	(*d*) 2	(*e*) 1
βa	0	0·52614	1·53263	1·84118	0
$\alpha a/i$	0	0·21480	0·76631	1·20534	3·6333
Γ_2	0	0·82874	28·3785	−12·7090	−45·529
Γ_4	0	0·78093	10·9652	19·2997	4·430
Γ_6	0	0·78416	11·3056	22·6800	10·281
Γ_8	0	0·79580	12·5337	26·6755	19·383
Γ_{10}	0	..	14·0881	31·379	30·225
Γ_{12}	0	..	16·105	36·386	42·109
A	0	0·29299	0·51133	0·91139	0·53030
B	0	0·10000	0·3900	0·86338	0·21245
C	0	..	..	1·10	0·15

all the information necessary to obtain a number of points on the longitudinal branches of the dispersion curve.

Using these results, phase velocities were calculated for three sections, an ellipse of eccentricity $e = \frac{1}{2}$, a square, and a rectangle with sides in the ratio 6 : 5. These were chosen for reasons which appear later. The coefficients b_s for these sections are given in the Appendix, together with the radius a of the cylinder with which they are compared. This radius a is the mean value of the radius vector r around the section.

TABLE 2

$c_s^2 = \mu/\rho$; ω = angular frequency; a = mean radius.

		c^2/c_s^2			
	$\omega a/c_s$	*Circle*	*Ellipse*	*Square*	*Rectangle*
(*a*)	0	2·6	2·6	2·6	2·6
(*b*)	0·6724	2·5781	2·5786	2·5777	2·5771
(*c*)	2·0275	2·3333	2·3140	2·3016	2·2549
(*d*)	2·6038	2·0000	2·0146	1·8921	1·9450
(*e*)	4·2990	1·0000	1·0304	0·9834	1·0558

The results are given in Table 2. In judging the results it should be remembered that the coefficients b_s in all three cases are probably as large as can be justified by using second-order perturbation theory. Moreover, (3.1) shows that, when $c^2 = 2c_s^2$ and $\beta = k$, the value of βa is completely determined for a circular cylinder, and is independent of Poisson's ratio. This value of the phase velocity, according to the approximate theory, also makes D_2 vanish as well as D_0, and although the true value for this to occur is a little less, it is close enough to upset the perturbation theory, for a rectangular or elliptical section. In fact, we see from Table 2 that for the ellipse the points for lower frequencies lie below those for the circle, and lie on one branch, and those for higher frequencies lie above those for the circle and lie on another branch. A similar comparison between the square and rectangle gives the same result, for sections with the same value of a.

We can compare these results for a square and rectangle with those of Morse (**2**) assuming, as he does, that the shear wave velocity is 2,160 metres per second and Poisson's ratio is 0·30. This enables us to calculate the frequencies corresponding to the three phase velocities near $c^2/c_s^2 = 7/3$, 2, and 1·5 (the set for 1·5 is estimated from the calculated values). The results are given in Table 3.† The difference in the values for a square at the lowest frequency can be explained by an error in Poisson's ratio, but this does not explain the difference at $c^2 = 2c_s^2$. This can only be due to

† We are grateful to Dr. Morse for his actual values which enabled this comparison to be made.

an error in the shear wave velocity of 3 per cent., which we can rule out, or to an error due to the use of perturbation theory. The error in the values for a rectangle may well be due to the fact that we are close to a zero of D_2. The fact that the difference between the calculated values for a square and a rectangle is less than the experimental may have the same cause.

In this table we have included for comparison calculated frequencies for a circular rod with the same cross-section as that of the square, both for $\sigma = 0{\cdot}30$ and $0{\cdot}35$, the latter value being chosen by Morse for this purpose.

TABLE 3

	$\left(\frac{\omega a}{c_s}\right)$	*Square*		*Rectangle*		*Circle*	
		(exp.)	*(calc.)*	*(exp.)*	*(calc.)*	$\sigma = 0{\cdot}30$	$\sigma = 0{\cdot}35$
(c)	2·03	3,350	3,270	3,260	3,250	3,295	3,317
(d)	2·60	3,050	2,980	3,240	3,040	3,053	3,053
Est.	3·00	2,700	2,680	2,810	2,740	2,750	2,751

In conclusion, the perturbation theory developed does not seem to be accurate enough for a square, using the circle as the unperturbed shape, but more experimental results for various sections are really necessary. One positive result, however, does emerge. It is that the two branches observed by Morse agree very well with the two branches obtained by an interaction between the longitudinal and screw vibrations, and are not the longitudinal branch and a harmonic.

Acknowledgement

One of us (W. A. G.) is indebted to the Department of Scientific and Industrial Research for a maintenance allowance covering the period in which this work was carried out.

APPENDIX

Apart from the factors involving z, t, and θ, the solutions used in section 2 are:

	$i = 1$	$i = 2$	$i = 3$
u_{ni}	$nJ_n(\beta r)/\beta r$	$J'_n(\beta r)$	$J'_n(\alpha r)$
v_{ni}	$-J'_n(\beta r)$	$-nJ_n(\beta r)/\beta r$	$-nJ_n(\alpha r)/\alpha r$
w_{ni}	0	$\beta J_n(\beta r)/k$	$-kJ_n(\alpha r)/\alpha$

where $k = 2\pi/\lambda$ is the wave-number, and α and β are defined by

$$\rho\omega^2/\mu = \beta^2 + k^2, \qquad \rho\omega^2/(\lambda + 2\mu) = \alpha^2 + k^2.$$

The dash denotes a derivative with respect to the argument βr or αr. These include $n = 0$. When $n = 0$, $u = w = 0$ for $i = 1$, and $v = 0$ for $i = 2, 3$. For the solutions $i = 1, 2$ the dilatation $\delta = 0$ and for $i = 3$, $\delta = -(\alpha^2 + k^2)J_n(\alpha r)/\alpha$.

The following are the elements of the determinant P, to the desired order in the coefficients b_s, using $x = \beta a$ and $y = \alpha a$. (K is defined below equation (3.1).)

D_0:
$$P_{20}^{20} = J_0''(x) + \sum \tfrac{1}{4}b_s^2\{x^2J_0(x) - J_0(x) - 2J_0'(x)/x\}$$
$$P_{30}^{20} = (\beta^2 - k^2)/2\beta k[J_0'(x) - \sum \tfrac{1}{4}b_s^2\{xJ_0(x) + x^2J_0'(x)\}]$$
$$P_{20}^{30} = J_0''(y) - (K-1)J_0(y) + \sum \tfrac{1}{4}b_s^2\{(y^2-1)J_0(y) - 2J_0'(y)/y - (K-1)(yJ_0' - y^2J_0)\}$$
$$P_{30}^{30} = -kJ_0'(y)/\alpha + \sum \tfrac{1}{4}b_s^2\, ka\{J_0(y) + yJ_0'(y)\}.$$

D_n:

$j =$	P_{jn}^{in} $i = 1$	$i = 2$	$i = 3$
1	$n(xJ_n' - J_n)/2x^2$	$\tfrac{1}{2}J_n''(x)$	$\tfrac{1}{2}\{J_n''(y) - (K-1)J_n(y)\}$
2	$(xJ_n' + \tfrac{1}{2}x^2J_n - n^2J_n)/2x^2$	$\tfrac{1}{2}n(J - xJ_n')/x^2$	$n(J_n - yJ_n')/2y^2$
3	$-nkaJ_n/4x^2$	$-(k^2-\beta^2)J_n'/4k\beta$	$-kJ_n'(y)/2\alpha$

D_{0n}:

$i =$	P_{20}^{in}	P_{30}^{in}
1	$\tfrac{1}{2}nb_n\{J_n(1-\tfrac{1}{2}x^2) - xJ_n'\}/x^2$	0
2	$\tfrac{1}{2}b_n\{xJ_n'(1-x^2) - n^2J_n\}/x^2$	$\tfrac{1}{4}b_n\, ka(k^2-\beta^2)J_n(x)/k^2$
3	$\tfrac{1}{2}b_n\{(y^2-n^2)J_n/y^2 + J_n'/y - K(J_n + yJ_n')\}$	$\tfrac{1}{2}b_n\, kaJ_n(y)$

D_{n0}:

$j =$	P_{jn}^{20}	P_{jn}^{30}
1	$\tfrac{1}{2}b_n J_0'(x)(1-x^2)/x$	$\tfrac{1}{2}b_n\{J_0(y) + J_0'/y - K(J_0 + yJ_0')\}$
2	$\tfrac{1}{2}nb_n J_0'(x)/x$	$\tfrac{1}{2}nb_n\{J_0 + J_0'/y - KJ_0(y)\}$
3	$\tfrac{1}{4}b_n(k^2-\beta^2)kaJ_0(x)/k^2$	$\tfrac{1}{2}b_n\, kaJ_0(y)$

Coefficients b_s for various sections. The following values were used:

Ellipse of eccentricity $e = \frac{1}{2}$:
$b_2 = 0{\cdot}07184$, $b_4 = 0{\cdot}00387$, $b_6 = 0{\cdot}00023$, $b_8 = 0{\cdot}00002$.

Square of side $2s$, *where* $a = 1{\cdot}12s$:
$b_4 = -0{\cdot}13941$, $b_8 = 0{\cdot}04397$.

Rectangle, with sides in ratio 6:5; $a = 1{\cdot}0218d$, *where* d *is the longer side*:
$b_2 = 0{\cdot}10985$, $b_4 = -0{\cdot}12713$, $b_6 = -0{\cdot}04359$, $b_8 = 0{\cdot}03148$.

REFERENCES

1. R. M. Davies, *App. Mech. Rev.* **6** (1953), 1.
2. R. W. Morse, *J. Amer. Acous. Soc.* **20** (1948), 833.
3. A. E. H. Love, *Mathematical Theory of Elasticity*, 4th edn., 1944.
4. R. M. Davies, *Phil. Trans.* A **240** (1948), 375.
5. D. Bancroft, *Phys. Rev.* **59** (1941), 588.
6. G. E. Hudson, ibid. **63** (1943), 46.
7. G. J. Kynch, *Nature*, **175** (1955), 559.

VIBRATIONS OF BEAMS

II. TORSIONAL MODES

By W. A. GREEN

(*University College of Wales, Aberystwyth*)

[Received 9 February 1956]

SUMMARY

The second order perturbation method developed in the previous paper (**1**) is adopted for the consideration of torsional waves in a bar of general section. The determinantal frequency equation is obtained correct to second order, for the first mode of torsional oscillations of the bar. This equation is solved for particular wavelengths and dispersion curves sketched for bars whose sections approximate to a square, rectangle, and ellipse. As in the longitudinal case it is found that the method breaks down for the rectangle and the ellipse at a certain point due to degeneracy between the torsional and screw modes.

1. Introduction

In the previous paper I the theory of longitudinal vibrations of an infinitely long bar of elastic material having the cross-section

$$r = a(1 + \sum b_s \cos s\theta) \tag{1.1}$$

has been examined by means of a perturbation method. The method is equally applicable to the case of torsional vibrations which will be considered here.

The torsional vibrations of a bar of circular cross-section have been investigated by Chree (**2**), Bancroft (**3**), and Davies and Owen (**4**). In this paper the results obtained for the bar of general section (1.1) are applied to cylinders of square, elliptical, and rectangular cross-sections whose Fourier expansions are terminated at convenient points, to obtain the appropriate dispersion curves for the fundamental mode. The results obtained being correct to second order in the coefficients b_s.

As in the longitudinal case it is found that at certain wavelengths degeneracy occurs between the fundamental mode of torsional vibrations and the screw mode. This does not affect the perturbation theory for a square, as pointed out in I, but the method is not valid in this region for the ellipse and rectangle.

2. Method

The method employed is exactly similar to that of paper I. The general solutions of the elastic equations are obtained in polar coordinates and made to satisfy the boundary conditions for the bar. On expanding the

stresses in these boundary conditions in Fourier series a set of linear simultaneous equations in the arbitrary constants of the general solutions of the displacements are obtained and the condition that these have a solution gives rise to two determinantal equations

$$|P^{in}_{jm}| = 0; \qquad |Q^{in}_{jm}| = 0 \quad \begin{pmatrix} i, j = 1, 2, 3, \\ m, n = 0, 1, 2, \ldots \end{pmatrix}. \tag{2.1}$$

These determinants have been discussed in paper I where it is shown that $|P|$ corresponds to the longitudinal oscillations of the cylinder and $|Q|$ to the torsional oscillations.

For a circular cylinder $|Q|$ consists only of diagonal minors D_0, D_1, D_2,..., where D_0 is (1×1) and D_n is (3×3). For the general cylinder considered here $|Q|$ contains the same terms together with terms of order b_s or more everywhere.

The modes of torsional vibrations of a circular cylinder are given by the equation $D_0 = 0$. Similarly, those for the general cylinder will be given by $D'_0 = 0$, where D'_0 is the new first element of $|Q|$ obtained by reducing all elements in the first row and column, apart from the first one, to zero. As in the longitudinal case, however, we only consider the solution to order b_s^2, and it is therefore sufficient to eliminate from the first row of $|Q|$, apart from the first term, all terms of order b_s. This is done by adding to the first row suitable multiples of all the other rows. The frequency equation for the torsional oscillations of the general cylinder is then given, to order b_s^2, by the equation

$$D''_0 = 0, \tag{2.2}$$

where D''_0 is the resulting element in the first row and first column of $|Q|$.

We will consider the first mode of vibration only. As the perturbation is assumed to be small, the multiples of the rows of D_n which eliminate the terms of order b_n in D_{0n} are evaluated at any point by using the corresponding solutions for the circular cylinder at that point.

3. Results

The general displacements obtained by solving the elastic equations in polar coordinates are given in paper I (Appendix). These give rise to the elements Q^{in}_{jm} shown in Table 1.

The frequency equation for torsional vibrations of a circular cylinder is

$$D_0 = 1 + \tfrac{1}{2}\phi_0(x) = 0, \tag{3.1}$$

where

$$\phi_0(x) = xJ_0(x)/J'_0(x)$$

and x is defined in paper I.

For the fundamental mode of vibration this has the solution

$$x = 0.$$

Using this value of x to eliminate the terms of order b_s in the first row of $|Q|$ we obtain the frequency equation for the general cylinder, correct to order b_s^2,

$$D_0'' = 1+\tfrac{1}{2}\phi_0+\sum \tfrac{1}{4}z^2 s b_s^2 \Gamma_s = 0, \tag{3.2}$$

where $(1/\Gamma_s) = 1+(2s-3)z^2/2s(s^2-1)-\bar{\theta}_s z^4/\{4s^2(s+1)^2(1-\bar{\theta}_s)\}$

and z and $\bar{\theta}_s$ are defined in Table 1.

TABLE 1

Elements Q_{jm}^{in} of the determinant Q

D_0:

$$Q_{10}^{10} = 1+\phi_0/2+\sum_s b_s^2\{1+\phi_0/2-x^2(1+\phi_0)/4\}/2$$

D_n:

Q_{jn}^{in}	$i=1$	$i=2$	$i=3$
$j=1$	$-1-x^2\theta_n/n+n\theta_n$	$n-\theta_n$	$-1-Ky^2\hat{\theta}_n/n+n\hat{\theta}_n$
$j=2$	$n-\theta_n$	$-1-x^2\theta_n/2n+n\theta_n$	$n-\hat{\theta}_n$
$j=3$	$(1-x^2/z^2)/2$	$\theta_n/2$	1

D_{0n}:

$$Q_{10}^{1n} = b_n(\theta_n-x^2\theta_n-n)$$
$$Q_{10}^{2n} = b_n(1-2x^2+x^2\theta_n/2n-n\theta_n)$$
$$Q_{10}^{3n} = b_n(\hat{\theta}_n-Ky^2\hat{\theta}_n-n)$$

D_{m0}:

$$Q_{1m}^{10} = b_m\, m(1+\phi_0/2)/2$$
$$Q_{2m}^{10} = b_m(-1-\phi_0/2+x^2/2)$$
$$Q_{3m}^{10} = b_m(-m/4)$$

where

$$\phi_0 = xJ_0(x)/J_0'(x)$$
$$\theta_n = nJ_n(x)/xJ_n'(x)$$
$$\hat{\theta}_n = nJ_n(y)/yJ_n'(y)$$
$$z = ka$$

TABLE 2

Values of Γ_s ($s = 2, 4, 6, 8$). $\sigma = 0{\cdot}3$

$(ka)^2$	Γ_2	Γ_4	Γ_6	Γ_8
0	1·0000000	1·0000000	1·0000000	1·0000000
1·4	1·0526623	0·9911516	0·9934799	0·9956126
2·8	1·1193416	0·9832335	0·9867866	0·9913374
4·2	1·2041572	0·9761920	0·9812849	0·9871714
5·6	1·3133640	0·9699798	0·9755883	0·9831112
7·0	1·4568390	0·9645553	0·9701457	0·9791562
14·0	4·3785101	0·9481332	0·9464404	0·9608491

The values of Γ_s for $s = 2, 4, 6, 8$, are given in Table 2 for a number of values of ka and a Poisson's ratio $\sigma = 0{\cdot}3$. This enables the phase velocity at these wavelengths to be determined for any bar whose cross-section can be put in the form (1.1) provided the b_s are sufficiently small. Equation (3.2) has been solved to give these phase velocities for bars of square, rectangular, and elliptical cross-sections whose Fourier expansions are taken up to $s = 8$, and the resulting dispersion curves are shown in Fig. 1.

4. Degeneracy

As has been pointed out in I, the method applied here breaks down when D_0 and any D_n vanish together. That occurs when the dispersion curves for the torsional mode of vibrations of the circular cylinder and any other mode intersect. It is in fact found to happen for $ka \simeq 4$, when the torsion curve intersects that of the screw mode $D_2 = 0$. However,

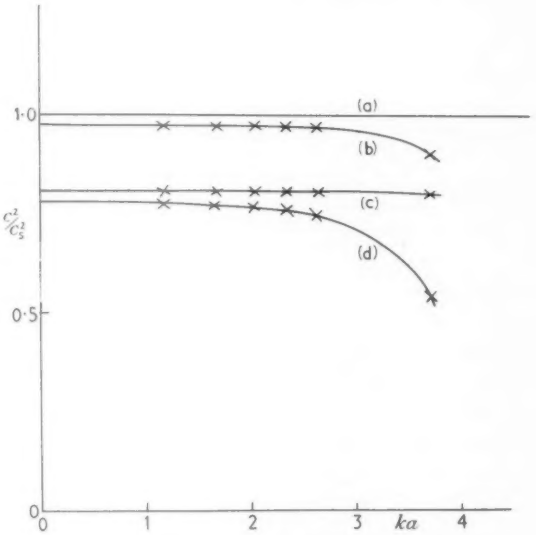

FIG. 1. Dispersion curves for torsional vibrations
(*a*) Circular cylinder (*b*) Ellipse (eccentricity $\frac{1}{2}$)
(*c*) Square (*d*) Rectangle (side ratio 6:5)

as explained in I, this does not affect the results for sections such as a square or triangle which do not contain a term in b_2, but will affect the results for a rectangle and ellipse as can be seen from Fig. 1.

Calculations have been started to obtain the dispersion curves for the screw vibration $D_2 = 0$, for different values of Poisson's ratio. A sketch curve for $\sigma = 0{\cdot}3$ through the three points given in Table 3 is shown in Fig. 2.

TABLE 3

Points on dispersion curve for screw vibrations ($\sigma = 0{\cdot}3$)

c^2/c_s^2	3·5	2·0	1·0
ka	1·031	1·773	4·112

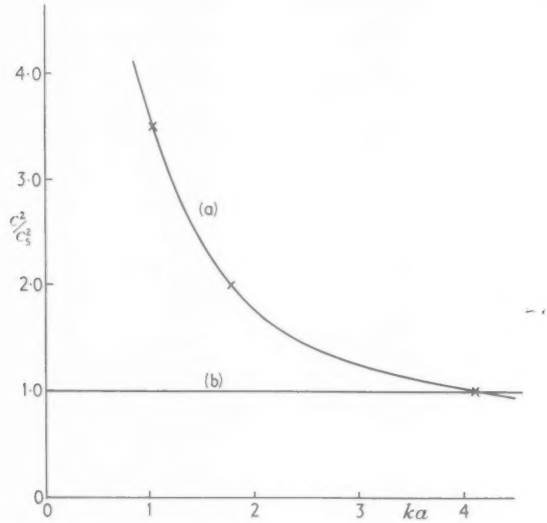

FIG. 2. Dispersion curves for (*a*) screw and (*b*) torsional vibrations of a circular cylinder

Acknowledgement

I am indebted to the Department of Scientific and Industrial Research for a maintenance allowance covering the period in which this work was carried out.

REFERENCES

1. G. J. KYNCH and W. A. GREEN, *Quart. J. Mech. Appl. Math.* (1956) (previous paper).
2. C. CHREE, *Trans. Camb. Phil. Soc.* **14** (1889), 250.
3. D. BANCROFT, *Phys. Rev.* **59** (1941), 588.
4. R. M. DAVIES and J. D. OWEN, *Proc. Roy. Soc.* A, **204** (1950), 17. (Detailed calculations are given in an unpublished thesis by Owen, 1950.)

A TRANSIENT MAGNETIC DIPOLE SOURCE ABOVE A TWO-LAYER EARTH

By J. S. LOWNDES (*University College of North Staffordshire*)

[Received 23 February 1956]

SUMMARY

The problem of a magnetic dipole acting as a transient current source when situated over a two-layer earth is considered by using the methods of integral transforms. The general expressions have been applied to deduce the induced field at the surface of the earth when the dipole is located on the surface, in the cases when the earth has homogeneous conductivity, and when the conductivities of the two layers are nearly equal. The expressions obtained for the induced magnetic field components are in a form suitable for numerical calculation.

1. Introduction

Using some results obtained by Price (**1**), Gordon (**2**) has considered the problem of an oscillating magnetic dipole outside a semi-infinite conductor and Bhattacharyya (**3**) the problem of an oscillating magnetic dipole over a two-layer earth.

In this paper, using the methods of integral transforms, we consider the case of a magnetic dipole, acting as a transient current source, when it is situated above a two-layer earth. In particular we confine our attention to a step function and an impulsive current source situated over a homogeneous earth and also over a two-layer earth where the conductivities of the layers are nearly equal.

Expressions for the induced magnetic field components are deduced in forms which can be readily calculated numerically. For geophysical exploration this may prove useful for the interpretation of field data.

The use of integral transforms enables the field components to be obtained directly from Maxwell's equations, avoiding the use of a Hertzian vector and the vector and scalar potential functions.

2. Statement of the problem

A magnetic dipole is situated above a semi-infinite two-layer earth. Cylindrical coordinates (ρ, ϕ, z) will be used in which the z-axis is along the upward vertical. Let the surface of the earth be taken as the plane $z = 0$ and the source be located at $(0, 0, a)$ in a region 1 defined by

$$0 \leqslant z < \infty,$$

with characteristics σ_1, ϵ_1, μ_1, and let the earth ($z < 0$) be considered as stratified horizontally into two regions,

Region 2, $0 \geqslant z \geqslant -h$, characteristics, σ_2, ϵ_2, μ_2,

Region 3, $-h \geqslant z > -\infty$, characteristics, σ_3, ϵ_3, μ_3.

The characteristics σ, ϵ, μ denote respectively the electrical conductivity, dielectric constant, and permeability. We assume axial symmetry and denote the current density in region 1 by $J_\phi(\rho, z, t)$. Maxwell's equations (in m.k.s. units) are then

$$\left.\begin{aligned} \frac{\partial E_{i\phi}}{\partial z} &= \mu_i \frac{\partial H_{i\rho}}{\partial t} \\ \frac{1}{\rho}\frac{\partial}{\partial \rho}(\rho E_{i\phi}) &= -\mu_i \frac{\partial H_{iz}}{\partial t} \\ \frac{\partial H_{i\rho}}{\partial z} - \frac{\partial H_{iz}}{\partial \rho} &= \left(\sigma_i + \epsilon_i \frac{\partial}{\partial t}\right) E_{i\phi} + J_\phi(\rho, z, t) \end{aligned}\right\}, \tag{1}$$

where $i = 1, 2, 3$, denotes the components of the separate regions and $J_\phi = 0$ when $i = 2, 3$. The boundary conditions are

$$\left.\begin{aligned} &(a) \quad H_{1\rho} = H_{2\rho} \\ &(b) \quad E_{1\phi} = E_{2\phi} \\ &(c) \quad \mu_1 H_{1z} = \mu_2 H_{2z} \end{aligned}\right\} \text{at } z = 0, \qquad \left.\begin{aligned} &(d) \quad H_{2\rho} = H_{3\rho} \\ &(e) \quad E_{2\phi} = E_{3\phi} \\ &(f) \quad \mu_2 H_{2z} = \mu_3 H_{3z} \end{aligned}\right\} \text{at } z = -h.$$

Applying a Laplace transformation in t defined by

$$\bar{E}_{i\phi}(\rho, z, s) = \int_0^\infty E_{i\phi}(\rho, z, t) e^{-st}\, dt$$

to equations (1), we find

$$\left.\begin{aligned} \frac{\partial \bar{E}_{i\phi}}{\partial z} &= \mu_i s \bar{H}_{i\rho} \\ \frac{1}{\rho}\frac{\partial}{\partial \rho}(\rho \bar{E}_{i\phi}) &= -\mu_i s \bar{H}_{i\rho} \\ \frac{\partial \bar{H}_{i\rho}}{\partial z} - \frac{\partial \bar{H}_{iz}}{\partial \rho} &= (\sigma_i + \epsilon_i s)\bar{E}_{i\phi} + \bar{J}_\phi(\rho, z, s) \end{aligned}\right\}. \tag{2}$$

Transforming equations (2) by a Hankel transform defined by

$$\mathscr{H}_{iz}(\theta, z, s) = \int_0^\infty \rho J_n(\theta\rho) \bar{H}_{iz}(\rho, z, s)\, d\rho,$$

of order zero for $\bar{H}_{iz}$ and order one for $\bar{J}_\phi$, $\bar{H}_{i\rho}$, $\bar{E}_{i\phi}$, we have

$$\frac{d\mathscr{E}_{i\phi}}{dz} = \mu_i s\mathscr{H}_{i\rho},$$

$$\theta\mathscr{E}_{i\phi} = -\mu_i s\mathscr{H}_{iz},$$

$$\frac{d\mathscr{H}_{i\rho}}{dz} + \theta\mathscr{H}_{iz} = (\sigma_i + \epsilon_i s)\mathscr{E}_{i\phi} + \mathscr{J}_\phi(\theta, z, s). \tag{3}$$

Solving the above for $\mathscr{E}_{i\phi}$, we find

$$\frac{d^2\mathscr{E}_{i\phi}}{dz^2} - \eta_i^2\mathscr{E}_{i\phi} = \mu_i s\,\mathscr{J}_\phi(\theta, z, s), \tag{4}$$

where $\eta_i^2 = \theta^2 + \mu_i s(\sigma_i + \epsilon_i s)$.

The solutions of (4) corresponding to each of the three regions can now be given.

Region 1

Since $\mathscr{E}_{1\phi} \to 0$ as $z \to +\infty$,

$$\mathscr{E}_{1\phi} = -\frac{\mu_1 s}{2\eta_1}\int_{-\infty}^{\infty} \mathscr{J}_\phi(\theta, \lambda, s)e^{-\eta_1 z - \lambda}\,d\lambda + A(\theta, s)e^{-\eta_1 z}. \tag{5}$$

Substituting (5) into (3), we get

$$\mathscr{H}_{1z} = \frac{\theta}{2\eta_1}\int_{-\infty}^{\infty} \mathscr{J}_\phi(\theta, \lambda, s)e^{-\eta_1 z - \lambda}\,d\lambda - \frac{\theta}{\mu_1 s}Ae^{-\eta_1 z}, \tag{6}$$

and

$$\mathscr{H}_{1\rho} = \frac{1}{2}\int_{-\infty}^{\infty}\left(\frac{z-\lambda}{|z-\lambda|}\right)\mathscr{J}_\phi(\theta, \lambda, s)e^{-\eta_1 z - \lambda}\,d\lambda - \frac{\eta_1}{\mu_1 s}Ae^{-\eta_1 z}. \tag{7}$$

Region 2

Since $\mathscr{J}_\phi = 0$ we have

$$\mathscr{E}_{2\phi} = B(\theta, s)e^{-\eta_2 z} + C(\theta, s)e^{\eta_2 z},$$

$$\mathscr{H}_{2\rho} = -\frac{\eta_2}{\mu_2 s}Be^{-\eta_2 z} + \frac{\eta_2}{\mu_2 s}Ce^{\eta_2 z},$$

$$\mathscr{H}_{2z} = -\frac{\theta}{\mu_2 s}Be^{-\eta_2 z} - \frac{\theta}{\mu_2 s}Ce^{\eta_2 z}. \tag{8}$$

Region 3

Since $\mathscr{J}_\phi = 0$, $\mathscr{E}_{3\phi} \to 0$, as $z \to -\infty$, then

$$\mathscr{E}_{3\phi} = D(\theta, s)e^{\eta_3 z},$$

$$\mathscr{H}_{3\rho} = \frac{\eta_3}{\mu_3 s}De^{\eta_3 z},$$

$$\mathscr{H}_{3z} = -\frac{\theta}{\mu_3 s}De^{\eta_3 z}. \tag{9}$$

The problem now reduces to the following: given a particular form of J_ϕ and applying the boundary conditions, to evaluate the terms A, B, C, D, and hence the field components.

3. General solution of the problem

We regard the dipole, located at $z = a$, as an infinitesimal loop with its axis in the z-direction. The dipole can be represented by the form

$$\lim_{b\to 0} \frac{\delta(\rho-b)\delta(z-a)}{2\pi\rho},$$

where $2\pi\rho$ is the normalizing factor and $\delta(x)$ the Dirac delta function. The current density is then seen to be

$$J_\phi(\rho, z, t) = \lim_{b\to 0} MT(t) \frac{\delta(\rho-b)\delta(z-a)}{\pi\rho^2}, \tag{10}$$

where M is the magnetic moment of the current loop and $T(t)$ is a function of time only.

Transforming (10) with respect to t by means of a Laplace transformation,

$$\bar{J}_\phi(\rho, z, s) = \lim_{b\to 0} M\bar{T}(s) \frac{\delta(\rho-b)\delta(z-a)}{\pi\rho^2},$$

then applying a Hankel transformation in ρ, we find

$$\mathscr{J}_\phi(\theta, z, s) = \frac{M\bar{T}(s)\delta(z-a)}{\pi} \lim_{b\to 0} \frac{J_1(\theta b)}{b}.$$

Proceeding to the limit,

$$\mathscr{J}_\phi(\theta, z, s) = \frac{M\bar{T}(s)\theta\delta(z-a)}{2\pi}. \tag{11}$$

Substituting (11) in (5), (6), (7) we have for the transformed field components in region 1,

$$\begin{aligned}
\mathscr{E}_{1\phi} &= -\frac{M\theta\mu_1 s\bar{T}(s)}{4\pi\eta_1} e^{-\eta_1|z-a|} + Ae^{-\eta_1 z}, \\
\mathscr{H}_{1z} &= \frac{M\theta^2\bar{T}(s)}{4\pi\eta_1} e^{-\eta_1|z-a|} - \frac{\theta}{\mu_1 s} Ae^{-\eta_1 z}, \\
\mathscr{H}_{1\rho} &= \frac{M\theta}{4\pi}\left(\frac{z-a}{|z-a|}\right)\bar{T}(s)e^{-\eta_1|z-a|} - \frac{\eta_1}{\mu_1 s} Ae^{-\eta_1 z}.
\end{aligned} \tag{12}$$

Henceforth we set $\mu_i = 1$, and apply the boundary conditions to (8), (9), and (12); we find

$$\left.\begin{aligned}
&(a) \quad -\frac{M\theta s\bar{T}(s)}{4\pi} e^{-\eta_1 a} - \eta_1 A = -\eta_2 B + \eta_2 C \\
&(b) \quad -\frac{M\theta s\bar{T}(s)}{4\pi\eta_1} e^{-\eta_1 a} + A = B + C \\
&(c) \quad -\eta_2 Be^{\eta_2 h} + \eta_2 Ce^{-\eta_2 h} = \eta_3 De^{-\eta_3 h} \\
&(d) \quad Be^{\eta_2 h} + Ce^{-\eta_2 h} = De^{-\eta_3 h}
\end{aligned}\right\}. \tag{13}$$

Solving the above for A we find

$$A = \frac{M\theta s\bar{T}(s)}{4\pi\eta_1}\left[\frac{(\eta_2+\eta_1)(\eta_2-\eta_3)e^{-2h\eta_2}-(\eta_2-\eta_1)(\eta_2+\eta_3)}{(\eta_2-\eta_1)(\eta_2-\eta_3)e^{-2h\eta_2}-(\eta_2+\eta_1)(\eta_2+\eta_3)}\right]e^{-\eta_1 a}, \quad (14)$$

and substituting for A in (12) we get

$$\mathscr{H}_{1z} = \frac{M\theta^2\bar{T}(s)}{4\pi\eta_1}e^{-\eta_1|z-a|}+\mathscr{H}^*_{1z}. \quad (15)$$

The first term in the above expression corresponds to the inducing field and the second term, $\mathscr{H}^*_{1z}$, is the induced field. We are here only concerned with the induced field

$$\mathscr{H}^*_{1z} = -\frac{M\theta^2\bar{T}(s)}{4\pi\eta_1}I(\eta_1,\eta_2,\eta_3)e^{-\eta_1(z+a)}. \quad (16)$$

Similarly,
$$\mathscr{H}^*_{1\rho} = -\frac{M\theta\bar{T}(s)}{4\pi}I(\eta_1,\eta_2,\eta_3)e^{-\eta_1(z+a)}, \quad (17)$$

where

$$I(\eta_1,\eta_2,\eta_3) = \left[\frac{(\eta_2+\eta_1)(\eta_2-\eta_3)e^{-2h\eta_2}-(\eta_2-\eta_1)(\eta_2+\eta_3)}{(\eta_2-\eta_1)(\eta_2-\eta_3)e^{-2h\eta_2}-(\eta_2+\eta_1)(\eta_2+\eta_3)}\right]. \quad (18)$$

The above are the general expressions for the transformed magnetic field components.

4. The induced magnetic field over a homogeneous earth

For a homogeneous earth $\eta_2 = \eta_3$. In this case (18) becomes

$$I(\eta_1,\eta_2) = \frac{\eta_2-\eta_1}{\eta_2+\eta_1}. \quad (19)$$

We will now make the following assumptions:

(i) $\sigma_1 = 0$.

(ii) We neglect the displacement currents in both media, i.e. set $\epsilon_1 = \epsilon_2 = 0$. This means that the transient response is valid for times $t \gg \epsilon/\sigma$.

(iii) The dipole is situated at the origin of coordinates and the induced field observed in the plane $z = 0$.

Substituting (19) in (16) and (17), and inverting with respect to the Hankel transform, we find

$$\bar{H}'_{1z} = -\frac{M\bar{T}(s)}{4\pi}\int_0^\infty \theta^2\left(\frac{\eta_2-\theta}{\eta_2+\theta}\right)J_0(\theta\rho)\,d\theta, \quad (20)$$

$$\bar{H}'_{1\rho} = -\frac{M\bar{T}(s)}{4\pi}\int_0^\infty \theta^2\left(\frac{\eta_2-\theta}{\eta_2+\theta}\right)J_1(\theta\rho)\,d\theta, \quad (21)$$

where now $\eta_2^2 = \theta^2+\sigma s$, $\sigma = \sigma_2$.

Evaluating the above integrals by Gordon's method and inverting the resulting expressions with respect to the Laplace transform,

$$H'_{1z} = \frac{M}{8\pi^2 i}\mathscr{D}\int_{\gamma-i\infty}^{\gamma+i\infty}\bar{T}(s)\left[\frac{1}{\rho}+\frac{2}{b^2\rho}\frac{d}{d\rho}\left(\frac{1-e^{-b\rho}}{\rho}\right)\right]e^{st}\,ds, \tag{22}$$

$$H'_{1\rho} = -\frac{M}{8\pi^2 i}\left[\frac{d}{d\rho}\left(\frac{1}{\rho}\frac{d}{d\rho}\right)\right]\int_{\gamma-i\infty}^{\gamma+i\infty}\bar{T}(s)I_1(as^{\frac{1}{2}})K_1(as^{\frac{1}{2}})e^{st}\,ds, \tag{23}$$

where $$\mathscr{D} = \frac{1}{\rho}\frac{d}{d\rho}\left(\rho\frac{d}{d\rho}\right), \qquad b^2 = \sigma s, \qquad 4a^2 = \sigma\rho^2.$$

4.1. Application A

A magnetic dipole acting as a step function current source over a homogeneous earth

In this particular case $T(t) = H(t)$, the Heaviside unit function. Applying

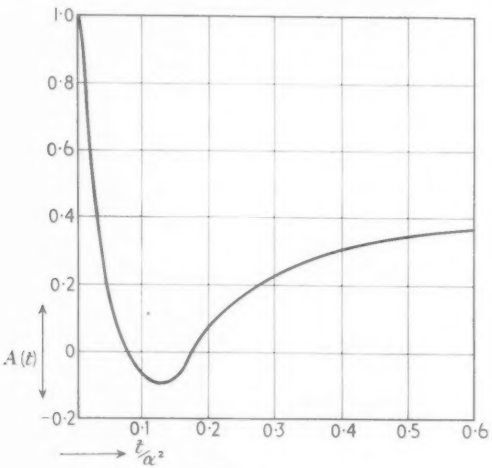

FIG. 1

a Laplace transform in t we find $\bar{T}(s) = s^{-1}$. Substituting for $\bar{T}(s)$ in (22) and evaluating the complex integral by tables (**4**) we have

$$H'_{1z} = \frac{M}{4\pi}\mathscr{D}\left\{\left(\frac{1}{\rho}-\frac{2t}{\sigma\rho^3}\right)-\frac{2}{\sigma\rho}\frac{d}{d\rho}\left[\left(\frac{t}{\rho}+\frac{\sigma\rho}{2}\right)\mathrm{erfc}\left(\frac{\alpha}{2t^{\frac{1}{2}}}\right)-\left(\frac{\sigma t}{\pi}\right)^{\frac{1}{2}}e^{-\alpha^2/4t}\right]\right\} \tag{24}$$

where $\alpha^2 = \sigma\rho^2$. Performing the differentiations we find

$$H'_{1z} = \frac{M}{4\pi\rho^3}A(t), \tag{25}$$

where

$$A(t) = \left[1 - 18\left(\frac{t}{\alpha^2}\right)\right]\operatorname{erf}\left(\frac{\alpha}{2t^{\frac{1}{2}}}\right) + \left[9\left(\frac{t}{\alpha^2}\right)^{\frac{1}{2}} + 3\left(\frac{\alpha}{2t^{\frac{1}{2}}}\right)\right]\operatorname{erf}'\left(\frac{\alpha}{2t^{\frac{1}{2}}}\right),$$

$$\operatorname{erf}' x = \frac{d}{dx}\operatorname{erf} x.$$

The function $A(t)$ is shown in Fig. 1. Substituting for $\overline{T}(s)$ in (23) and evaluating the integral using the Faltung theorem for Laplace transforms we have

$$H'_{1\rho} = -\frac{M}{4\pi}\left\{\frac{d}{d\rho}\left(\frac{1}{\rho}\frac{d}{d\rho}\right)\right\}\int_0^t \frac{e^{-\alpha^2/8\tau}}{\tau} I_1\left(\frac{\alpha^2}{8\tau}\right) d\tau. \tag{26}$$

4.2. Application B

A magnetic dipole acting as an impulsive current source over a homogeneous earth

In this case $T(t) = \delta(t)$. Applying a Laplace transform we have

$$\overline{T}(s) = 1.$$

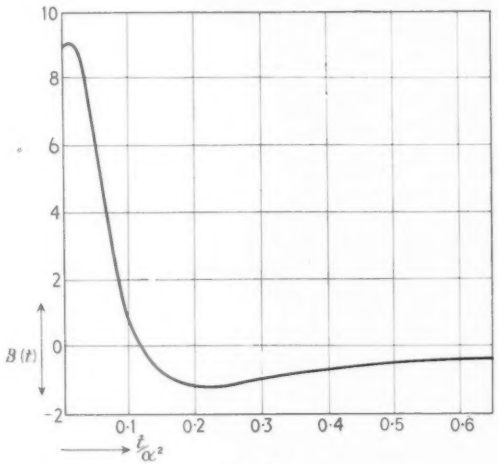

FIG. 2

The expressions for the induced fields are, after evaluating the complex integrals,

$$H'_{1z} = \frac{M}{2\pi\sigma}\mathscr{D}\left\{\frac{1}{\rho}\left(\frac{d}{d\rho}\frac{1}{\rho}\right)\right\}\operatorname{erf}\left(\frac{\alpha}{2t^{\frac{1}{2}}}\right), \tag{27}$$

$$H'_{1\rho} = -\frac{M}{4\pi t}\left\{\frac{d}{d\rho}\left(\frac{1}{\rho}\frac{d}{d\rho}\right)\right\}e^{-\alpha^2/8t} I_1\left(\frac{\alpha^2}{8t}\right). \tag{28}$$

Performing the differentiations we have

$$H'_{1z} = -\frac{M}{2\pi\sigma\rho^5}B(t), \qquad H'_{1\rho} = \frac{M}{2\pi\sigma\rho^5}C(t), \tag{29}$$

where

$$B(t) = 9\,\mathrm{erf}\left(\frac{\alpha}{2t^{\frac{1}{2}}}\right) - \left[9\left(\frac{\alpha}{2t^{\frac{1}{2}}}\right) + 8\left(\frac{\alpha}{2t^{\frac{1}{2}}}\right)^3 + 4\left(\frac{\alpha}{2t^{\frac{1}{2}}}\right)^5\right]\mathrm{erf}'\left(\frac{\alpha}{2t^{\frac{1}{2}}}\right),$$

$$C(t) = 16z[(2z^2+z)I_0(z) - 2(z^2+z+1)I_1(z)]e^{-z},$$

$$z = \frac{\alpha^2}{8t}.$$

The functions $B(t)$ and $C(t)$ are shown in Figs. 2 and 3.

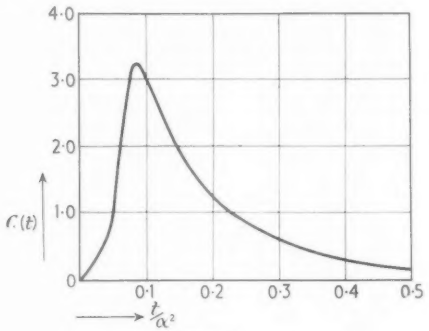

FIG. 3

5. The induced magnetic field over a two-layer earth when the conductivities are nearly equal

We now make the following assumptions:

(i) $\sigma_1 = 0$.

(ii) We neglect the displacement currents, i.e. set $\epsilon_1 = \epsilon_2 = \epsilon_3 = 0$.

(iii) The dipole is situated at the origin of coordinates and the induced field measured in the plane $z = 0$.

(iv) The conductivities of the two layers are nearly equal, i.e.

$$\Delta\sigma = \sigma_2 - \sigma_3 \ll \frac{\sigma_2+\sigma_3}{2}.$$

Inverting (16) and (17) with respect to the Hankel transform and following the method of (**3**) we see that the resulting expressions can be reduced with sufficient accuracy to

$$\bar{H}^*_{1z} = \bar{H}'_{1z} + \bar{H}''_{1z},$$
$$\bar{H}^*_{1\rho} = \bar{H}'_{1\rho} + \bar{H}''_{1\rho}. \tag{30}$$

The terms $\bar{H}'_{1z}$ and $\bar{H}'_{1\rho}$ have been evaluated in section 4 and the terms arising from the inhomogeneity in the earth's conductivity are

$$\bar{H}''_{1z} = \frac{M\bar{T}(s)}{4\pi}\int_0^\infty \theta^2\left(\frac{\eta_2-\eta_3}{\eta_2+\eta_3}\right)e^{-2h\eta_2}J_0(\theta\rho)\,d\theta, \tag{31}$$

$$\bar{H}''_{1\rho} = \frac{M\bar{T}(s)}{4\pi}\int_0^\infty \theta^2\left(\frac{\eta_2-\eta_3}{\eta_2+\eta_3}\right)e^{-2h\eta_2}J_1(\theta\rho)\,d\theta. \tag{32}$$

As in (3) we can write with sufficient accuracy the above in the form

$$\bar{H}''_{1z} = \frac{\Delta\sigma M\bar{T}(s)s}{16\pi}\int_0^\infty \theta^2\frac{e^{-2h\eta}}{\eta^2}J_0(\theta\rho)\,d\theta, \tag{33}$$

$$\bar{H}''_{1\rho} = \frac{\Delta\sigma M\bar{T}(s)s}{16\pi}\int_0^\infty \theta^2\frac{e^{-2h\eta}}{\eta^2}J_1(\theta\rho)\,d\theta, \tag{34}$$

where $\eta = \frac{1}{2}(\eta_2+\eta_3) = (\theta^2+\sigma s)^{\frac{1}{2}}$, and σ denotes the average conductivity.

Inverting (33) and (34) with respect to the Laplace transform and reversing the order of integration we have

$$H''_{1z} = \frac{\Delta\sigma M}{16\pi\sigma}\int_0^\infty \theta^2 J_0(\theta\rho)\Phi(\theta,t)\,d\theta, \tag{35}$$

$$H''_{1\rho} = \frac{\Delta\sigma M}{16\pi\sigma}\int_0^\infty \theta^2 J_1(\theta\rho)\Phi(\theta,t)\,d\theta, \tag{36}$$

where

$$\Phi(\theta,t) = \frac{1}{2\pi i}\int_{\gamma-i\infty}^{\gamma+i\infty}\frac{\bar{T}(s)s}{s+\beta}\exp[-\lambda(s+\beta)^{\frac{1}{2}}+st]\,ds, \tag{37}$$

$$\lambda^2 = 4h^2\sigma, \qquad \beta = \theta^2/\sigma.$$

5.1. Application C

A magnetic dipole acting as a step function source over a two-layer earth

As before we take $T(t) = H(t)$ and find $\bar{T}(s) = s^{-1}$. Substituting for $\bar{T}(s)$ in (37) we have

$$\Phi(\theta,t) = e^{-\beta t}\operatorname{erfc}\left(\frac{h^2\sigma}{t}\right)^{\frac{1}{2}}. \tag{38}$$

Therefore (35) and (36) become

$$H''_{1z} = -\frac{\Delta\sigma M}{16\pi\sigma}\operatorname{erfc}\left(\frac{h^2\sigma}{t}\right)^{\frac{1}{2}}\mathscr{D}\int_0^\infty J_0(\theta\rho)e^{-\beta t}\,d\theta, \tag{39}$$

$$H''_{1\rho} = -\frac{\Delta\sigma M}{16\pi\sigma}\operatorname{erfc}\left(\frac{h^2\sigma}{t}\right)^{\frac{1}{2}}\frac{d}{d\rho}\int_0^\infty \theta J_0(\theta\rho)e^{-\beta t}\,d\theta, \tag{40}$$

where $\mathscr{D} = \frac{1}{\rho}\frac{d}{d\rho}\left(\rho\frac{d}{d\rho}\right)$. By (**5**, p. 394)

$$H''_{1z} = -\frac{\Delta\sigma M}{32}\left(\frac{1}{\pi\sigma t}\right)^{\frac{1}{2}}\operatorname{erfc}\left(\frac{h^2\sigma}{t}\right)^{\frac{1}{2}}\mathscr{D}\left[e^{-\alpha^2/8t}I_0\left(\frac{\alpha^2}{8t}\right)\right], \tag{41}$$

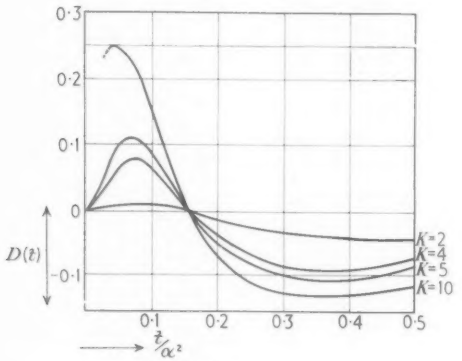

FIG. 4

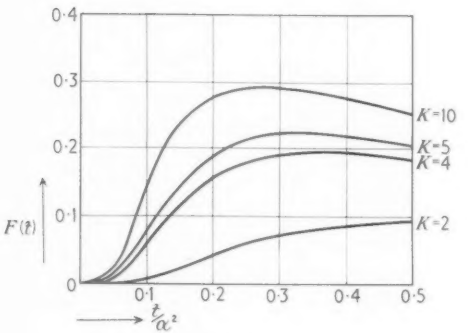

FIG. 5

and by (**5**, p. 393)

$$H''_{1\rho} = -\frac{\Delta\sigma M}{32\pi t}\operatorname{erfc}\left(\frac{h^2\sigma}{t}\right)^{\frac{1}{2}}\frac{d}{d\rho}e^{-\alpha^2/4t}. \tag{42}$$

Performing the differentiations we have

$$H''_{1z} = -\frac{\Delta\sigma M}{4\pi\sigma\rho^3}D(t), \qquad H''_{1\rho} = -\frac{\Delta\sigma M}{16\pi\rho}F(t), \tag{43}$$

where

$$D(t) = \operatorname{erfc}\left(\frac{\sigma\rho^2}{\kappa^2 t}\right)^{\frac{1}{2}}[(2z-1)I_0(z)-2zI_1(z)](2\pi z^3)^{-\frac{1}{2}}e^{-z},$$

$$F(t) = \operatorname{erfc}\left(\frac{\sigma\rho^2}{\kappa^2 t}\right)^{\frac{1}{2}}\left[\left(\frac{\alpha^2}{4t}\right)e^{-\alpha^2/4t}\right],$$

$$z = \frac{\sigma\rho^2}{8t}, \qquad \kappa^2 h^2 = \rho^2.$$

The functions $D(t)$ and $F(t)$ are shown in Figs. 4 and 5.

5.2. Application D

A magnetic dipole acting as an impulsive current source over a two-layer earth

In this case $\overline{T}(s) = 1$. Evaluating the integral (37) we find that (35) and (36) give

$$H''_{1z} = -\frac{\Delta\sigma M}{16\pi\sigma^2}\mathscr{D}\left[\operatorname{erfc}\left(\frac{h^2\sigma}{t}\right)^{\frac{1}{2}}\mathscr{D} - \frac{h}{2}\left(\frac{\sigma}{t}\right)^{\frac{3}{2}}\operatorname{erf}'\left(\frac{h^2\sigma}{t}\right)^{\frac{1}{2}}\right]\int_0^\infty J_0(\theta\rho)e^{-\beta t}\,d\theta, \quad (44)$$

$$H''_{1\rho} = -\frac{\Delta\sigma M}{16\pi\sigma^2}\frac{d}{d\rho}\left[\operatorname{erfc}\left(\frac{h^2\sigma}{t}\right)^{\frac{1}{2}}\mathscr{D} - \frac{h}{2}\left(\frac{\sigma}{t}\right)^{\frac{3}{2}}\operatorname{erf}'\left(\frac{h^2\sigma}{t}\right)^{\frac{1}{2}}\right]\int_0^\infty \theta J_0(\theta\rho)e^{-\beta t}\,d\theta. \quad (45)$$

Evaluating the integrals as before we have

$$H''_{1z} = -\frac{\Delta\sigma M}{32}\left(\frac{1}{\pi\sigma^3 t}\right)^{\frac{1}{2}}\mathscr{D}\left[\operatorname{erfc}\left(\frac{h^2\sigma}{t}\right)^{\frac{1}{2}}\mathscr{D} - \frac{h}{2}\left(\frac{\sigma}{t}\right)^{\frac{3}{2}}\operatorname{erf}'\left(\frac{h^2\sigma}{t}\right)^{\frac{1}{2}}\right]e^{-\alpha^2/8t}I_0\left(\frac{\alpha^2}{8t}\right), \quad (46)$$

$$H''_{1\rho} = -\frac{\Delta\sigma M}{32\pi\sigma}\frac{d}{d\rho}\left[\operatorname{erfc}\left(\frac{h^2\sigma}{t}\right)^{\frac{1}{2}}\mathscr{D} - \frac{h}{2}\left(\frac{\sigma}{t}\right)^{\frac{3}{2}}\operatorname{erf}'\left(\frac{h^2\sigma}{t}\right)^{\frac{1}{2}}\right]e^{-\alpha^2/4t}, \quad (47)$$

where $\alpha^2 = \sigma\rho^2$.

Acknowledgements

I wish to thank Professor I. N. Sneddon and Mr. B. Noble for valuable advice during the writing of this paper. I am indebted to the Department of Scientific and Industrial Research for a maintenance grant during the period in which the work described in this paper was done.

REFERENCES

1. A. T. Price, *Quart. J. Mech. Appl. Math.* **3** (1950), 385.
2. A. N. Gordon, ibid. **4** (1951), 106.
3. B. K. Bhattacharyya, *J. Geophys. Research*, **60** (1955), 279.
4. Erdélyi *et al.*, *Tables of Integral Transforms* (McGraw-Hill, 1954).
5. G. N. Watson, *Theory of Bessel Functions* (Cambridge, 1944).

THE DIFFRACTION OF A DIPOLE FIELD BY A HALF-PLANE

By BETTY D. WOODS
(*Department of Mathematics, Manchester University*)

[Received 7 March 1956]

SUMMARY

The problem of the diffraction of an electromagnetic dipole field by a perfectly conducting half-plane is discussed. Solutions for arbitrary orientations of the dipole are determined by extending a method due to Bromwich, which was based on the solution of a scalar problem and valid only when the axis of the dipole is parallel to the edge of the screen. Results are given for an electric dipole with its axis normal to the screen and for an electric dipole with its axis normal to the edge of the screen and lying in a plane parallel to the screen.

1. Introduction

THE problem discussed in this paper is that of the diffraction of the electromagnetic field of an oscillating dipole by an infinitely thin, perfectly conducting half-plane. This problem has been discussed by Senior (**1**), who obtains a solution by expanding the dipole field in plane waves. The method can be used for any position and orientation of the dipole but the calculation is laborious. Senior gives an explicit solution only for an electric dipole with its axis perpendicular to the plane. Another method has recently been given in a paper by Heins (**2**).†

Bromwich (**3**) has given a simpler solution for a dipole parallel to the edge of the conducting plane based on the solution of the corresponding scalar problem, that of the diffraction of the sound waves of a point source by a rigid screen. The purpose of the present paper is to extend Bromwich's method to arbitrary orientations of the dipole.

The solution of the scalar problem is the determination of a function ϕ which satisfies the wave equation everywhere except at points on the screen and at the singularity which represents the source. Also it contains only diverging waves at infinity and its normal derivative is zero on the screen. There is a similar problem in which ϕ, instead of its normal derivative, is to be zero on the screen. Solutions to both problems, which are closely related, have been given by Macdonald (**4**), *inter alia*.

Bromwich's method is to take this function ϕ multiplied by a constant unit vector in the direction of the axis of the dipole as the Hertz potential for the electromagnetic field problem. The resultant field satisfies Maxwell's equations, has the correct singularity at the position of the dipole and

† *Note added in proof.* Investigation of this problem has also been carried out by Yu. V. Vandakurov, *Zh. Eksp. Teor. Fiz.* **26** (1954), 3–18.

contains only diverging waves. By using the value of ϕ which satisfies the appropriate boundary condition for each of three mutually perpendicular orientations of the dipole the tangential component of the electric field on the screen can be made to vanish. Thus Bromwich's method leads to a field, for arbitrary orientation of the dipole, which satisfies Maxwell's equations and the appropriate boundary conditions.

It is known, however, that for diffracting bodies with sharp edges these boundary conditions are not sufficient to determine a unique solution of the field equations. Recent investigations by several authors (Copson (**5**), Meixner (**6**), Jones (**7**), Heins and Silver (**8**)) agree that the correct solution to the physical problem is defined by the order of the singularities of the various field components near the edge. It is only for an electric dipole with its axis parallel to the edge of the diffracting half-plane that Bromwich's solution satisfies the edge conditions.

The difference between any two solutions of the field equations which satisfy the boundary conditions on the screen and at the source is a field which satisfies Maxwell's equations everywhere except on the screen and satisfies the boundary conditions there. The method adopted in this paper is to determine the solution of this 'homogeneous' problem which, when added to Bromwich's solution of the diffraction problem gives a field which satisfies the edge conditions and which is therefore the correct solution of the diffraction problem. In this way the problem involving either an electric, magnetic, or sound dipole can be solved. The details are given here for two cases, one being that of an electric dipole with its axis normal to the screen, for which the solution is shown to be the same as that given by Senior, and the other that of an electric dipole with its axis normal to the edge of the screen and lying in a plane parallel to the screen. The solutions for these two positions of the dipole, together with that given by Bromwich for a dipole parallel to the edge of the screen, can then be used to determine the field of a dipole orientated in any way.

I wish to express my thanks to Mr. D. S. Jones for suggesting this problem and to him and Mr. E. Wild for their valuable advice and criticism.

2. Bromwich's method

Suppose that an infinitely thin, perfectly conducting half-plane occupies the region $y = 0, x > 0$ of a cartesian coordinate system $O(x, y, z)$ and that either an electric or magnetic dipole is situated at some point in space, its direction being represented by the unit vector $\mathbf{u}$.

The electromagnetic field must be such that:

(i) It satisfies Maxwell's equations everywhere except on the screen, and at the dipole where there must be a dipole singularity.

(ii) It represents diverging waves at large distances from the origin.

(iii) The tangential electric field component vanishes on the screen.

(iv) In terms of cylindrical polar coordinates r, θ, z, the x and y components of the electric and magnetic fields are of order $r^{-\frac{1}{2}}$ and the z-components are of order $r^{\frac{1}{2}}$ near the edge of the screen.

For the case of an electric dipole Bromwich's solution

$$\mathcal{E}^{(B)}(x,y,z)e^{ickt}, \qquad \mathcal{H}^{(B)}(x,y,z)e^{ickt}$$

is given in m.k.s. units by

$$\mathcal{E}^{(B)} = (\nabla\nabla . + k^2)\phi\mathbf{u}, \qquad \mathcal{H}^{(B)} = ikY(\nabla \wedge \phi\mathbf{u}),$$

where Y is the intrinsic admittance of free space.

The function ϕ is the solution of the wave equation $(\nabla^2+k^2)\phi = 0$, which either vanishes or has vanishing normal derivatives on the screen and is such that near the position of the dipole $\phi \sim e^{-ikR}/R$, where R is the distance from the dipole.

$\mathcal{E}^{(B)}$ and $\mathcal{H}^{(B)}$ satisfy (i) and (ii) and can be made to satisfy (iii) by using the ϕ which satisfies the appropriate boundary conditions for each position of the dipole. Thus for the dipole parallel to the x-axis

$$\mathcal{E}_x^{(B)} = \frac{\partial^2\phi}{\partial x^2} + k^2\phi, \qquad \mathcal{E}_z^{(B)} = \frac{\partial^2\phi}{\partial x \partial z},$$

$$\mathcal{E}_x^{(B)} = \mathcal{E}_z^{(B)} = 0 \quad \text{on } y = 0,\ x > 0, \text{ when } \phi = 0 \text{ there.}$$

For the dipole parallel to the y-axis

$$\mathcal{E}_x^{(B)} = \frac{\partial^2\phi}{\partial x \partial y}, \qquad \mathcal{E}_z^{(B)} = \frac{\partial^2\phi}{\partial y \partial z},$$

$$\mathcal{E}_x^{(B)} = \mathcal{E}_z^{(B)} = 0 \quad \text{on } y = 0,\ x > 0, \text{ when } \partial\phi/\partial y = 0 \text{ there,}$$

and for the dipole parallel to the z-axis

$$\mathcal{E}_x^{(B)} = \frac{\partial^2\phi}{\partial x \partial z}, \qquad \mathcal{E}_z^{(B)} = \frac{\partial^2\phi}{\partial z^2} + k^2\phi,$$

$$\mathcal{E}_x^{(B)} = \mathcal{E}_z^{(B)} = 0 \quad \text{on } y = 0,\ x > 0, \text{ when } \phi = 0 \text{ there.}$$

For the case of the magnetic dipole Bromwich's solution is given by

$$\mathcal{E}^{(B)} = -\frac{ik}{Y}(\nabla \wedge \phi\mathbf{u}), \qquad \mathcal{H}^{(B)} = -(\nabla\nabla . + k^2)\phi\mathbf{u},$$

where again $\mathcal{E}^{(B)}$ and $\mathcal{H}^{(B)}$ satisfy (i) and (ii) and satisfy (iii) when ϕ is suitably chosen for each position of the dipole.

For the dipole parallel to the x-axis,

$$\mathcal{E}_x^{(B)} = 0, \qquad \mathcal{E}_z^{(B)} = -\frac{ik}{Y}\frac{\partial\phi}{\partial y},$$

$$\mathcal{E}_z^{(B)} = 0 \quad \text{on } y = 0,\ x > 0, \text{ when } \partial\phi/\partial y = 0 \text{ there.}$$

For the dipole parallel to the y-axis

$$\mathcal{E}_x^{(B)} = -\frac{ik}{Y}\frac{\partial\phi}{\partial z}, \qquad \mathcal{E}_z^{(B)} = \frac{ik}{Y}\frac{\partial\phi}{\partial x},$$

$$\mathcal{E}_x^{(B)} = \mathcal{E}_z^{(B)} = 0 \quad \text{on } y = 0, x > 0 \text{ when } \phi = 0 \text{ there,}$$

and for the dipole parallel to the z-axis

$$\mathcal{E}_x^{(B)} = \frac{ik}{Y}\frac{\partial\phi}{\partial y}, \qquad \mathcal{E}_z^{(B)} = 0,$$

$$\mathcal{E}_x^{(B)} = 0 \quad \text{on } y = 0, x > 0 \text{ when } \partial\phi/\partial y = 0 \text{ there.}$$

3. Behaviour of Bromwich's solution near the edge of the screen

We consider the case of an electric dipole with axis parallel to the y-axis and situated at the point (x_0, y_0, z_0), for which Bromwich's solution is

$$\boldsymbol{\mathcal{E}}^{(B)} = \left(\frac{\partial^2\phi}{\partial x\partial y}, \frac{\partial^2\phi}{\partial y^2} + k^2\phi, \frac{\partial^2\phi}{\partial y\partial z}\right), \tag{3.1}$$

$$\boldsymbol{\mathcal{H}}^{(B)} = ikY\left(-\frac{\partial\phi}{\partial z}, 0, \frac{\partial\phi}{\partial x}\right), \tag{3.2}$$

where $\phi = \phi_1 + \phi_2$ and in the form given by Senior (**1**),

$$\phi_1 = -\frac{i}{2}\int_{-\infty}^{\mu_R} H_1^{(2)}(kR\cosh\mu)\,d\mu, \qquad \phi_2 = -\frac{i}{2}\int_{-\infty}^{\mu_S} H_1^{(2)}(kS\cosh\mu)\,d\mu,$$

where $R = [r^2 + r_0^2 - 2rr_0\cos(\theta-\theta_0) + (z-z_0)^2]^{\frac{1}{2}}$ is the distance from the dipole, and $S = [r^2 + r_0^2 - 2rr_0\cos(\theta+\theta_0) + (z-z_0)^2]^{\frac{1}{2}}$ is the distance from the image of the dipole in the plane $y = 0$; r_0, θ_0, z_0 are the cylindrical polar coordinates which specify the position of the dipole. Also

$$\mu_R = \sinh^{-1}\left[\frac{2\sqrt{(r_0 r)}}{R}\cos\frac{(\theta-\theta_0)}{2}\right], \qquad \mu_S = \sinh^{-1}\left[\frac{2\sqrt{(r_0 r)}}{S}\cos\frac{(\theta+\theta_0)}{2}\right].$$

The solution of the homogeneous problem is most easily determined by using Fourier transforms, and therefore to determine the difference between Bromwich's solution and the correct solution we introduce the Fourier transforms $\mathbf{E}^{(B)}$, $\mathbf{H}^{(B)}$ with respect to z of $\boldsymbol{\mathcal{E}}^{(B)}$, $\boldsymbol{\mathcal{H}}^{(B)}$ defined by

$$\mathbf{E}^{(B)} = \frac{1}{\sqrt{(2\pi)}}\int_{-\infty}^{\infty} \boldsymbol{\mathcal{E}}^{(B)} e^{-isz}\,dz, \qquad \mathbf{H}^{(B)} = \frac{1}{\sqrt{(2\pi)}}\int_{-\infty}^{\infty} \boldsymbol{\mathcal{H}}^{(B)} e^{-isz}\,dz,$$

and we consider the behaviour of $\mathbf{E}^{(B)}$ and $\mathbf{H}^{(B)}$ near the edge of the screen.

It is seen from (3.1) and (3.2) that

$$\mathbf{E}^{(B)} = \left(\frac{\partial^2\Phi}{\partial x\partial y}, \frac{\partial^2\Phi}{\partial y^2}+k^2\Phi, is\frac{\partial\Phi}{\partial y}\right), \tag{3.3}$$

$$\mathbf{H}^{(B)} = ikY\left(-is\Phi, 0, \frac{\partial\Phi}{\partial x}\right), \tag{3.4}$$

where
$$\Phi = \frac{1}{\sqrt{(2\pi)}}\int_{-\infty}^{\infty}\phi e^{-isz}\,dz.$$

Now Φ is easily determined, for as ϕ satisfies

$$\nabla^2\phi+k^2\phi+\delta(x-x_0)\delta(y-y_0)\delta(z-z_0) = 0,$$

Φ must satisfy

$$\nabla_2^2\Phi+\kappa^2\Phi+\frac{e^{-isz_0}}{\sqrt{(2\pi)}}\delta(x-x_0)\delta(y-y_0) = 0, \tag{3.5}$$

where $\nabla_2^2 = \left(\frac{\partial^2}{\partial x^2}+\frac{\partial^2}{\partial y^2}\right)$ and δ is the Dirac delta-function; also $\kappa^2 = k^2-s^2$ and we define κ as the branch of $(k^2-s^2)^{\frac{1}{2}}$ for which $\kappa > 0$ for $|s| < k$ and $i\kappa > 0$ for $|s| > k$. Equation (3.5) is the same as the equation satisfied by the magnetic force, $e^{isz}\sqrt{(2\pi)}\Phi$, of a line source on the line r_0, θ_0 in the presence of the screen and from the solution of this problem given by MacDonald (**4**) we find that

$$\Phi = \Phi_1+\Phi_2,$$

where

$$\Phi_1 = \frac{e^{-isz_0}}{k\sqrt{(2\pi)}}\int_{-\infty}^{\mu_{R_1}} e^{-i\kappa R_1\cosh\mu}\,d\mu, \tag{3.6}$$

$$\Phi_2 = \frac{e^{-isz_0}}{k\sqrt{(2\pi)}}\int_{-\infty}^{\mu_{S_1}} e^{-i\kappa S_1\cosh\mu}\,d\mu, \tag{3.7}$$

$$R_1 = [r^2+r_0^2-2rr_0\cos(\theta-\theta_0)]^{\frac{1}{2}}, \qquad S_1 = [r^2+r_0^2-2rr_0\cos(\theta+\theta_0)]^{\frac{1}{2}},$$

$$\mu_{R_1} = \sinh^{-1}\left[\frac{2\sqrt{(r_0 r)}}{R_1}\cos\frac{(\theta-\theta_0)}{2}\right], \qquad \mu_{S_1} = \sinh^{-1}\left[\frac{2\sqrt{(r_0 r)}}{S_1}\cos\frac{(\theta+\theta_0)}{2}\right].$$

Equations (3.6) and (3.7) can be verified from the inverse Fourier transform using the substitution

$$t = -i\kappa(r+r_0)+is(z-z_0)$$

given at the end of section 4.

To derive the edge singularities in the transformed components $E_x^{(B)}$,

$E_y^{(B)}$, $E_z^{(B)}$, and $H_x^{(B)}$, $H_y^{(B)}$, $H_z^{(B)}$ it is sufficient to determine the leading terms in the expansion of Φ in powers of $r^{\frac{1}{2}}$ near $r = 0$. Thus

$$\Phi_1 = \frac{e^{-isz_0}}{k\sqrt{(2\pi)}} \int_{-\infty}^{0} e^{-ikr_0 \cosh \mu}\, d\mu + \frac{e^{-ikr_0 - isz_0}}{k} \left(\frac{2r}{\pi r_0}\right)^{\frac{1}{2}} \cos \frac{(\theta - \theta_0)}{2} + O(r),$$

$$\Phi_2 = \frac{e^{-isz_0}}{k\sqrt{(2\pi)}} \int_{-\infty}^{0} e^{-ikr_0 \cosh \mu}\, d\mu + \frac{e^{-ikr_0 - isz_0}}{k} \left(\frac{2r}{\pi r_0}\right)^{\frac{1}{2}} \cos \frac{(\theta + \theta_0)}{2} + O(r)$$

as $r \to 0$. Hence

$$\Phi = \frac{e^{-isz_0}}{k} \left(\frac{2}{\pi}\right)^{\frac{1}{2}} \int_{-\infty}^{0} e^{-ikr_0 \cosh \mu}\, d\mu + \frac{2e^{-ikr_0 - isz_0}}{k} \left(\frac{2r}{\pi r_0}\right)^{\frac{1}{2}} \cos \frac{\theta_0}{2} \cos \frac{\theta}{2} + O(r)$$

as $r \to 0$.

Using this result and carrying out the differentiation in (3.3) and (3.4) we find as $r \to 0$,

$$E_x^{(B)} = -\frac{C}{2r^{\frac{1}{2}}} \sin \frac{3\theta}{2} + O\left(\frac{1}{r^{\frac{1}{2}}}\right), \qquad H_x^{(B)} = sYe^{-isz_0} \left(\frac{2}{\pi}\right)^{\frac{1}{2}} \int_{-\infty}^{0} e^{-ikr_0 \cosh \mu}\, d\mu + O(r^{\frac{1}{2}}),$$

$$E_y^{(B)} = \frac{C}{2r^{\frac{1}{2}}} \cos \frac{3\theta}{2} + O\left(\frac{1}{r^{\frac{1}{2}}}\right), \qquad H_y^{(B)} = 0,$$

$$E_z^{(B)} = \frac{isC}{r^{\frac{1}{2}}} \sin \theta + O(1), \qquad H_z^{(B)} = \frac{ikYC}{r^{\frac{1}{2}}} \cos \frac{\theta}{2} + O(1),$$

where $C = \dfrac{e^{-ikr_0 - isz_0}}{k} \left(\dfrac{2}{\pi r_0}\right)^{\frac{1}{2}} \cos \dfrac{\theta_0}{2}$.

4. The homogeneous problem

To eliminate the incorrect edge singularities in Bromwich's solution we have to find an electromagnetic field $\boldsymbol{\mathcal{E}}^{(C)} e^{ickt}$, $\boldsymbol{\mathcal{H}}^{(C)} e^{ickt}$ which satisfies Maxwell's equations everywhere except on the screen, represents only diverging waves at infinity and has a vanishing tangential electric field component on the screen. We consider only solutions $\boldsymbol{\mathcal{E}}^{(C)}$ and $\boldsymbol{\mathcal{H}}^{(C)}$ which have Fourier transforms $\mathbf{E}^{(C)}$ and $\mathbf{H}^{(C)}$ with respect to z.

The equations to be satisfied by the Fourier transforms $E_x^{(C)}$, $E_y^{(C)}$, $E_z^{(C)}$, and $H_x^{(C)}$, $H_y^{(C)}$, $H_z^{(C)}$ of the field components are

$$-\frac{ikH_x^{(C)}}{Y} = \frac{\partial E_z^{(C)}}{\partial y} - isE_y^{(C)}, \qquad ikYE_x^{(C)} = \frac{\partial H_z^{(C)}}{\partial y} - isH_y^{(C)},$$

$$-\frac{ikH_y^{(C)}}{Y} = isE_x^{(C)} - \frac{\partial E_z^{(C)}}{\partial x}, \qquad ikYE_y^{(C)} = isH_x^{(C)} - \frac{\partial H_z^{(C)}}{\partial x},$$

$$-\frac{ikH_z^{(C)}}{Y} = \frac{\partial E_y^{(C)}}{\partial x} - \frac{\partial E_x^{(C)}}{\partial y}, \qquad ikYE_z^{(C)} = \frac{\partial H_y^{(C)}}{\partial x} - \frac{\partial H_x^{(C)}}{\partial y}.$$

From these it can be seen that all the transformed components can be expressed in terms of $E_z^{(C)}$, $H_z^{(C)}$ and their derivatives. Thus

$$E_x^{(C)} = \frac{is}{\kappa^2}\frac{\partial E_z^{(C)}}{\partial x} - \frac{ik}{Y\kappa^2}\frac{\partial H_z^{(C)}}{\partial y}, \qquad H_x^{(C)} = \frac{iYk}{\kappa^2}\frac{\partial E_z^{(C)}}{\partial y} + \frac{is}{\kappa^2}\frac{\partial H_z^{(C)}}{\partial x},$$

$$E_y^{(C)} = \frac{is}{\kappa^2}\frac{\partial E_z^{(C)}}{\partial y} + \frac{ik}{Y\kappa^2}\frac{\partial H_z^{(C)}}{\partial x}, \qquad H_y^{(C)} = -\frac{iYk}{\kappa^2}\frac{\partial E_z^{(C)}}{\partial x} + \frac{is}{\kappa^2}\frac{\partial H_z^{(C)}}{\partial y}. \tag{4.1}$$

It can be seen from (3.3), (3.4), (3.5) that $E_x^{(B)}$, $E_y^{(B)}$, $H_x^{(B)}$, and $H_y^{(B)}$ can be expressed in the same way in terms of $E_z^{(B)}$ and $H_z^{(B)}$. From (4.1) and the boundary conditions $E_x^{(C)} = E_z^{(C)} = 0$ on the screen there follow the boundary conditions

$$E_z^{(C)} = \frac{\partial H_z^{(C)}}{\partial y} = 0 \quad \text{on the screen.}$$

As $\mathscr{E}_z^{(C)}$ must satisfy $(\nabla^2+k^2)\mathscr{E}_z^{(C)} = 0$ then $E_z^{(C)}$ must satisfy $(\nabla_2^2+\kappa^2)E_z^{(C)} = 0$, and the only solutions of this equation which satisfy the boundary condition and the condition that $E_z^{(C)} \sim Qe^{-i\kappa r}/r^{\frac{1}{2}}$ for large r, Q a constant (which is necessary in order that the solution of the original problem should contain only outward travelling waves at infinity) are

$$E_z^{(C)} = \sum_n A_{\frac{1}{2}n} H_{\frac{1}{2}n}^{(2)}(\kappa r)\sin\frac{n\theta}{2}, \tag{4.2}$$

where n has integral values and the coefficients $A_{\frac{1}{2}n}$ are arbitrary functions of s. We define $H_\nu^{(2)}(\kappa r)$ for κ real or imaginary as a Bessel function of order ν which has the asymptotic form $(2/\pi\kappa r)^{\frac{1}{2}}e^{-i(\kappa r-\frac{1}{2}\nu\pi-\frac{1}{4}\pi)}$ for large r.

In the same way for $H_z^{(C)}$ we obtain

$$H_z^{(C)} = \sum_n B_{\frac{1}{2}n} H_{\frac{1}{2}n}^{(2)}(\kappa r)\cos\frac{n\theta}{2}, \tag{4.3}$$

where the coefficients $B_{\frac{1}{2}n}$ are arbitrary functions of s.

We consider now the electromagnetic field whose Fourier transform is given by $\mathbf{E} = \mathbf{E}^{(B)}+\mathbf{E}^{(C)}$, $\mathbf{H} = \mathbf{H}^{(B)}+\mathbf{H}^{(C)}$, and we determine $A_{\frac{1}{2}n}$ and $B_{\frac{1}{2}n}$ by equating to zero the terms of order $r^{-\frac{1}{2}}$ in the expansion near $r = 0$ of E_z and H_z, which are thus made to satisfy the edge condition. It follows from the relations (4.1) for the B and C fields that the other components of $\mathbf{E}$ and $\mathbf{H}$ will also satisfy the edge condition.

For the values of the coefficients we find

$$A_{\frac{1}{2}} = -sC\left(\frac{\pi\kappa}{2}\right)^{\frac{1}{2}}, \qquad B_{\frac{1}{2}} = -kYC\left(\frac{\pi\kappa}{2}\right)^{\frac{1}{2}}.$$

Hence

$$E_z^{(C)} = -\frac{ise^{-i\kappa(r+r_0)-isz_0}}{k}\left(\frac{2}{\pi r_0 r}\right)^{\frac{1}{2}}\cos\frac{\theta_0}{2}\sin\frac{\theta}{2},$$

$$H_z^{(C)} = -iYe^{-i\kappa(r+r_0)-isz_0}\left(\frac{2}{\pi r_0 r}\right)^{\frac{1}{2}}\cos\frac{\theta_0}{2}\cos\frac{\theta}{2},$$

and therefore

$$E_z = is\frac{\partial\Phi}{\partial y} - \frac{ise^{-i\kappa(r+r_0)-isz_0}}{k}\left(\frac{2}{\pi r_0 r}\right)^{\frac{1}{2}}\cos\frac{\theta_0}{2}\sin\frac{\theta}{2},$$

$$H_z = ikY\frac{\partial\Phi}{\partial x} - iYe^{-i\kappa(r+r_0)-isz_0}\left(\frac{2}{\pi r_0 r}\right)^{\frac{1}{2}}\cos\frac{\theta_0}{2}\cos\frac{\theta}{2}.$$

From the definitions (3.6) and (3.7) and the fact that R_1 is a function of $(x-x_0)$ and $(y-y_0)$ and S_1 a function of $(x-x_0)$ and $(y+y_0)$ it follows easily that

$$\frac{\partial\Phi}{\partial y} = \frac{\partial(\Phi_2-\Phi_1)}{\partial y_0} + \frac{e^{-i\kappa(r+r_0)-isz_0}}{k}\left(\frac{2}{\pi r_0 r}\right)^{\frac{1}{2}}\cos\frac{\theta_0}{2}\sin\frac{\theta}{2},$$

$$\frac{\partial\Phi}{\partial x} = -\frac{\partial\Phi}{\partial x_0} + \frac{e^{-i\kappa(r+r_0)-isz_0}}{k}\left(\frac{2}{\pi r_0 r}\right)^{\frac{1}{2}}\cos\frac{\theta_0}{2}\cos\frac{\theta}{2}.$$

Using these relations we can express E_z and H_z in the form

$$E_z = is\frac{\partial}{\partial y_0}(\Phi_2-\Phi_1), \qquad H_z = -ikY\frac{\partial\Phi}{\partial x_0}.$$

For the other components of **E** and **H** we have, using (4.1),

$$E_x = \frac{\partial^2}{\partial x\partial y_0}(\Phi_2-\Phi_1) + \frac{ike^{-i\kappa(r+r_0)-isz_0}}{\kappa}\left(\frac{2}{\pi r_0 r}\right)^{\frac{1}{2}}\cos\frac{\theta_0}{2}\sin\frac{\theta}{2},$$

$$E_y = \frac{\partial^2}{\partial y\partial y_0}(\Phi_2-\Phi_1) + k^2\Phi - \frac{ike^{-i\kappa(r+r_0)-isz_0}}{\kappa}\left(\frac{2}{\pi r_0 r}\right)^{\frac{1}{2}}\cos\frac{\theta_0}{2}\cos\frac{\theta}{2},$$

$$H_x = skY\Phi + Y\frac{\partial}{\partial z_0}\left[\frac{e^{-i\kappa(r+r_0)-isz_0}}{\kappa}\right]\left(\frac{2}{\pi r_0 r}\right)^{\frac{1}{2}}\cos\frac{\theta_0}{2}\cos\frac{\theta}{2},$$

$$H_y = Y\frac{\partial}{\partial z_0}\left[\frac{e^{-i\kappa(r+r_0)-isz_0}}{\kappa}\right]\left(\frac{2}{\pi r_0 r}\right)^{\frac{1}{2}}\cos\frac{\theta_0}{2}\sin\frac{\theta}{2}.$$

Finally, by taking the inverse Fourier transforms of **E** and **H** we obtain the correct solution $\mathscr{E}$, $\mathscr{H}$ of the problem. Thus for the x-component of the electric force $\mathscr{E}_x$ we have

$$\mathscr{E}_x = \frac{1}{\sqrt{(2\pi)}}\int_{-\infty}^{\infty} E_x e^{isz}\,ds$$

$$= \frac{\partial^2}{\partial x\partial y_0}(\phi_2-\phi_1) + \frac{ik}{\pi\sqrt{(r_0 r)}}\cos\frac{\theta_0}{2}\sin\frac{\theta}{2}\int_{-\infty}^{\infty} e^{-i\kappa(r+r_0)+is(z-z_0)}\frac{ds}{\kappa}. \quad (4.4)$$

To evaluate the integral in (4.4) we make the substitution

$$t = -i\kappa(r+r_0)+is(z-z_0).$$

Then $$s = -it(z-z_0)+(r+r_0)(k^2U^2+t^2)^{\frac{1}{2}},$$

where $$U = [(r+r_0)^2+(z-z_0)^2]^{\frac{1}{2}}.$$

The integral becomes $$-i\int_C \frac{e^t\,dt}{(k^2U^2+t^2)^{\frac{1}{2}}},$$

where C is a contour which can be deformed into the imaginary axis taken from $-i\infty$ to $i\infty$ with $(k^2U^2+t^2)^{\frac{1}{2}} > 0$ for $|t| < kU$ and $i(k^2U^2+t^2)^{\frac{1}{2}} > 0$ for $|t| > kU$. This contour can be further deformed into a Hankel loop round the branch point $t = -ikU$, which gives for the value of the integral $\pi H_0^{(2)}(kU)$. Therefore

$$\mathscr{E}_x = \frac{\partial^2}{\partial x\partial y_0}(\phi_2-\phi_1)+\frac{ik}{\sqrt{(r_0 r)}}H_0^{(2)}(kU)\cos\frac{\theta_0}{2}\sin\frac{\theta}{2}.$$

The other field components can be determined in a similar way. Hence for the complete solution we have

$$\mathscr{E}_x = \frac{\partial^2}{\partial x\partial y_0}(\phi_2-\phi_1)+\frac{ik}{\sqrt{(r_0 r)}}H_0^{(2)}(kU)\cos\frac{\theta_0}{2}\sin\frac{\theta}{2},$$

$$\mathscr{E}_y = \frac{\partial^2}{\partial y\partial y_0}(\phi_2-\phi_1)+k^2\phi-\frac{ik}{\sqrt{(r_0 r)}}H_0^{(2)}(kU)\cos\frac{\theta_0}{2}\cos\frac{\theta}{2},$$

$$\mathscr{E}_z = \frac{\partial^2}{\partial z\partial y_0}(\phi_2-\phi_1),$$

$$\mathscr{H}_x = ikY\frac{\partial\phi}{\partial z_0}+\frac{kY(z-z_0)}{U\sqrt{(r_0 r)}}H_1^{(2)}(kU)\cos\frac{\theta_0}{2}\cos\frac{\theta}{2},$$

$$\mathscr{H}_y = \frac{kY(z-z_0)}{U\sqrt{(r_0 r)}}H_1^{(2)}(kU)\cos\frac{\theta_0}{2}\sin\frac{\theta}{2},$$

$$\mathscr{H}_z = -ikY\frac{\partial\phi}{\partial x_0}.$$

It is seen that $\mathscr{E}$, $\mathscr{H}$ in the above form is the solution given by Senior for this problem.

5. The dipole with its axis parallel to the x-axis

For the case of an electric dipole with axis parallel to the x-axis and situated at the point (x_0, y_0, z_0) the procedure is the same. Bromwich's solution is

$$\mathscr{E}^{(B)} = \left(\frac{\partial^2\phi}{\partial x^2}+k^2\phi, \frac{\partial^2\phi}{\partial x\partial y}, \frac{\partial^2\phi}{\partial x\partial z}\right), \qquad \mathscr{H}^{(B)} = ikY\left(0, \frac{\partial\phi}{\partial z}, -\frac{\partial\phi}{\partial y}\right),$$

where now $\phi = \phi_1-\phi_2$.

The Fourier transforms of $\mathfrak{E}^{(B)}$ and $\mathfrak{H}^{(B)}$ are

$$\mathbf{E}^{(B)} = \left(\frac{\partial^2\Phi}{\partial x^2}+k^2\Phi, \frac{\partial^2\Phi}{\partial x\partial y}, is\frac{\partial\Phi}{\partial x}\right), \qquad \mathbf{H}^{(B)} = ikY\left(0, is\Phi, -\frac{\partial\Phi}{\partial y}\right),$$

where $\Phi = \Phi_1 - \Phi_2$.

Near the edge of the sheet

$$E_z^{(B)} = -\frac{isD}{r^{\frac{1}{2}}}\sin\frac{\theta}{2}+O(1), \qquad H_z^{(B)} = -\frac{ikYD}{r^{\frac{1}{2}}}\cos\frac{\theta}{2}+O(1), \qquad (5.1)$$

where

$$D = \frac{e^{-i\kappa r_0 - isz_0}}{k}\left(\frac{2}{\pi r_0}\right)^{\frac{1}{2}}\sin\frac{\theta_0}{2}.$$

The coefficients $A_{\frac{1}{2}n}$ and $B_{\frac{1}{2}n}$ involved in the homogeneous problem are determined by eliminating the terms of order $r^{-\frac{1}{2}}$ in (5.1) in the way described.

Thus we find

$$A_{\frac{1}{2}} = sD\left(\frac{\pi\kappa}{2}\right)^{\frac{1}{2}}, \qquad B_{\frac{1}{2}} = kYD\left(\frac{\pi\kappa}{2}\right)^{\frac{1}{2}}.$$

Hence

$$E_z^{(C)} = \frac{ise^{-i\kappa(r+r_0)-isz_0}}{k}\left(\frac{2}{\pi r_0 r}\right)^{\frac{1}{2}}\sin\frac{\theta_0}{2}\sin\frac{\theta}{2},$$

$$H_z^{(C)} = iYe^{-i\kappa(r+r_0)-isz_0}\left(\frac{2}{\pi r_0 r}\right)^{\frac{1}{2}}\sin\frac{\theta_0}{2}\cos\frac{\theta}{2}.$$

Then for E_z and H_z we obtain

$$E_z = is\frac{\partial\Phi}{\partial x}+\frac{ise^{-i\kappa(r+r_0)-isz_0}}{k}\left(\frac{2}{\pi r_0 r}\right)^{\frac{1}{2}}\sin\frac{\theta_0}{2}\sin\frac{\theta}{2},$$

$$H_z = -ikY\frac{\partial\Phi}{\partial y}+iYe^{-i\kappa(r+r_0)-isz_0}\left(\frac{2}{\pi r_0 r}\right)^{\frac{1}{2}}\sin\frac{\theta_0}{2}\cos\frac{\theta}{2},$$

which can be written as

$$E_z = is\frac{\partial}{\partial x_0}(\Phi_2-\Phi_1), \qquad H_z = ikY\frac{\partial}{\partial y_0}(\Phi_1+\Phi_2).$$

By using the relations (4.1) the other components of **E** and **H** can be found. Thus

$$E_x = \frac{\partial^2}{\partial x\partial x_0}(\Phi_2-\Phi_1)+k^2\Phi-\frac{ike^{-i\kappa(r+r_0)-isz_0}}{\kappa}\left(\frac{2}{\pi r_0 r}\right)^{\frac{1}{2}}\sin\frac{\theta_0}{2}\sin\frac{\theta}{2},$$

$$E_y = \frac{\partial^2}{\partial y\partial x_0}(\Phi_2-\Phi_1)+\frac{ike^{-i\kappa(r+r_0)-isz_0}}{\kappa}\left(\frac{2}{\pi r_0 r}\right)^{\frac{1}{2}}\sin\frac{\theta_0}{2}\cos\frac{\theta}{2},$$

$$H_x = -Y\frac{\partial}{\partial z_0}\left[\frac{e^{-i\kappa(r+r_0)-isz_0}}{\kappa}\right]\left(\frac{2}{\pi r_0 r}\right)^{\frac{1}{2}}\sin\frac{\theta_0}{2}\cos\frac{\theta}{2},$$

$$H_y = -skY(\Phi_1-\Phi_2)-Y\frac{\partial}{\partial z_0}\left[\frac{e^{-i\kappa(r+r_0)-isz_0}}{\kappa}\right]\sin\frac{\theta_0}{2}\sin\frac{\theta}{2}.$$

Hence by taking the inverse Fourier transforms of the components of **E** and **H** we have for the solution

$$\mathscr{E}_x = -\frac{\partial^2\phi}{\partial x\partial x_0} + k^2\phi - \frac{ik}{\sqrt{(r_0 r)}} H_0^{(2)}(kU)\sin\frac{\theta_0}{2}\sin\frac{\theta}{2},$$

$$\mathscr{E}_y = -\frac{\partial^2\phi}{\partial y\partial x_0} + \frac{ik}{\sqrt{(r_0 r)}} H_0^{(2)}(kU)\sin\frac{\theta_0}{2}\cos\frac{\theta}{2},$$

$$\mathscr{E}_z = -\frac{\partial^2\phi}{\partial z\partial x_0},$$

$$\mathscr{H}_x = -\frac{kY(z-z_0)}{U\sqrt{(r_0 r)}} H_1^{(2)}(kU)\sin\frac{\theta_0}{2}\cos\frac{\theta}{2},$$

$$\mathscr{H}_y = -ikY\frac{\partial\phi}{\partial z_0} - \frac{kY(z-z_0)}{U\sqrt{(r_0 r)}} H_1^{(2)}(kU)\sin\frac{\theta_0}{2}\sin\frac{\theta}{2},$$

$$\mathscr{H}_z = ikY\frac{\partial\phi_1}{\partial y_0} + ikY\frac{\partial\phi_2}{\partial y_0}.$$

The field due to a dipole orientated in any way can now easily be determined from the solutions for the above two cases together with Bromwich's solution for an electric dipole parallel to the z-axis.

REFERENCES

1. T. B. A. Senior, *Quart. J. Mech. App. Math.* **6** (1953), 101.
2. A. E. Heins, Tech. Report No. 17, Carnegie Inst. of Tech.
3. T. J. I'A. Bromwich, *Proc. London Math. Soc.* **14** (1915), 450.
4. H. M. Macdonald, ibid. 410.
5. E. T. Copson, *Proc. Roy. Soc.* A, **202** (1950), 277.
6. J. Meixner, *Ann. d. Phys.* **6** (1949), 2.
7. D. S. Jones, *Quart. J. Mech. App. Math.* **3** (1950), 420.
8. A. E. Heins and S. Silver, *Proc. Camb. Phil. Soc.* **51** (1955), 149.

THE PERIODIC SOLUTIONS OF THE DIFFERENTIAL EQUATION OF A RESISTANCE-CAPACITANCE OSCILLATOR

By A. W. GILLIES (*Northampton Polytechnic, London*)

[Received 5 April 1956]

SUMMARY

A third-order differential equation is considered of a form which arises in connexion with a resistance-capacity oscillator, the equation being normalized to the form

$$\left\{(D^2+1)\left(D+\frac{\sqrt{6}}{5}\right)+\epsilon D^3\right\}x+g(D)\sum_{n=2}c_n\mu^{n-1}x^n=g(D)\,2B\cos\omega t,$$

where ϵ and μ are small parameters which in the main part of the discussion are related by $\epsilon=\mu^2$, and $g(D)$ is a particular polynomial operator of the third degree.

The procedure previously applied to a second-order equation with unsymmetrical non-linear damping, is used to obtain the periodic solutions having the period of the forcing term when ω is near to 1, i.e. for the case of fundamental resonance. It is shown that the resonance curves are of the same form as those obtained for the second-order equation and that the stability of the periodic solutions is determined by variational equations which are likewise identical in form to those previously obtained for the second-order equation.

1. Derivation of the differential equation

THE equations of a triode oscillator may be written in the form (cf. (1))

$$v_g=e_g+\alpha Zi_a,$$

$$Zi_a=e_a-v_a,$$

where v_a, v_g are the anode and grid voltages, Z is the impedance of the linear circuit at the anode terminals when the grid terminals are open, α is the voltage transfer ratio from anode to grid through the linear circuit, and e_a, e_g are the effective e.m.f.s in the anode and grid meshes of the linear circuit.

The currents and voltages are increments from the quiescent point, and it is assumed that the circuit is biased so that no grid current flows.

If it is assumed further that i_a is a function of mv_g+v_a, with m the amplification factor of the valve, and if we set

$$v=mv_g+v_a,$$

$$e=me_g+e_a$$

then we obtain

$$(1-m\alpha)Zi_a=e-v.$$

If we refer to the series C, shunt R circuit, Fig. 1, we obtain

$$(1-m\alpha)Z = \frac{R_0\{(m+1)R^3+6R^2X+5RX^2+X^3\}}{R_0\{3R^2+4RX+X^2\}+\{R^3+6R^2X+5RX^2+X^3\}},$$

with $1/X = j\omega C$, from which we get

$$R_0\{(m+1)R^3+6R^2X+5RX^2+X^3\}i_a$$
$$= \{R_0(3R^2+4RX+X^2)+(R^3+6R^2X+5RX^2+X^3)\}(e-v).$$

Since we have been concerned only with the linear circuit we may obtain the differential equation by replacing $R/X = j\omega RC$ by $CR\,d/dt$, and by

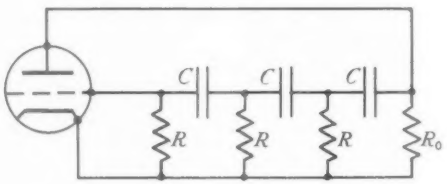

FIG. 1

a change of time scale this may be replaced by $d/dt \equiv D$. If further R_0/R is assumed negligible in comparison with unity we obtain the differential equation

$$\{(m+1)D^3+6D^2+5D+1\}R_0 i_a = \{D^3+6D^2+5D+1\}(e-v).$$

in which e will be a known function of the time (in particular a simple periodic function) and the valve characteristic determines a non-linear functional relation between i_a and v. It is usual to express i_a as a power series in v, but in the present case the number of parameters in the final equation is smaller if v is expressed in powers of i_a, and this will be done, although the difference is not important. It is assumed that such a representation is valid over the operating range of the characteristic.

Write $x_1 = R_0 i_a$ and y instead of v, so that we have

$$\{(m+1)D^3+6D^2+5D+1\}x_1+\{D^3+6D^2+5D+1\}y$$
$$= \{D^3+6D^2+5D+1\}e.$$

Suppose that in the operating range y can be expressed as a series in powers of x_1, of the form

$$y = c_1 x_1+c_2'\mu x_1^2+c_3'\mu^2 x_1^3+\ldots$$

in which c_1 is positive, and in a normal valve characteristic c_3' will also be

positive, μ is a small parameter characterizing the magnitude of the non-linear terms. The equation then becomes

$$\left\{\left(\frac{m}{1+c_1}+1\right)D^3+6D^2+5D+1\right\}x_1+\{D^3+6D^2+5D+1\}\sum_{n=2}\frac{c_n'\mu^{n-1}x^n}{1+c_1}$$

$$=\{D^3+6D^2+5D+1\}\frac{e}{1+c_1}.$$

If the non-linear terms are omitted ($\mu = 0$), and we set $e = 0$, we are left with the linear equation

$$\left\{\left(\frac{m}{1+c_1}+1\right)D^3+6D^2+5D+1\right\}x_1 = 0.$$

This equation has a simple periodic normal mode if

$$\frac{m}{1+c_1} = 29,$$

when it reduces to $(6D^2+1)(5D+1)x_1 = 0.$

This represents the condition of critical regeneration. The linear equation has an exponentially increasing normal mode if $m > 29(1+c_1)$, a decreasing mode if the inequality is reversed. Set

$$\frac{m}{1+c_1}+1 = 30(1+\epsilon)$$

and $$30x_1 = x;$$

the full equation then becomes

$$\{(1+\epsilon)D^3+\tfrac{1}{5}D^2+\tfrac{1}{6}D+\tfrac{1}{30}\}x+\{D^3+6D^2+5D+1\}\sum_{n=2}\frac{c_n'\mu^{n-1}}{1+c_1}\left(\frac{x}{30}\right)^n$$

$$=\{D^3+6D^2+5D+1\}\frac{e}{1+c_1}.$$

A further change of time scale, replacing dt by $\sqrt{6}\,dt$, brings the equation to the form

$$\left\{(D^2+1)\left(D+\frac{\sqrt{6}}{5}\right)+\epsilon D^3\right\}x+\{D^3+6\sqrt{6}D^2+30D+6\sqrt{6}\}\sum_{n=2}\frac{c_n'\mu^{n-1}}{1+c_1}\left(\frac{x}{30}\right)^n$$

$$=\{D^3+6\sqrt{6}D^2+30D+6\sqrt{6}\}\frac{e}{1+c_1}.$$

It is convenient to associate a numerical factor with the operator $\{D^3+6\sqrt{6}D^2+30D+6\sqrt{6}\}$ and set

$$29g(D) = D^3+6\sqrt{6}D^2+30D+6\sqrt{6}, \tag{1}$$

$$\frac{29c_n'}{30^n(1+c_1)} = c_n, \quad n = 2, 3, \ldots.$$

If we further assume $$\frac{29e}{1+c_1} = 2B\cos\omega t,$$

the equation becomes

$$\left\{(D^2+1)\left(D+\frac{\sqrt{6}}{5}\right)+\epsilon D^3\right\}+g(D)\sum_{n=2}c_n\mu^{n-1}x^n = g(D)\,2B\cos\omega t. \tag{2}$$

The operator $g(D)$ on the right-hand side of this equation produces a variation in amplitude and phase which will be small if only a small frequency interval is considered. This factor may therefore be absorbed by replacing $g(D)\,2B\cos\omega t$ by $2B_1\cos\omega t$.

The equation is then of the general form

$$\{(D^2+1)(D+\alpha)-\epsilon k(D)\}x+g(D)\sum_{n=2}c_n\mu^{n-1}x^n = 2B_1\cos\omega t, \tag{3}$$

in which α is a positive constant, ϵ and μ are small parameters, and $k(D)$, $g(D)$ are polynomials in D, of degree not exceeding 3.

The equation is thus of the third order, containing small non-linear terms dependent on the parameter μ, and such that if these, together with small linear terms dependent on ϵ, are omitted we are left with a linear equation with constant coefficients having a simple periodic normal mode of angular frequency normalized to unity together with a decreasing exponential mode of time constant $1/\alpha$.

The present paper will treat the special equation (2), though it will be clear that the method is applicable to equation (3). The generalization to a wider class of equations which will include (3) is however deferred to another paper.

2. Outline of the method

We are concerned with (2) where $g(D)$ is defined by (1). The c_n are assumed to be $O(1)$; ϵ and μ are small parameters which will at first be treated as independent, but later they will be related by $\epsilon = \mu^2$. In the case worked out in detail B will be taken as $O(\epsilon)$ and $(\omega-1)$ likewise, i.e. the amplitude of the forcing term is small, and its frequency near to resonance with the simple periodic normal mode of the approximate linear equation.

In the equations of the first approximation only c_2 and c_3 occur, so that effectively the valve characteristic is approximated by a third-degree polynomial.

The method of solution will follow closely that used in connexion with the equation
$$\ddot{v}-(\epsilon+\mu kv-\mu^2v^2)\dot{v}+v = 2B\omega_1\sin\omega_1 t,$$
which was solved in a previous paper (**2**). The procedure for determining periodic solutions having the frequency of the forcing term is exactly the same; but in considering stability account has to be taken of the fact that the present equation is of the third order.

In a normal characteristic c_3 is positive, and if ϵ is positive, regeneration is beyond critical. It will be shown in this case that, if the ratio c_2^2/c_3 is less than a certain value, the resonance curves are of the same general form as for the second-order equation, and that the stability of the periodic solutions is likewise determined by variational equations of the same form as those previously obtained. If, however, c_2^2/c_3 exceeds this value, the amplitude of oscillation increases and the final state cannot be determined from the equations of the first approximation.

If ϵ is negative the regeneration is less than critical. In this case, in the absence of the forcing term a small oscillation will not grow from zero. With the forcing term, when c_2^2/c_3 is less than a certain value, the resonance curves resemble those of a system with a non-linear restoring force, such as a compound pendulum. If, on the other hand, c_2^2/c_3 exceeds a certain value it appears that if an oscillation of sufficient amplitude can be started it will grow, and again the final state cannot be determined from the equations of the first approximation.

3. Periodic solution developed in powers of B

Equation (2) may be rearranged in the form
$$2B\cos\omega t = \zeta(D)x+\sum_{n=2} c_n\mu^{n-1}x^n, \tag{4}$$
with
$$\zeta(D) = \{1/g(D)\}\left\{(D^2+1)\left(D+\frac{\sqrt{6}}{5}\right)+\epsilon D^3\right\},$$
which is of exactly the same form as (7) of (**2**). We may therefore proceed as in (**2**), writing
$$x = x^{(1)}B+x^{(2)}B^2+...+x^{(n)}B^n+.... \tag{5}$$
Substitute into (4) and equate coefficients of like powers of B; we thereby obtain the $x^{(n)}$ in succession as periodic functions of t of period $2\pi/\omega$.

Using exponential notation, and reverting to i instead of j for $\sqrt{(-1)}$ we thus obtain
$$\left.\begin{aligned}\exp i\omega t+\exp(-i\omega t) &= \zeta(D)x^{(1)}\\ 0 &= \zeta(D)x^{(2)}+c_2\mu x^{(1)^2}\\ 0 &= \zeta(D)x^{(3)}+2c_2\mu x^{(1)}x^{(2)}+c_3\mu^2x^{(1)^3}\\ &\cdots\cdots\end{aligned}\right\} \tag{6}$$

from which $$x^{(1)} = x_1^{(1)} + x_{-1}^{(1)},$$

where $$x_1^{(1)} = \frac{1}{\zeta_1}\exp i\omega t, \qquad x_{-1}^{(1)} = \frac{1}{\zeta_{-1}}\exp(-i\omega t).$$

Similarly $$x^{(2)} = x_2^{(2)} + x_0^{(2)} + x_{-2}^{(2)},$$

where

$$\left.\begin{aligned} x_2^{(2)} &= -\frac{\mu c_2}{\zeta_2}x_1^{(1)^2} = -\frac{\mu c_2}{\zeta_1^2\zeta_2}\exp 2i\omega t \\ x_0^{(2)} &= -\frac{2\mu c_2}{\zeta_0}x_1^{(1)}x_{-1}^{(1)} = -\frac{2\mu c_2}{\zeta_1\zeta_{-1}\zeta_0} \\ x_{-2}^{(2)} &= -\frac{\mu c_2}{\zeta_{-2}}x_{-1}^{(1)^2} = -\frac{\mu c_2}{\zeta_{-1}^2\zeta_{-2}}\exp(-2i\omega t) \end{aligned}\right\}. \tag{7}$$

Again $$x^{(3)} = x_{-3}^{(3)} + x_1^{(3)} + x_{-1}^{(3)} + x_{-3}^{(3)},$$

where

$$\left.\begin{aligned} x_3^{(3)} &= \frac{1}{\zeta_3}\left(\frac{2c_2^2}{\zeta_2} - c_3\right)\mu^2 x_1^{(1)^3} \\ x_1^{(3)} &= \frac{1}{\zeta_1}\left(\frac{2c_2^2}{\zeta_2} + \frac{4c_2^2}{\zeta_0} - 3c_3\right)\mu^2 x_1^{(1)^2}x_{-1}^{(1)} \end{aligned}\right\} \tag{8}$$

and $x_{-3}^{(3)}$ and $x_{-1}^{(3)}$ the corresponding conjugates. In these equations $\zeta_{\pm r}$ denotes $\zeta(\pm ri\omega)$.

Proceeding in this way the $x^{(n)}$ are determined in succession in the general form $$x^{(n)} = \sum x_r^{(n)} \tag{9}$$

with r running through alternate integers from $-n$ to $+n$. $x_{-r}^{(n)}$ is the complex conjugate of $x_r^{(n)}$ and the two together give a real term of rth harmonic frequency.

The series (5) then gives a formal solution of (2) which is periodic with period $2\pi/\omega$. The series is in powers of B, but, since $x^{(n)}$ contains μ^{n-1} as a factor, it may equally be regarded as a power series in μ.

An interval of assured convergence is obtained by considering the equation $$\xi = N\eta - c\mu_1\eta^2 - c\mu_1^2\eta^3 - \ldots, \tag{10}$$

where $$|c_n| \leqslant c \quad (n = 2, 3, \ldots)$$

and N, μ_1 are positive constants to be chosen later. Equation (10) with $N \neq 0$ defines η as a function of ξ, vanishing at $\xi = 0$ and analytic in a circle extending to the branch point nearest to the origin given by

$$\frac{d\xi}{d\eta} = 0.$$

This branch point is at $\xi = R$, $\eta = S$ where

$$R = (1/\mu_1)\{N + 2c - 2c(1 + N/c)^{\frac{1}{2}}\}, \tag{11}$$

$$S = (1/\mu_1)\{1 - (1 + N/c)^{-\frac{1}{2}}\}; \tag{12}$$

η may therefore be developed in powers of ξ provided $\xi < R$, ξ and η now being assumed real and positive. If this series is obtained by setting

$$\eta = \eta^{(1)}\xi + \eta^{(2)}\xi^2 + \ldots + \eta^{(n)}\xi^n + \ldots, \tag{13}$$

substituting in (10) and equating coefficients of like powers of ξ to determine the $\eta^{(n)}$ in succession, it is clear, on comparing with (4) et seq., that, provided

$$2B \leqslant \xi < R \tag{14}$$

and N is chosen so that

$$N < |\zeta(\pm ri\omega)| \quad (r = 0, 1, 2, \ldots), \tag{15}$$

the series (13) dominates (5) in the sense that

$$|x^{(n)}|B^n \leqslant \sum |x_r^{(n)}|B^n \leqslant \eta^{(n)}\xi^n \tag{16}$$

for any $\mu < \mu_1$.

The absolute and uniform convergence with respect to t of the series (5) is thus established in a definite interval of sufficiently small values of B and μ, and it may be rearranged according to frequency to give the Fourier expansion of the solution.

The interval of assured convergence is

$$B < \frac{1}{2\mu_1}\left\{N + 2c - 2c\left(1 + \frac{N}{c}\right)^{\frac{1}{2}}\right\}. \tag{17}$$

If N can be chosen independently of μ, and μ_1 is chosen to make the right-hand member of (17) greater than B_1, then the interval of assured convergence is $B < B_1$, for any $\mu < \mu_1$; here B_1 is any convenient constant.

If, however, $\omega = 1$, we have $|\zeta(i\omega)| = \epsilon$, so that to satisfy (15) when any $r\omega$ is near to 1, N must have a value less than ϵ which is small in the conditions contemplated. If ϵ is independent of μ it is still possible to choose μ_1, i.e. if the non-linearity is sufficiently small the series in powers of B will still converge.

When N is small (17) becomes approximately

$$B < N^2/(4\mu_1 c).$$

When N is $O(\epsilon)$ the interval of assured convergence may be fixed independently of the magnitude of the non-linear terms if ϵ is larger than or of the same order as $\mu^{\frac{1}{2}}$; but if ϵ is of a higher order of smallness in relation to μ, the interval of convergence will tend to zero with μ. In this last case the solution in powers of B fails if any $r\omega$ is near to 1. This situation may be dealt with by the methods of the following sections in which the special case $\epsilon = \mu^2$ and ω near to 1 (i.e. fundamental resonance) is treated in detail.

4. Periodic solution in powers of b

Whatever the values of ϵ and μ, (17) determines a definite interval of convergence, provided ϵ is not actually zero, so that for a sufficiently small

value of B a solution of period $2\pi/\omega$ certainly exists. (The stability of such a solution remains to be discussed.) Let the fundamental mode of such a solution be

$$2b\cos(\omega t+\phi),$$

and replace (5) by

$$x = x^{(1)}b+x^{(2)}b^2+\ldots+x^{(n)}b^n+\ldots \tag{18}$$

with $$x^{(1)} = x_1^{(1)}+x_{-1}^{(1)} = \exp i(\omega t+\phi)+\exp i(-\omega t-\phi).$$

Following the procedure developed in (**2**), substitute (18) into (4) and choose the $x^{(2)}$, $x^{(3)}$,... to annul all terms in the successive powers of b of other than fundamental frequency. When expressed in terms of $x_1^{(1)}$ and $x_{-1}^{(1)}$ we obtain the same expressions for the $x^{(n)}$ as before, with the omission of $x_1^{(n)}$ and $x_{-1}^{(n)}$ when n is odd, and the omission of terms derived from these in the higher orders. Thus the terms of $x^{(2)}$ are still given by the first expressions in (7) and $x^{(3)} = x_3^{(3)}+x_{-3}^{(3)}$ with $x_3^{(3)}$ given by the first of the equations (8).

The terms which were previously cancelled by the $x_1^{(n)}$ and $x_{-1}^{(n)}$, now remain to form an equation containing only terms of fundamental frequency, i.e. containing either $\exp i\omega t$ or $\exp(-i\omega t)$. These two sets of terms are conjugate complex numbers, and the full equation will be satisfied if we satisfy the equation formed with one set of terms only. Those in $\exp i\omega t$ give the equation

$$B\exp i\omega t = \zeta(i\omega)x_1^{(1)}b-\left(\frac{2c_2^2}{\zeta_2}+\frac{4c_2^2}{\zeta_0}-3c_3\right)\mu^2x_1^{(1)^2}x_{-1}^{(1)}b^3+\ldots. \tag{19}$$

Since $$x_1^{(1)} = \exp i(\omega t+\phi)$$

this may be rewritten

$$B\exp(-i\phi) = \zeta(i\omega)b-\left(\frac{2c_2^2}{\zeta_2}+\frac{4c_2^2}{\zeta_0}-3c_3\right)\mu^2b^3+\ldots$$

the right side of which is an infinite series of the form

$$\sum_{n=0}^{\infty}A_{2n+1}\mu^{2n}b^{2n+1},$$

where the A_{2n+1} are functions of the c_r $(r\leqslant n)$ and of the

$$\zeta(\pm ri\omega)\quad (r = 0, 2, 3,\ldots, 2n)$$

when $n > 0$, while $A_1 = \zeta(i\omega)$.

The relationship between the series for x and η remains valid provided

$$2b < \eta^{(1)}\xi < R/N$$

and N satisfies (15) for $r = 0, 2, 3,\ldots$ but no longer for $r = 1$. N can therefore now be chosen independently of ϵ; and so, given b_1, we can always find μ_1 so that the series (18) converges for $b < b_1$ provided $\mu < \mu_1$.

The series on the right of (19) is likewise dominated by the η series multiplied by N and will therefore converge under the same conditions.

The possibility of finding a periodic solution of (2) now depends on obtaining real solutions of (19) for b and ϕ, with b positive and nec s-sarily less than b_1. Equation (19) will be called the amplitude equation.

In the present paper the solution of (19) will be considered when $|\zeta(i\omega)|$ is small, but it may be noted that if this is not so, then the previous solution in powers of B may be recovered by reversing (19).

5. Solution of the amplitude equation

Now $\zeta(i\omega)$ is only small when ω is near to 1. Set $\omega = 1+\Delta\omega$ and expand $\zeta(z)$ about $z = i$ to give

$$\begin{aligned}\zeta(i\omega) &= \zeta(i)+i\Delta\omega\zeta'(i)+\ldots \\ &= -\epsilon+i\Delta\omega\, 2\left(i+\frac{\sqrt{6}}{5}\right)\left(1+\frac{30\epsilon}{29}\right)+\ldots.\end{aligned}$$

Let $2\Delta\omega = \epsilon\sigma$, making $\Delta\omega = O(\epsilon)$ and

$$\zeta(i\omega) = -\epsilon\left[1+\sigma-\frac{i\sqrt{6}\sigma}{5}\right]+O(\epsilon^2).$$

The coefficient $3c_3-\dfrac{2c_2^2}{\zeta_2}-\dfrac{4c_2^2}{\zeta_0}$ which occurs in the second term on the right of (19) may likewise be expanded in powers of ϵ with a non-zero constant term which we denote by $\lambda+i\lambda'$.

The amplitude equation now becomes

$$B\exp(-i\phi) = \left[-\epsilon\left(1+\sigma-\frac{i\sqrt{6}\sigma}{5}\right)+O(\epsilon^2)\right]b+(\lambda+i\lambda'+O(\epsilon))\mu^2b^3+O(\mu^4). \tag{20}$$

Clearly if ϵ and μ are both small, B must also be small if a solution is to exist for which higher powers in the series may be neglected in a first approximation. Therefore let

$$B = \epsilon E, \tag{21}$$

with $E = O(1)$, and suppose that ϵ is of order μ^2. By modifying the c_n if necessary, leaving them still $O(1)$, we may set

$$\epsilon = \mu^2. \tag{22}$$

The amplitude equation then becomes

$$E\exp(-i\phi) = -\left(1+\sigma-\frac{i\sqrt{6}\sigma}{5}\right)b+(\lambda+i\lambda')b^3+O(\epsilon). \tag{23}$$

Omitting the $O(\epsilon)$ and separating real and imaginary parts we obtain the equations of the first approximation

$$E\cos\phi = -(1+\sigma)b+\lambda b^3, \tag{24}$$

$$E\sin\phi = -\frac{\sqrt{6}}{5}\sigma b-\lambda' b^3. \tag{25}$$

If $E = 0$, ϕ is indeterminate and these equations will only be consistent if σ satisfies

$$(1+\sigma)\lambda'+\frac{\sqrt{6}}{5}\sigma\lambda = 0,$$

i.e.

$$\sigma = -\frac{\lambda'}{(\sqrt{6}/5)\lambda+\lambda'},$$

which determines the frequency of free oscillation. For the amplitude of free oscillation we then have

$$b^2 = \frac{1}{\lambda+(5/\sqrt{6})\lambda'}.$$

If the oscillator is biased to an inflexion on the non-linear characteristic, $c_2 = 0$ and therefore $\lambda' = 0$. Thus $\sigma = 0$ and $b^2 = 1/\lambda = 1/(3c_3)$. Therefore c_3 must be positive for a real solution to exist.

If c_2 is not zero, and at the same time not too large, there is a deviation of frequency towards lower frequencies since λ' may be shown to be positive. In fact

$$\lambda+i\lambda' = 3c_3-\frac{17020}{4611}c_2^2+\frac{1160\sqrt{6}}{4611}ic_2^2.$$

This makes

$$\lambda+(5/\sqrt{6})\lambda' = 3c_3-\frac{11220}{4611}c_2^2.$$

Thus the effect of increasing $|c_2|$ is to increase λ' and also to decrease $\lambda+(5/\sqrt{6})\lambda'$, and so to increase the frequency deviation and the amplitude of free oscillation. The analysis will clearly break down if c_2^2 approaches equality with $\frac{13833}{11220}c_3$ so that $\lambda+(5/\sqrt{6})\lambda'$ becomes $O(\mu)$. Then the frequency would no longer differ from unity by $O(\epsilon)$ and it would no longer be possible to choose μ so that the amplitude of free oscillation remained within the interval of convergence of the series. It will therefore be assumed in what follows that c_2^2 is limited to say $c_2^2 < c_3$ so that the situation just mentioned is excluded.

Denote the amplitude of free oscillation by a so that

$$a^2 = \frac{1}{\lambda+(5/\sqrt{6})\lambda'}.$$

Now multiply (25) by $5/\sqrt{6}$ and subtract (24), whence

$$E\left(\frac{5}{\sqrt{6}}\sin\phi-\cos\phi\right)=b-\left(\lambda+\frac{5}{\sqrt{6}}\lambda'\right)b^3,$$

or

$$\frac{E}{a}\left(\frac{5}{\sqrt{6}}\sin\phi-\cos\phi\right)=\frac{b}{a}\left(1-\frac{b^2}{a^2}\right). \tag{26}$$

Also from (24) and (25),

$$E\left(-\sin\phi-\frac{5}{\sqrt{6}}\cos\phi\right)=\left(\frac{5}{\sqrt{6}}+\frac{31}{5\sqrt{6}}\sigma\right)b-\left(\frac{5}{\sqrt{6}}\lambda-\lambda'\right)b^3,$$

or

$$\frac{E}{a}\left(-\sin\phi-\frac{5}{\sqrt{6}}\cos\phi\right)=\left(\frac{5}{\sqrt{6}}+\frac{31}{5\sqrt{6}}\sigma\right)\frac{b}{a}-\frac{(5/\sqrt{6})\lambda-\lambda'}{\lambda+(5/\sqrt{6})\lambda'}\frac{b^3}{a^3}. \tag{27}$$

If we now set $\phi'=\phi-\pi+\tan^{-1}(5/\sqrt{6})$, $F=(E/a)\sqrt{(31/6)}$,

$$\sigma'=5/\sqrt{6}+31\sigma/(5\sqrt{6}),$$

$\nu=-((5/\sqrt{6})\lambda-\lambda')/(\lambda+(5/\sqrt{6})\lambda')$, and $b'=b/a$, these changes involving only origins and scales, (26) and (27) become

$$F\cos\phi'=b'(1-b'^2), \tag{28}$$

$$F\sin\phi'=b'(\sigma'+\nu b'^2). \tag{29}$$

The equations of the first approximation (28), (29) are now identical in form with (27) of (**2**). The resonance curves are therefore of the same form as was then obtained for the second-order equation with unsymmetrical damping. If the circuit is biased to an inflexion of the characteristic, $c_2=0$, $\lambda'=0$, and $\nu=-5/\sqrt{6}\doteq-2{\cdot}04$. The resonance curves therefore closely resemble those of Fig. 2 of (**2**), which is drawn for $\nu=2$, reflected in the y-axis so that they lean over towards the high frequency side, the ordinate y of that figure corresponding to the present b'^2 and the abscissa corresponding to σ'.

As in (**2**) we may use implicit function theory to show that if $\epsilon=\mu^2$ is sufficiently small, the full amplitude equation has solutions differing at most by $O(\epsilon)$ from the solutions of the equations of the first approximation, and each such solution determines a periodic solution of the differential equation. The error in the approximate solution may likewise be discussed as in (**2**).

6. Differential equations for the amplitude and phase of non-periodic solutions

Equations (2) and (3) may be rewritten as

$$\left\{(D^2+1)\left(D+\frac{\sqrt{6}}{5}\right)+\epsilon D^3\right\}x+g(D)\sum_{n=2}c_n\mu^{n-1}x^n-g(D)\,2B\cos\omega t=0, \tag{30}$$

$$\zeta(D)x+\sum_{n=2}c_n\mu^{n-1}x^n-2B\cos\omega t=0, \tag{31}$$

the first being obtained from the second by the operation $g(D)$. If the formal solution (18) is substituted in (31) the residual terms are those forming the amplitude equation (19) together with their conjugates, namely

$$\zeta(i\omega)x_1^{(1)}b+\left(3c_3-\frac{2c_2^2}{\zeta_2}-\frac{4c_2^2}{\zeta_0}\right)\mu^2x_1^{(1)^2}x_{-1}^{(1)}b^3+\ldots-B\exp(i\omega t)+\text{conjugates},$$

i.e. if we set $\theta=\omega t+\phi$, so that $x_1^{(1)^n}x_{-1}^{(1)^{n-1}}=\exp(i\theta)$,

$$\exp(i\theta)\left\{\zeta(i\omega)b+\left(3c_3-\frac{2c_2^2}{\zeta_2}-\frac{4c_2^2}{\zeta_0}\right)\mu^2b^3+\ldots\right\}-B\exp(i\omega t)+\text{conjugates}.$$

When the formal solution is substituted in (30) the residual terms are

$$g(i\omega)[\exp(i\theta)\{\zeta(i\omega)b+\ldots\}-B\exp(i\omega t)]+\text{conjugates}$$

obtained from the previous line by the operation $g(D)$. Let these residual terms be denoted by $2\,dH/dt$ with

$$\begin{aligned}H(b,\phi,t)&=\frac{g(i\omega)}{2i\omega}[\exp(i\theta)\{\zeta(i\omega)b+\ldots\}-B\exp(i\omega t)]+\text{conjugates}\\&=\frac{\epsilon}{2}\left[\exp(i\theta)\left\{\left(\frac{i\sqrt{6}\sigma}{5}-1-\sigma\right)b+(\lambda+i\lambda')b^3\right\}-E\exp(i\omega t)\right]+\\&\qquad+\text{conjugates}+O(\epsilon^2).\end{aligned}$$

Denote the formal solution by $K(b,\phi,t)$, i.e.

$$\begin{aligned}K(b,\phi,t)&=x^{(1)}b+x^{(2)}b^2+\ldots\\&=b\exp(i\theta)+b\exp(-i\theta)+O(\mu),\end{aligned}$$

and returning to (30), denote the group of small terms by

$$\mu S(x)=\mu^2D^3x+g(D)\sum_{n=2}c_n\mu^{n-1}x^n.$$

The differential equation (30) is then equivalent to the system of two equations in u and x, namely

$$(D^2+1)u+\mu S(x)-g(D)\,2B\cos\omega t=0, \tag{32}$$

$$u=\left(D+\frac{\sqrt{6}}{5}\right)x, \tag{33}$$

the formal solution of which is

$$x=K(b,\phi,t), \tag{34}$$

$$\begin{aligned}u&=\left(D+\frac{\sqrt{6}}{5}\right)K(b,\phi,t)\\&=K_1(b,\phi,t),\end{aligned} \tag{35}$$

say, where

$$K_1(b,\phi,t)=\left(i+\frac{\sqrt{6}}{5}\right)b\exp(i\theta)+\left(-i+\frac{\sqrt{6}}{5}\right)b\exp(-i\theta)+O(\mu).$$

The residual terms when (34) and (35) are substituted into (32) are $2\,dH/dt$, which vanishes when b, ϕ satisfy the amplitude equation.

If we now regard b and ϕ as variables this is equivalent to

$$\left(\frac{\partial^2}{\partial t^2}+1\right)K_1+\mu S(K)-g(D)\,2B\cos\omega t = 2\frac{\partial H}{\partial t}, \tag{36}$$

where $$\mu S(K) = \mu^2\frac{\partial^3}{\partial t^3}K+g\left(\frac{\partial}{\partial t}\right)\sum_{n=2} c_n\,\mu^{n-1}x^n.$$

Now introduce b and ϕ as new dependent variables by using the equations

$$u = K_1(b,\phi,t), \tag{37}$$

$$\frac{du}{dt} = \frac{\partial K_1}{\partial t}-H. \tag{38}$$

These require that $$\frac{\partial K_1}{\partial b}\frac{db}{dt}+\frac{\partial K_1}{\partial \phi}\frac{d\phi}{dt}+H = 0. \tag{39}$$

Substituting in (32) we obtain

$$\frac{\partial^2 K_1}{\partial t^2}-\frac{\partial H}{\partial t}+\frac{\partial}{\partial b}\left(\frac{\partial K_1}{\partial t}-H\right)\frac{db}{dt}+\frac{\partial}{\partial \phi}\left(\frac{\partial K_1}{\partial t}-H\right)\frac{d\phi}{dt}+K_1+$$
$$+\mu\,S(x)-g(D)\,2B\cos\omega t = 0.$$

Subtracting (36) gives

$$\frac{\partial}{\partial b}\left(\frac{\partial K_1}{\partial t}-H\right)\frac{db}{dt}+\frac{\partial}{\partial \phi}\left(\frac{\partial K_1}{\partial t}-H\right)\frac{d\phi}{dt}+\mu\{S(x)-S(K)\}+\frac{\partial H}{\partial t} = 0. \tag{40}$$

Solving (39) and (40) for db/dt and $d\phi/dt$ we obtain

$$\frac{db}{dt} = \frac{1}{\Delta}\left\{L\frac{\partial K_1}{\partial \phi}-H\frac{\partial}{\partial \phi}\left(\frac{\partial K_1}{\partial t}-H\right)\right\} \tag{41}$$

$$\frac{d\phi}{dt} = \frac{1}{\Delta}\left\{-L\frac{\partial K_1}{\partial b}+H\frac{\partial}{\partial b}\left(\frac{\partial K_1}{\partial t}-H\right)\right\}, \tag{42}$$

where $$L = \mu\{S(x)-S(K)\}+\frac{\partial H}{\partial t}$$

and $$\Delta = \frac{\partial K_1}{\partial b}\frac{\partial}{\partial \phi}\left(\frac{\partial K_1}{\partial t}-H\right)-\frac{\partial K_1}{\partial \phi}\frac{\partial}{\partial b}\left(\frac{\partial K_1}{\partial t}-H\right).$$

Instead of the original equation we now have a system of three equations (41), (42) together with

$$\left(D+\frac{\sqrt{6}}{5}\right)x = K_1 \tag{43}$$

in the three unknowns b, ϕ, x. These are satisfied if b and ϕ have constant values satisfying the amplitude equation for which H and $\partial H/\partial t$ both vanish, and $x = K(b,\phi,t)$, i.e. by the periodic solutions of the original equation.

We proceed to expand the right-hand members of (41) and (42) in powers of μ, replacing ε by μ^2. Evaluating only the lowest powers of μ we find

$$\Delta = -\tfrac{124}{25}b + O(\mu) \tag{44}$$

and

$$\frac{db}{dt} = \{S(x)-S(K)\}\left\{\frac{5}{2\sqrt{31}}\mu\sin(\theta+\alpha)+O(\mu^2)\right\}+ \\ +\frac{5\sqrt{6}}{62}\mu^2\left\{b-\left(\lambda+\frac{5}{\sqrt{6}}\lambda'\right)b^3+E\sqrt{\tfrac{31}{6}}\cos(\phi+\alpha)\right\}+O(\mu^3), \tag{45}$$

$$b\frac{d\phi}{dt} = \{S(x)-S(K)\}\left\{\frac{5\mu}{2\sqrt{31}}\cos(\theta+\alpha)+O(\mu^2)\right\}- \\ -\frac{5\sqrt{6}\mu^2}{62}\left\{\left(\frac{5}{\sqrt{6}}+\frac{31\sigma}{5\sqrt{6}}\right)b-\left(\frac{5\lambda}{\sqrt{6}}-\lambda'\right)b^3+E\sqrt{\tfrac{31}{6}}\sin(\phi+\alpha)\right\}+O(\mu^3), \tag{46}$$

in which $\alpha = \tan^{-1}(5/\sqrt{6})$.

With the changes of origin and scale that were used to obtain (28) and (29) these become

$$\frac{db'}{dt} = -\{S(x)-S(K)\}\left\{\frac{5\mu}{2\sqrt{31}a}\sin(\omega t+\phi')+O(\mu^2)\right\}+ \\ +\frac{5\sqrt{6}\mu^2}{62}\{b'(1-b'^2)-F\cos\phi'\}+O(\mu^3), \tag{47}$$

$$b'\frac{d\phi'}{dt} = -\{S(x)-S(K)\}\left\{\frac{5\mu}{2\sqrt{31}a}\cos(\omega t+\phi')+O(\mu^2)\right\}- \\ -\frac{5\sqrt{6}\mu^2}{62}\{b'(\sigma'+\nu b'^2)-F\sin\phi'\}+O(\mu^3). \tag{48}$$

We now have the system of three first-order equations (45), (46), or the equivalent pair (47), (48), together with (43) replacing the original equation of the third order.

7. Qualitative character of the solutions

If $x = K(b,\phi,t)$ with b and ϕ having constant values satisfying the amplitude equation, then H and $\partial H/\partial t$ both vanish and $S(x) = S(K)$. Hence, (45) and (46) give $db/dt = 0$, $d\phi/dt = 0$, and the system (43), (45), (46) is satisfied. This gives the periodic solutions of the original equation.

If an existing periodic solution is slightly disturbed so that $S(x)-S(K)$ is small of $O(\mu^2)$ then db/dt and $b\,d\phi/dt$ are also small of $O(\mu^2)$ and differ only by $O(\mu^3)$ from the values given by the autonomous system

$$\frac{db'}{dt} = \frac{5\sqrt{6}\mu^2}{62}\{b'(1-b'^2)-F\cos\phi'\}, \tag{49}$$

$$b'\frac{d\phi'}{dt} = \frac{5\sqrt{6}\mu^2}{62}\{-b'(\sigma'+\nu b'^2)+F\sin\phi'\}. \tag{50}$$

The singular points of this system correspond to the first approximation to the periodic solutions, and one may infer at once that the stability or instability of the periodic solutions to small disturbances is determined by the character of the singular points of this system. With a change of time scale the equations are identical with the variational equations, (44), (45) of (2), obtained for the second-order equation in (2), and the stability character of the periodic solutions is therefore the same as was obtained in that paper.

The question next arises, whether a periodic solution will be realized or approached when the physical system is released from an arbitrary initial state.

If values are given for x, dx/dt, d^2x/dt^2 at $t = 0$, a solution of (2) is determined which may be represented by a trajectory Γ in a space $\mathscr{S}$ with x, dx/dt, and d^2x/dt^2 as cartesian coordinates. The space $\mathscr{S}$ is transformed into $\mathscr{S}'$ with x, u, du/dt as coordinates by the non-singular linear transformation

$$x = x,$$

$$u = \frac{dx}{dt} + \frac{\sqrt{6}}{5}x,$$

$$\frac{du}{dt} = \frac{d^2x}{dt^2} + \frac{\sqrt{6}}{5}\frac{dx}{dt},$$

and the trajectory Γ transforms into Γ' representing the corresponding solution of the system (32), (33).

Now transform $\mathscr{S}'$ into $\mathscr{S}''$ with cylindrical coordinates x, b, ϕ by (37), (38) with Jacobian Δ which for μ sufficiently small vanishes only when $b = 0$ and ϕ is indeterminate on the x-axis. The trajectory Γ' transforms into Γ'' representing the corresponding solution of the system (43), (45), (46).

Now given b_1 we may choose μ_1 so that the series for K and H converge for $b < b_1$ and $\mu < \mu_1$. This determines a cylindrical region $\mathscr{R}''$ in $\mathscr{S}''$ with axis along the x-axis within which the series converge. It is certainly possible to define a sphere $\mathscr{R}$ centre at the origin of $\mathscr{S}$ which corresponds to an ellipsoid $\mathscr{R}'$ in $\mathscr{S}'$, which in turn transforms to a region within $\mathscr{R}''$ in $\mathscr{S}''$, whatever the value of t since the series converge uniformly with respect to t.

If the initial values of x, dx/dt, d^2x/dt^2 define a point P in $\mathscr{R}$, then to the trajectory Γ starting at P will correspond trajectories Γ' and Γ'' in $\mathscr{R}'$ and $\mathscr{R}''$ respectively which may be continued in their respective regions either for t tending to infinity, or until some finite value of t at which Γ reaches the boundary of $\mathscr{R}$.

Now since the initial values are bounded, (45), (46) show that db/dt and $b\,d\phi/dt$ are not greater than $O(\mu)$, so that if P is not near to the boundary

the trajectories will remain within their respective regions for an interval of time T which is $O(1/\mu)$. Now, by (43),

$$\left(D+\frac{\sqrt{6}}{5}\right)x = K_1(b,\phi,t) = \left(\frac{\partial}{\partial t}+\frac{\sqrt{6}}{5}\right)K(b,\phi,t)$$

and so

$$\left(D+\frac{\sqrt{6}}{5}\right)(x-K(b,\phi,t)) = -\frac{\partial K}{\partial b}\frac{db}{dt}-\frac{\partial K}{\partial \phi}\frac{d\phi}{dt}.$$

If the initial values of x, b, ϕ are x_0, b_0, ϕ_0 then

$$x-K(b,\phi,t) = -e^{-\sqrt{6}t/5}\int_0^t\left(\frac{\partial K}{\partial b}\frac{db}{dt}+\frac{\partial K}{\partial \phi}\frac{d\phi}{dt}\right)e^{\sqrt{6}t/5}\,dt+ \\ +(x_0-K(b_0,\phi_0,0))e^{-\sqrt{6}t/5}. \quad (51)$$

If

$$\left|\frac{\partial K}{\partial b}\frac{db}{dt}+\frac{\partial K}{\partial \phi}\frac{d\phi}{dt}\right| < M$$

throughout the interval of integration, the modulus of the first term on the right of (51) is less than $(5\sqrt{6})M$. This is certainly the case with $M = O(\mu)$ in the interval $(0, T)$. Hence in an interval of time of order $\log(1/\mu)$ the second term on the right of (51) is reduced to $O(\mu)$ and therefore the difference between x and $K(b,\phi,t)$ is reduced to $O(\mu)$. In fact this difference is reduced to $O(\mu)$ in the same way as the damped exponential mode of the approximate linear equation with time constant $5/\sqrt{6}$. Equations (45) and (46) then show that db/dt and $b\,d\phi/dt$ are $O(\mu^2)$. A repetition of the same argument with M now $O(\mu^2)$ shows that in a further interval of the same duration, the difference $x-K(b,\phi,t)$ will be reduced to $O(\mu^2)$, and will thereafter remain not greater than $O(\mu^2)$.

The values of db/dt and $b\,d\phi/dt$ will then be given within $O(\mu^3)$ by the autonomous system (49), (50), and db/dt, $b\,d\phi/dt$ are $O(\mu^2)$. Consequently, in a further interval of order $O(1/\mu)$ the projection of Γ'' on the b, ϕ plane will not differ by more than $O(\mu^2)$ from the trajectory Γ_1'' of the autonomous system (49), (50), which starts from the same point at the beginning of this interval.

There are now two cases to consider. If Γ_1'' approaches a stable singular point it is clear that x approaches the periodic solution with b, ϕ the solutions of the amplitude equation for which the values of the singular point of the autonomous system are the first approximation. Otherwise Γ_1'' must wind asymptotically on to a limit cycle. In this case, at the end of the interval last considered, the projection of the representative point of Γ'' may differ by $O(\mu^2)$ from the corresponding point on Γ_1'' and will coincide with a point of another trajectory Γ_2'' of the autonomous system. We may in this way obtain a succession of arcs Γ_1'', Γ_2'', Γ_3'',... of trajectories of the autonomous

system, such that the projection of the representative point of Γ'' follows each one in turn within $O(\mu^2)$ in intervals of time of order $O(1/\mu)$, the end point of one arc differing from the starting-point of the next by $O(\mu^2)$. It is clear that, unless Γ_1'' was very close to a separatrix, all these arcs will belong to trajectories winding on to the same limit cycle, and that ultimately the projection of Γ'' will come within $O(\mu^2)$ of this limit cycle.

Such a solution is evidently an almost periodic solution having the character of a combination oscillation. The period of the cycle of variation of amplitude and phase will be $O(1/\mu^2)$, and it will be given within a fractional error of $O(\mu)$ by the period of the limit cycle of the autonomous system.

8. The variational equations

Summarizing, it has been shown that the autonomous system (49), (50) is sufficient to determine the stability or otherwise of the periodic solutions of (2). By a change of the time scale this system may be brought to the form

$$\frac{db'}{dt} = b'(1-b'^2) - F\cos\phi', \tag{52}$$

$$b'\frac{d\phi'}{dt} = F\sin\phi' - b'(\sigma' + \nu b'^2), \tag{53}$$

which is identical with the variational equations obtained for the second-order equation in (**2**), where the singular points of this system are discussed.

Furthermore it has been shown that a solution starting at any point in a sphere $\mathscr{R}$ of the phase space $\mathscr{S}$ will have a transient stage in which the difference between x and $K(b, \phi, t)$ decreases at a rate determined by the time constant of the exponential normal mode of the approximate linear equation and is reduced to $O(\mu^2)$ in a time which is $O(\log(1/\mu))$. Thereafter the solution is determined within $O(\mu^2)$ by the variational equations and approaches asymptotically either a periodic solution or a combination oscillation represented by a limit cycle of the variational equations.

Finally, it may be noted that the variational equations may be obtained very easily from the amplitude equation by the same symbolic procedure as was used in (**2**). Equations equivalent to these were in fact derived on an intuitive basis in an earlier paper, (**1**), in which the resonance curves of this system were derived. The present paper provides the justification for that procedure.

Some experimental work has been published by Tucker (**3, 4**), but though there is qualitative agreement, Tucker's results are not expressed in a form which makes detailed comparison with the present solution possible. In any case it is unlikely that a cubic approximation to the valve characteristic

would be sufficiently accurate to give numerical agreement except very close to critical regeneration.

9. Degenerative circuit

We conclude with a brief indication of some situations which have been excluded from the previous discussion, taking first the case when the circuit is degenerative. This will be the case if the sign of ϵ is reversed in the differential equation (2). This will reverse the sign of ϵ in the term $\zeta(i)$ of the amplitude equation. The variational equations then take the form

$$\frac{db'}{dt} = \frac{5\sqrt{6}\mu^2}{62}[-b'(1+b'^2)-F\cos\phi'],$$

$$b'\frac{d\phi'}{dt} = \frac{5\sqrt{6}\mu^2}{62}[-b'(\sigma'+\nu b'^2)+F\sin\phi'],$$

where now $$\sigma' = -5/\sqrt{6}+31\sigma/(5\sqrt{6}).$$

Changing the time scale and dropping the accents, these become

$$\dot{b} = -b(1+b^2)-F\cos\phi,$$

$$b\dot{\phi} = F\sin\phi-b(\sigma+\nu b^2).$$

Each resonance curve of $y\,(=b^2)$ against σ for fixed F is now a single branch. The system of resonance curves resembles that of an oscillator with non-linear restoring force, the curves leaning over towards the high frequency side. When $\nu^2 > 3$ this gives an interval in which there are three stationary oscillations, the system of variational equations having three singular points, the middle one a col, the other two both stable. When only one singularity exists it is stable and there are no limit cycles. The amplitude equation gives for $F = 0$

$$b^2 = -a^2 = -1\Big/\Big(\lambda+\frac{5}{\sqrt{6}}\lambda'\Big),$$

so that no free oscillation occurs.

10. The case when c_2^2 is not restricted

Given a constant c such that $|c_n| < c$ $(n = 2, 3,...)$ and a constant b_1, we can determine μ_1 so that the series defining K and H converge for $b < b_1$ and $\mu < \mu_1$. The regions $\mathscr{R}$, $\mathscr{R}'$, $\mathscr{R}''$ may then be defined within which the transformation from (2) to the system (43), (45), (46) is defined and the analysis of section 7 is valid. The equations (45) and (46) will require modification, as was done in the foregoing section, if different assumptions are made within the general restrictions just set out.

(i) Suppose the circuit is regenerative and that c_2 and c_3 have values such that $\lambda+(5/\sqrt{6})\lambda'$ is $O(\mu)$. The term containing this factor in (45) is then

$O(\mu^3)$ and does not therefore appear in the first approximation. Equations (45) and (46) then become

$$\frac{db}{dt} = \frac{5\sqrt{6}\mu^2}{62}\{b + E\sqrt{\tfrac{31}{6}}\cos(\phi+\alpha)\},$$

$$b\frac{d\phi}{dt} = -\frac{5\sqrt{6}\mu^2}{62}\left\{\left(\frac{5}{\sqrt{6}}+\frac{31\sigma}{5\sqrt{6}}\right)b - \left(\frac{5}{\sqrt{6}}\lambda-\lambda'\right)b^3 + E\sqrt{\tfrac{31}{6}}\sin(\phi+\alpha)\right\}$$

omitting the terms which are $O(\mu^3)$ and assuming that $S(x)-S(K)$ is already reduced to $O(\mu^2)$. With a change of time scale, and writing

$$\sigma_1 = 5/\sqrt{6}+31\sigma/(5\sqrt{6}),\quad \nu_1 = (5/\sqrt{6})\lambda-\lambda',\quad F_1 = E\sqrt{(31/6)},\quad \phi' = \phi-\pi+\alpha,$$

these may be written

$$\frac{db}{dt} = b - F\cos\phi', \tag{54}$$

$$b\frac{d\phi}{dt} = F\sin\phi - b(\sigma_1-\nu_1 b^2), \tag{55}$$

which correspond to (52), (53) respectively.

The resonance curves of this system have no loops as in the case of an oscillator with non-linear restoring force, but are more correctly compared with the portion of the resonance curve diagram of (52), (53) which lies below the resonance curve for $F^2 = 4/27$ (Fig. 2 of (**2**)). They have reversed slope within the hyperbola

$$1+(\sigma_1-\nu_1 y)(\sigma_1-3\nu_1 y) = 0,$$

so that there may be three singular points, the middle one being a col, the others unstable nodes or foci. When only one singular point exists it is an unstable node or focus.

Bendixon's first theorem shows that there are no limit cycles, so that for any initial conditions not coinciding exactly with an unstable singular point, the representative point moves outwards until it eventually leaves the region of validity of the equations of the first approximation.

The solution of (2) will then consist of an oscillation of increasing amplitude and varying phase, the final state not being determinable from the equations of the first approximation.

(ii) If we suppose that the circuit is regenerative, and that c_2 and c_3 have values such that $\lambda+(5/\sqrt{6})\lambda'$ is negative and $O(1)$, and write

$$a^2 = -1/(\lambda+(5/\sqrt{6})\lambda'),$$

the variational equations may be reduced to the form

$$\frac{db}{dt} = b(1+b^2) - F\cos\phi,$$

$$b\frac{d\phi}{dt} = F\sin\phi - b(\sigma+\nu b^2)$$

with ν positive, by changes of scale and origins analogous to those previously employed.

This case resembles the previous one, the outward radial velocity being increased by the b^3 term of the first equation. Again the amplitude of oscillation increases until the equations of first approximation cease to be valid.

(iii) Lastly there is the case in which the circuit is degenerative and $\lambda+(5/\sqrt{6})\lambda'$ is negative and $O(1)$. The variational equations now take the form

$$\frac{db}{dt} = -b(1-b^2) - F\cos\phi,$$

$$b\frac{d\phi}{dt} = F\sin\phi - b(\sigma+\nu b^2).$$

If ϕ is replaced by $\phi+\pi$ these equations make the component velocities of the representative point of the b, ϕ plane the negatives of those given by (52), (53), except that ν is now positive. The trajectories are therefore of the same form but are described in the reverse sense as t increases. The resonance curves are therefore of the same form with asymmetry of the opposite kind, but the stabilities of the nodes and foci are interchanged. The zero amplitude is stable when $F = 0$ and when $F \neq 0$ the oscillation is stable when $b^2 < \frac{1}{2}$ if only one singular point exists, or the oscillation of smallest amplitude is stable if three exist. It appears, however, that if an oscillation of sufficiently large amplitude could be initiated, so that the representative point was at a sufficiently large radius, the representative point would then move outwards, and the oscillation amplitude would increase until again the equations of the first approximation ceased to be valid.

In the last three cases it may be that, depending on higher powers in the series, there are other singular points or limit cycles determining periodic solutions or solutions of combination type. The expressions for the higher terms of the series are, however, excessively cumbersome and no attempt has been made to evaluate them. On the other hand, the amplitude of oscillation may grow beyond the limits of convergence of the series and the determination of the ultimate form of the solution for large values of t

will not be possible by the present methods. We may then be in a situation similar to that mentioned by Cartwright (**5**) in connexion with the equation

$$\ddot{v}-(\alpha+\beta v-\gamma v^2)\dot{v}+\omega^2 v = f(t)$$

when β is large compared with α and γ.

The situations discussed in this section do not appear to have been observed experimentally.

REFERENCES

1. A. W. Gillies, 'The application of power series to the solution of non-linear circuit problems', *Proc. Inst. Elec. Eng.* **96** (1949), 453.
2. —— 'The periodic solution of a non-linear differential equation of the second order with unsymmetrical non-linear damping and a forcing term', *Quart. J. Mech. App. Math.* **8** (1955), 108.
3. D. G. Tucker, 'Forced oscillations in oscillator circuits and the synchronisation of oscillators', *J. Inst. Elec. Eng.* **92** (1945), 226.
4. —— and G. G. Jamieson, 'Discrimination of a synchronised oscillator against interfering tones and noise', *Proc. Inst. Elec. Eng.*, Monograph No. 146R, August 1955.
5. M. L. Cartwright, 'Forced oscillations in nearly sinusoidal systems', *J. Inst. Elec. Eng.* **95** (1948), 88.

WIDENING THE APPLICABILITY OF LIN'S ITERATION PROCESS FOR DETERMINING QUADRATIC FACTORS OF POLYNOMIALS

By J. W. HEAD†

[Received 22 December 1955.—Revise received 20 March 1956]

SUMMARY

If an approximation is known to a real or complex root of an algebraic equation, the root can be determined from two applications of Lin's process by an adaptation of Steffensen's device (Aitken's δ^2-process), whether Lin's process is convergent or divergent, provided that the divergence is not too violent and the roots of the algebraic equation are sufficiently well separated. The basic principle used is that for a sufficiently close starting approximation and a real or complex linear divisor, successive approximations have their first differences in geometric progression. The question of finding a suitable starting approximation is not considered. Two numerical examples, one with real roots and one with complex roots, are discussed fully.

1. Introduction

Olver (**1**) has suggested that the solution of an algebraic equation should be carried out in two stages: first a 'direct' method such as repeated root-squaring should be applied to obtain good approximations to the roots sought, and thereafter these approximations should be improved where necessary by means of an iterative method. Olver also gives techniques for locating groups of clustered roots and for transforming an equation having a group of clustered roots into one (usually of much lower degree) in which the clustered roots become well separated from the point of view of root-squaring. Here we shall mainly be concerned with the second stage, where an approximation to the root sought is known and we wish to improve that approximation by an iterative method. Of all known iterative methods, that due to Lin (**2**, **3**) has the advantage of great simplicity, but the disadvantage of uncertain convergence because the conditions of convergence involve the unknown roots being sought (**3**, **4**). Lin's method, when convergent, may be used to find a factor of any degree, but here we shall confine our attention to the case of a linear divisor, real or complex, because in this case (as shown in (**3**)) the successive differences between consecutive divisors arising in the iteration form a geometric progression provided that the initial approximation is sufficiently close. If a is complex, division by $(x+a)$ only differs in the last stage from division by the real quadratic factor $(x+a)(x+\bar{a})$, $\bar{a}$ being the conjugate of a.

† Research Department, B.B.C. Engineering Division.

[Quart. Journ. Mech. and Applied Math., Vol. X, Pt. 1 (1957)]

We can roughly divide equations to which Lin's process is applied into six classes, according to the rate of convergence, which may be (*a*) rapid convergence, (*b*) rather slow convergence, (*c*) very slow convergence, (*d*) very slow divergence, (*e*) rather slow divergence, or (*f*) rapid divergence. In case (*a*) Lin's original process is quite adequate and no further improvement is needed. In cases (*c*) and (*d*) the presence of equal or clustered roots must be suspected; this can be confirmed by carrying out the 'H.C.F. process' between the original polynomial $f(x)$ and its derivative $f'(x)$; abnormally small coefficients in the remainders $r_{m+1}(x)$, $r_{m+2}(x)$,... obtained after a certain stage will indicate that $r_m(x)$ contains factors which are nearly repeated factors of $f(x)$. Alternatively, groups of clustered roots can be located by Olver's techniques already mentioned. However they are determined, Olver's transformation techniques (**1**, section 9) are probably an essential preliminary to the application of any iterative process. If the original polynomial $f(x)$ is replaced by $x^n f(1/x)$, case (*f*) is likely to become case (*a*), (*b*), or (*e*); we shall not consider cases where this does not happen. Our main object is to show that the root being sought can be determined in cases (*b*) and (*e*) using Steffensen's device (also known as Aitken's δ^2-process, cf. (**4**) and equations (5), (6) below) because, for a sufficiently good approximation, differences between successive linear divisors are in geometric progression. Aitken (**4**, p. 179) considered the behaviour of a divisor of any degree and noted that under certain conditions, automatically satisfied for a linear divisor in case (*b*), the differences between corresponding coefficients in successive divisors tended to geometric progression, and in 1926 used an accelerative process based upon this fact. Equation (5) is, in effect, derived by the application of this accelerative process to the case of a linear divisor here considered. The process here described is applied to the original equation; it is thus different from Aitken's 'catalytic multiplier' (**5**). In Aitken's 'catalytic multiplier' a trial divisor $d(x)$ is applied to the original polynomial $f(x)$ and if there is divergence or slow convergence, a factor $g(x)$ is determined in such a way that when $d(x)$ is applied as a trial divisor to the product $f(x)g(x)$, convergence is rapid provided that $d(x)$ is a sufficiently good approximation to a factor of $f(x)$. The multiplier $g(x)$ is of the same degree as $d(x)$. There is no reason why both the process here suggested and Aitken's should not be used in combination.

In the iterative solution of m linear simultaneous equations, the nth iterative approximation to each unknown is a linear combination of the nth powers of $(m-1)$ fixed quantities which depend upon the coefficients. Schmidt (**6**) has used this fact to solve the equations explicitly in terms of a number of the iterates although the iteration process itself may be divergent. Schmidt was mainly concerned with $m \geqslant 3$; when Lin's process

is divergent and the divisor is linear, the iteration behaves similarly to the simultaneous-equation iteration for $m = 2$. Basically our approach is the same as that of Schmidt, but considerable simplification is possible because m is only 2.

2. General description of Lin's process

Let $$F(x) = x^n + a_{n-1}x^{n-1} + a_{n-2}x^{n-2} + \ldots + a_1 x + a_0 \quad (1)$$

and suppose that $d_0(x)$ is an approximation to a factor $d(x)$ of $F(x)$ having any degree. Divide $F(x)$ by $d_0(x)$, stopping at the penultimate remainder $k_1 d_1(x)$, so that $$F(x) \equiv x d_0(x) Q_1(x) + k_1 d_1(x), \quad (2)$$

Q_1 being a polynomial of degree $(n-3)$ in x, and k_1 the coefficient of the term of highest degree in the penultimate remainder, so that $d_1(x)$ has unity for the coefficient of the term of highest degree. Now divide $F(x)$ by $x d_1(x)$, and let $d_2(x)$ be the remainder divided by the coefficient of the term of highest degree, and so on. Then the sequence $d_0(x)$, $d_1(x)$, $d_2(x)$,... if convergent, has a limit $d(x)$ which is a factor of $F(x)$.

3. The general case of a linear divisor

In reference (**3**) it is shown that, provided an approximation $(x-p_r)$ to a factor $(x-p)$ of a polynomial $F(x)$ is so close that $p_r - p = \xi_r$ can be regarded as a small quantity of the first order, then

$$\xi_r = \bar{\xi}\lambda^r, \quad (3)$$

where $\bar{\xi}$ is a constant and

$$\lambda = 1 + \frac{pF'(p)}{F(0)}, \quad (4)$$

so that the successive differences $(p_r - p)$ form a geometric progression. Now suppose that the trial divisor $(x-p_0)$ is such that $(p_0 - p)$ is a small quantity of the first order (that is, p_0 is a good approximation to the required root p) and that $(x-p_1)$ and $(x-p_2)$ are the divisors produced by the first two rounds of the Lin process, p_0 being real or complex. Then from (3) with $r = 0, 1, 2$, we obtain

$$p = \frac{p_1^2 - p_0 p_2}{2p_1 - p_0 - p_2}, \quad (5)$$

and this is in theory true whatever the values of $\bar{\xi}$, λ may be, so that (5) can be applied whether the original Lin process (with real or complex linear divisor) is convergent or divergent, subject only to the limitation that $\bar{\xi}$, $\bar{\xi}\lambda$, and $\bar{\xi}\lambda^2$ can be regarded as small quantities of the first order, which implies that p_0, p_1, and p_2 are all good approximations to p. Clearly (5) is likely to be unsatisfactory if λ is near 1, as its numerator and denominator then both involve differences between nearly equal quantities. The most

likely reason for λ to be near unity is, from (2), that $F'(p) \simeq 0$ so that $F(x)$ has a repeated or nearly repeated root for $x = p$. Formula (5) is equivalent to Steffensen's adjustment (4), also known as Aitken's δ^2-process, in which if three consecutive members of a sequence are u_{k-1}, u_k, u_{k+1} and the first differences Δu_k, Δu_{k+1},... are settling down to an approximate geometric progression, then the limit U of the sequence is nearly

$$U = u_{k+1} - (\Delta u_k)^2 / \Delta^2 u_{k-1}, \tag{6}$$

$\Delta^2 u_{k-1}$ being a second difference. It therefore seems that Steffensen's adjustment could also be applied, in a form analogous to (5), to sequences in general which have first differences diverging in approximately geometric progression, provided the divergence is not too violent; we can in this case treat the three members u_{k-1}, u_k, u_{k+1} of the diverging sequence as if they had been obtained in the reverse order.

4. A simple example with real roots

Consider first the equation

$$f(x) = x^3 + 18x^2 + 78{\cdot}75x + 81 = 0. \tag{7}$$

The actual roots are $-1{\cdot}5$, $-4{\cdot}5$, and -12. These roots might be regarded as obvious in the case of (7), but in general we might obtain rough approximations $-1{\cdot}7$, $-4{\cdot}3$, and -11 by considering the general behaviour of $f(x)$ for negative x. We now perform two rounds of Lin's process taking p_0 as successively $-1{\cdot}7$, $-4{\cdot}3$, and -11 and use the notation of (5) (except that the estimate of the root obtained from (5) will be called P so that p can be reserved for the exact root). Results are given in Table 1 below. P is then used instead of p_0 as a starting approximation and the whole process is repeated. Table 1 shows that the roots $-1{\cdot}5$ and $-4{\cdot}5$ are reached rapidly; the original Lin process is convergent in the first case and divergent in the second. When, however, we seek the root -12 in this way it is clear that the divergence is very violent, but this root is easily found by means of the reciprocal equation as already suggested. If the original Lin process is carried on with the starting divisor $x+11$, the factor $x+1{\cdot}5$ is eventually reached.

TABLE 1

Successive trial divisors for equation (7)

$-p_0$	$-p_1$	$-p_2$	$-P$
1·7	1·5870	1·5369	1·4970
1·4970	1·49875	1·49948	1·50000
4·3	4·0827	3·6936	4·5749
4·5749	4·6736	4·9187	4·5084
4·5084	4·5190	4·5431	4·5001
11	46·29	0·0583	..

5. A straightforward sextic equation with complex roots

Consider the sextic equation

$$x^6+3x^5+21x^4+30x^3+84x^2+48x+64 = 0 \tag{8}$$

which can also be written in the form

$$(x^2+1)(x^2+4)(x^2+16)+3x(x^2+2)(x^2+8) = 0. \tag{9}$$

Since the terms of even degree have real roots -1, -4, and -16 in x^2 which separate the corresponding roots -2, -8 associated with the terms of odd degree, (8) is free from roots with positive real parts, and the form (9) also suggests that a useful starting divisor for seeking the roots nearest $x = \pm i$ is $x^2+0{\cdot}4666x+1$, obtained by putting -1 for x^2 in (9) except in the factor (x^2+1); the corresponding factor for the roots nearest $x = \pm 2i$ is $x^2+0{\cdot}6666x+4$. Though better starting factors could have been obtained otherwise, e.g. by root squaring, these are adequate for our present purpose, which is to consider the situation after a starting approximation has been chosen rather than how to find a starting approximation.

Starting then with the trial divisor $x^2+0{\cdot}4666x+1$, and carrying out the division of the left-hand side of (8) by this in the original Lin manner, we obtain the quadratic remainder $56{\cdot}4631x^2+29{\cdot}3138x+64$. This remainder is divided by the factor $x+0{\cdot}2333+0{\cdot}9724i = x-p_0$ of the trial divisor, leaving the complex linear remainder

$$(16{\cdot}1410-54{\cdot}9047i)x+64, \tag{10}$$

which would also have been obtained if we had merely divided the left-hand side of (8) by $x+0{\cdot}2333+0{\cdot}9724i$. From (10) we deduce that the next complex linear divisor is

$$x+0{\cdot}3154+1{\cdot}0729i = x-p_1 \tag{11}$$

associated with a real quadratic factor

$$x^2+0{\cdot}6308x+1{\cdot}2506. \tag{12}$$

The process is now repeated by dividing (12) into the left-hand side of (8), yielding a quadratic remainder $51{\cdot}3792x^2+28{\cdot}5883x+64$, which is divided by (11) to yield a complex linear remainder

$$(12{\cdot}3833-55{\cdot}1247i)x+64,$$

and hence the next complex linear divisor would be

$$x+0{\cdot}2483+1{\cdot}1052i = x-p_2. \tag{13}$$

We now apply (5) to obtain the complex linear divisor $(x-P)$ actually used in preference to (13), and the whole process is repeated; the various divisors are given in Table 2. For the trial divisor $x+0{\cdot}2333+0{\cdot}9724i$ we have

been considering, there is no difference between Table 1 and Table 2 except that Table 1 has real numbers while Table 2 has complex ones. The root found repeats in the ordinary Lin process to five places. When we come to consider the trial divisor $x^2+0{\cdot}6666x+4$, however, a new feature appears: the divergence is such that two successive values of P have not brought us sufficiently close to the root. This indicates that the initial approximation is not sufficiently close. If the various values of p_0, p_1, p_2, and P are plotted, they indicate a general tendency for the successive values of P to circulate; this suggests that the centre of the circle formed by p_0 ($x-p_0$ being a factor of $x^2+0{\cdot}6666x+4$) and the first two P's is worth trying as a new starting approximation; finding this centre algebraically gives us a new value of p_0 which is $-0{\cdot}4115-1{\cdot}9615i$, and this is sufficiently close to the true root, $-0{\cdot}41705-1{\cdot}95601i$, to enable us to obtain this root in two applications of the geometric-progression process as indicated in Table 2; it checks satisfactorily if the ordinary Lin process is used.

The method of finding the successful value of p_0 in this case may have severe limitations; the important point, however, is that an adequate approximation must be found before an iterative process becomes useful, as contended by Olver (1). In favourable cases, a crude approximation may be quite sufficient; the case we have just considered was unfavourable; the divergence was on the border line between 'rather slow' and 'rapid', whereas the divergence associated with the factor $x+11$ and (7) was very rapid indeed.

For the third root pair of (8) it is advisable to use the reciprocal equation; when this is done, no new feature appears, and the actual value of the roots is $-0{\cdot}83015+3{\cdot}52800i$.

TABLE 2

Successive trial divisors for equation (8)

$-p_0$	$-p_1$	$-p_2$	$-P$
0·2333 +0·9724i	0·3154 +1·0729i	0·2483 +1·1052i	0·2565 +1·0724i
0·2565 +1·0724i	0·2534 +1·0763i	0·2517 +1·0745i	0·25273+1·07431i
0·25273+1·07431i	0·25279+1·07427i	0·25281+1·07430i	0·25279+1·07430i
0·3333 +1·9720i	0·0991 +2·1154i	−1·5513 +1·8572i	0·3433 +1·9217i
0·3433 +1·9217i	0·1221 +1·9108i	−0·6309 +1·4908i	0·4053 +1·8831i
0·4115 +1·9615i	0·4073 +1·9847i	0·4352 +2·0798i	0·4164 +1·9565i
0·4164 +1·9565i	0·4157 +1·9588i	0·4173 +1·9679i	0·41705 +1·95601i

6. Acknowledgement

The author wishes to thank the Chief Engineer of the B.B.C. for permission to publish this paper.

REFERENCES

1. F. W. J. Olver, 'The evaluation of zeros of high-degree polynomials', *Phil. Trans.* A, **244** (1952), 385.
2. Shih-Nge Lin, 'A method of successive approximations of evaluating the real and complex roots of cubic and higher order equations', *J. Math. Phys.* **20** (1941), 231.
3. J. Morris and J. W. Head, 'Note on Lin's iteration process for the extraction of complex roots of algebraic equations', *Quart. J. Mech. App. Math.* **6** (1953), 391.
4. A. C. Aitken, 'On the factorization of polynomials by iterative methods', *Proc. Roy. Soc. Edinburgh*, A, **63** (1951), 174.
5. —— 'Note on the acceleration of Lin's process of iterated penultimate remainder', *Quart. J. Mech. App. Math.* **8** (1955), 251.
6. R. J. Schmidt, 'On the numerical solution of linear simultaneous equations by an iterative method', *Phil. Mag.* **32** (1941), 369.

RELAXATION METHODS IN THEORETICAL PHYSICS

VOLUME II

By Sir Richard Southwell

55*s. net*

This volume completes a treatise of which Volume I was published separately (in 1946), for reasons given in its preface: '. . . in recent papers Relaxation Methods have dealt successfully with problems of greater difficulty. . . . But the papers have still to be released from the restrictions of war-time secrecy . . .'. Reviewing that volume in *Nature*, Professor G. Temple wrote that already relaxation methods had become 'well recognized and established weapons of numerical computation . . . clearly capable of wide extension to many other problems of mathematical physics.' Volume II fulfils that prediction, since it discusses equations of higher order than the second, equations involving *three* independent variables, and equations which are non-linear, also eigenvalue problems, for which more powerful methods have been devised quite recently. It aims, in fact, to record the position attained by the end of 1953; and even refers (in supplementary notes) to papers published in 1956, including one which describes stress-calculations made for the new Dokan Dam in Iraq—one of the most impressive of relaxational achievements. The number of items in its 'Index of problems solved' has risen from 35 (in Volume I) to 62.

By the same author, and in the same series:

RELAXATION METHODS IN THEORETICAL PHYSICS, *Vol. I*, 35*s. net*

RELAXATION METHODS IN ENGINEERING SCIENCE, 35*s. net*

AN INTRODUCTION TO THE THEORY OF ELASTICITY FOR ENGINEERS AND PHYSICISTS, 50*s. net*

OXFORD UNIVERSITY PRESS

THE QUARTERLY JOURNAL OF MECHANICS AND APPLIED MATHEMATICS

VOLUME X PART 1 FEBRUARY 1957

CONTENTS

The Editorial Board gratefully acknowledge the support given by: Blackburn & General Aircraft Limited; Bristol Aeroplane Company; Courtaulds Scientific and Educational Trust Fund; English Electric Company; Hawker Siddeley Group Limited.